W-PM-Sym 1

REGULATION OF ENDOMEMBRANE ACIDIFICATION. Dennis K. Stone, Dept. of Physiology, University of Texas Southwestern Medical Center, Dallas, TX 75235-9040.

W-PM-Sym 2

STRUCTURE AND ORGANIZATION OF MITOCHONDRIAL COMPLEX I. John Walker, Laboratory of Molecular Biology, Medical Research Council, Hills Road, Cambridge, England CB2 2QH.

W-PM-Sym 3

PROTON PUMPS, PROTON FLOW AND ATP-SYNTHESIS IN PHOTOSYNTHESIS OF GREEN PLANTS.

W. Junge, P. Jahns, G. Schönknecht, G. Althoff, & S. Engelbrecht. Universität Osnabrück, D-4500 Osnabrück, Germany

The proton pumping activity of photosystem II results from the oxidation of water (at a Mn-centre) and the reduction of a bound quinone (Q_b) at different sides of the thylakoid membrane. The protolytic reactions with the water phases do not directly reflect the events at bound Q and bound water but rather the transient electrostatic response of acids/bases on the protein surface. At the extreme, the net proton production and consumption has been totally occluded from bulk water. It became short-circuited through the protein and across the membrane by derivatisation with DCCD of acid side chains of certain polypeptides (LHC). While the stoichiometric pattern of proton uptake during the two stepped reduction of Q_b to the quinole is flat, 1:1 H^+/e^-, proton release upon the four stepped oxidation of water oscillates, but rather as 1:0.5:1:1.5 (pH7.5) and pH-dependent and not as 1:0:1:2 as published by various laboratories including our own.

The unit size of transmembrane electric events was titrated with picomolar concentrations of gramicidin. Regarding the electrical relaxation the connected membrane area was much larger than previously thought (at least 100 μm^2, $\simeq 2 \cdot 10^7$ molecules of chlorophyll, $\simeq 2 \cdot 10^4$ of the ATP synthase) of same order of magnitude as the total thylakoid content of one chloroplast. Diffusion (ohmic loss), however, limited the drainage basin for protons of the ATP synthase to narrower size.

The proton translocating ATP synthase (CFOCF1) is endowed with an access channel (CFO) with extreme proton selectivity (even at pH8 against 300 mM KCl). Its conductance is very high (turnover number $>>10^4 s^{-1}$) and seemingly independent of pH. The coupling of proton flow to ATP synthesis may involve mechanical transduction steps as suggested by the functionality of hybrid synthases mixed from subunits that were taken from different sources.

W-PM-Sym 4

THE CYSTIC FIBROSIS GENE PRODUCT AS A MEMBER OF THE TM6-NBF TRANSPORTER SUPER FAMILY. John R. Riordan, Dept. of Biochemistry, Research Institute, The Hospital for Sick Children, Toronto, Ontario M5G 1X8, Canada.

W-PM-Sym 5

SECONDARY STRUCTURE OF THE H+ K+ ATPase. George Sachs, Membrane Biology Lab, University of California, Los Angeles CURE, Wadsworth VA Medical Center, Los Angeles, CA, 90073.

W-PM-Sym 6

MECHANISTIC STUDIES OF THE CONFORMATIONAL CHANGE IN E1E2-TYPE ATPASES REPORTED BY FLUORESCEIN.

L. D. Faller, R. A. Diaz, G. Scheiner-Bobis, and R. A. Farley, CURE, Dept. of Medicine UCLA & Dept. of Veterans Affairs Medical Center, West Los Angeles, CA 90073, and Dept. of Physiology & Biophysics, University of Southern California School of Medicine, Los Angeles, CA 90033.

The working hypothesis in most models of mammalian active transport is that the carrier can assume different conformations, designated E1 and E2, in which the ion binding sites are alternately exposed to the cytosol and to the lumen. The mechanism of the conformational change is unknown. We have approached this problem by studying the temperature dependence of the rates of the conformational change reported by fluorescein. Analysis of the results by absolute reaction rate theory places constraints on the types of molecular chemical events that are occurring by resolving the energy which determines the rate and extent of reaction into heat changes resulting from formation, or cleavage, of chemical bonds and into changes in the organization of the system that increase, or decrease, the number of molecular degrees of freedom. Since proposals for the mechanism of the conformational change are not explicit enough to calculate the expected enthalpy and entropy changes, we have empirically varied the transport enzyme, the monovalent cation, and the solvent structure. There are striking differences between the sodium and proton pumps. For example, the E2K to E1K transition of the latter enzyme is more than an two orders of magnitude faster. Lithium can substitute for potassium in the sodium pump, but not in the proton pump. Enthalpy-entopy compensation is not observed with all metals.
Supported by grants from NIH, NSF, and the VA.

W-PM-A1

HOW MANY BALLS DOES IT TAKE TO INACTIVATE A K^+ CHANNEL? Roderick MacKinnon, William N. Zagotta and Richard W. Aldrich. Department of Cellular and Molecular Physiology, Harvard University and Department of Molecular and Cellular Physiology and the Howard Hughes Medical Institute, Stanford University.

The Shaker K^+ channel is an A-type K^+ channel: following voltage-activated opening it undergoes rapid, spontaneous closure (fast inactivation). Armstrong and Bezanilla proposed that inactivation in Na^+ channels results when a structural part of the channel, acting like a tethered ball, occludes the open channel from the inside. Recently, a region near the N-terminus of the Shaker K^+ channel protein was shown to have the functional properties of such an inactivation ball. Because the Shaker K^+ channel is a tetramer and can be composed of four identical subunits, we wondered whether four balls, one from each subunit, are necessary to inactivate the channel or is one ball enough? To answer this question we co-expressed in oocytes normal inactivating (WT) and mutant inactivation-removed (IR) channels. At the same time we selectively "tagged" either WT or IR by controlling charybdotoxin (CTX) sensitivity with a second, independent mutation. The pattern of CTX sensitivity directly demonstrates the functional expression of heteromerous channels containing both WT and IR subunits. A single inactivation ball is sufficient to inactivate a K^+ channel, although with slower kinetics.

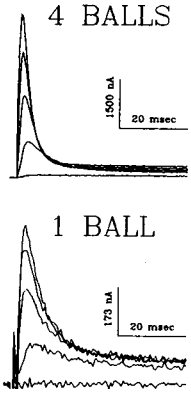

W-PM-A2

MODEL OF ION CHANNEL KINETICS: CHAOTIC MOTION IN A POTENTIAL THAT HAS TWO LOCAL MINIMA

Larry S. Liebovitch and Ferenc P. Czegledy
Dept. Ophthalmology, Columbia Univ.,NY

Most models of ion channel gating assume that the ion channel protein randomly switches between different conformational states. Liebovitch and Tóth (*J. Theoret. Biol.*, 1991, in press) developed a model where the switching between states was not random, but due to a deterministic chaotic process that mimics random behavior. That model was based on a mathematical formulation which could be given a physical interpretation. Now, we present a chaotic model based on physical principles.

We assume that the channel protein has a potential energy function with two local minima, corresponding to the open and closed states. The acceleration of a coordinate that controls the current is proportional to the sum of three forces: the gradient of the potential, a velocity dependent friction due to viscosity of the relative motions within the protein, and a deterministic driving function chosen to be periodic.

The predicted currents look qualitatively like experimental single channel data. The predicted histograms of open and closed times are approximately exponential. There are subconductance states due to subharmonic resonances. That is, there are long lived states due to dynamic resonances rather than local minima in the potential energy function.

Supported by Amer. Heart Assoc., Whitaker Found., and NIH EY6234.

W-PM-A3

CONSTANT FIELDS AND CONSTANT GRADIENTS IN OPEN IONIC CHANNELS.

D.P. Chen and R.S. Eisenberg, Department of Physiology, Rush Medical Center, Chicago IL 60612.

An open channel is no simpler than a pore in a dielectric, a pore filled with salt solution. Our goal is to predict current flow through such a pore, with as few assumptions as possible. The potentials in the dielectric and the pore are described by the relevant Maxwell equations in three dimensions. The potentials are coupled by a dielectric boundary condition assuming only induced polarization charge. Current flow in the pore is described by the Nernst–Planck equations, allowing net charge. A mathematical assumption and asymptotic expansion (exploiting the narrow diameter of the pore) reduce these non–linear partial differential equations to nonlinear ordinary differential equations or a (double) integral equation. Those equations are self–consistent and permit large interactions between ion and channel wall, unlike traditional constant field theory. The integral equation is solved by iteration, giving the profile of potential and concentration along the pore, and thus the flux and current through the channel.

This theory is distinct from, but related to traditional theories. A constant electric field is predicted (***not*** assumed) when the pore contains significant net charge because it is much shorter than a Debye length. A constant gradient is predicted in other cases: the gradient of the total concentration of possibly permeant ions is constant (but ***not*** the gradient of concentration of each ion, as in Henderson's theory of the liquid junction). When the gradient of total concentration vanishes, because the total concentration of possibly permeant ions is the same on both sides of the channel, a constant electric field is predicted for ***both*** short and long channels.

Thus, the theory predicts that an open channel will contain a constant electric field (usually producing a ***non***linear current voltage relation) and/or a constant concentration gradient (usually producing a linear current voltage relation), depending on the concentrations on each side of the channel (and other experimental conditions). Those concentrations can be easily manipulated in the laboratory: in that way measurements of current voltage relations can tell whether a channel is best described by a constant field or constant gradient approximation.

W-PM-A4

GATING CURRENTS OF POTASSIUM CHANNELS EXPRESSED IN *XENOPUS* OOCYTES

Stefan H. Heinemann, Walter Stühmer and Franco Conti*
Max-Planck-Institut für biophysikalische Chemie, Abt. Membranbiophysik, D-3400 Göttingen, FRG. * CNR, Istituto di Cibernetica e Biofisica, I-16146 Genova, Italy.

While the study of potassium gating currents has so far been hampered by the simultaneous presence of sodium channels in excitable cells, the approach of exogenous ion channel expression in oocytes meets the requirements for such investigations. We report recordings of gating currents from oocytes which were injected with cRNA corresponding to potassium channels from *Drosophila* and rat brain. Large inside-out patches provided high time resolution and low-noise performance. The rising phase of the recorded potassium gating currents is close to the recording bandwidth of 10 kHz ruling out slow initial steps in the activation process. The *"on"* gating currents show a double exponential time course between -60 and 0 mV. The fast recovery of Q_{on} upon repolarization is incomplete. In contrast to sodium channels, gating charge becomes totally immobilized for positive membrane potentials and long pulses regardless of whether the channels show inactivation or not. The ratio of Q_{on} and Q_{off} versus membrane potential is consistent with four independent gating units per channel. Figure: Gating currents in response to a depolarizing pulse from -100mV to 20mV.

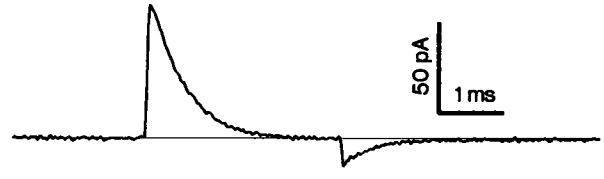

W-PM-A5

RECOVERY FROM INACTIVATION OF SHAKER K^+ CHANNELS: ROLE OF THE CARBOXYL DOMAIN. Lin, J.W., Moreno, H. and Rudy, B. Depts. of Physiology & Biophysics and Biochemistry, New York University Medical Center, New York, NY 10016. (Introduced by: J. Zadunaisky)

The Shaker gene in Drosophila generates several products by alternative splicing; these encode proteins with an identical central core region flanked by divergent amino and carboxyl domains. Shaker K^+ channel proteins may have one of two identified carboxyl domains which influence the rate of recovery from inactivation. Shaker channels with a type of 4 carboxyl domain recover from inactivation fast while channels with a type 37 carboxyl domain recover from inactivation extremely slowly. Channels with a type 4 carboxyl domain also recover slowly from inactivation if the membrane is depolarized for many seconds. Iverson and Rudy (1990) suggested that the carboxyl domain regulates the rate of entrance into a second inactivated state from which recovery is slow. Channels with type 4 carboxyl domain enter this second state slower than channels with a type 37 carboxyl domain. We now find that the rate of entrance into the slow recovery state in channels with a type 37 carboxyl domain is the same as the rate of decline of the currents during a depolarization. We also find that the rate of recovery depends on the type of amino domain, the voltage at which recovery takes place and the concentration of divalent cations. These results and the effects of structural changes on the carboxyl domain will be used to discuss possible mechanisms responsible for the slow recovery from inactivation in channels with a type 37 carboxyl domain. Supported by NIH Grant: GM26976 to BR.

W-PM-A6

PROBING THE ACTIVATION PROCESS OF THE DELAYED RECTIFIER K^+ CHANNEL WITH DEUTERIUM OXIDE. A MACROSCOPIC CURRENT AND SINGLE CHANNEL STUDY. Eduardo Perozo and Francisco Bezanilla. Department of Physiology, UCLA, Los Angeles, CA 90024.

The opening and closing of the delayed rectifier K^+ channel is well represented by a sequential model of several closed states and one open state. In such scheme, there are voltage dependent and voltage independent transitions which have been studied in detail with voltage clamp methods and single channel recordings. The possibility that the channel undergoes an electrically silent major conformational change during channel opening was explored using deuterium oxide as a probe.

The effects of D_2O on the kinetics of the delayed rectifier channel have been studied using internally dialyzed voltage clamped squid axons, and at the single channel level using the cut-open axon technique. The internal solution contained (in mM) 310 or 500 K^+, 4 Mg^{++}, 30 $PO_4^=$, 110 Glycine and 1 EGTA. The external solution was artificial sea water plus 300 nM TTX. The experimental solutions were identical, but prepared in 99.8 % pure D_2O. Both internal and external application of D_2O produced a reduction in the amplitude of the macroscopic ionic current, with a marked slow-down in its activation kinetics.

At the single channel level there is a slight decrease in the single channel conductance in the presence of D_2O. The effects of D_2O were studied at several temperatures, in macroscopic and single channel experiments, to distinguish the effects due to intrinsic solvent from those related to isotopic exchange. Supported by USPHS grant GM30376.

W-PM-A7

KINETIC AND STEADY-STATE PROPERTIES OF SLOW INACTIVATION OF THE DELAYED RECTIFIER K^+ CHANNEL. Eduardo Perozo and Francisco Bezanilla. Department of Physiology, UCLA, Los Angeles CA 90024.

The delayed rectifier potassium current of the squid giant axon is reduced by sustained depolarization, independently of K^+ accumulation in the periaxonal space (Ehrenstein and Gilbert, Biophys. J. 6:553, 1966). We have studied this slow inactivation process in macroscopic, single channel and gating current experiments. Internally dialyzed axons under voltage clamp conditions were used for the macroscopic and gating current experiments. The cut-open axon technique was used for the single-channel recordings. In general, the external solution was artificial sea water with 300 nM TTX and 1 mM NaCN. The internal solution contained (in mM) 310 K^+, 30 $PO_4^=$, 4 Mg^{++}, 110 glycine, and 1 EGTA. As measured with macroscopic ionic currents, the voltage dependence of the steady-state inactivation can be fitted with a Boltzmann distribution. The midpoint of the distribution depends on the phosphorylation state of the channel, as previously reported. The kinetics of inactivation was studied by tail analysis, using a high K^+ external solution and low internal K^+. The onset of inactivation showed two distinct components with time constants near 4 and 30 s, and it displayed very little or no voltage dependence. The recovery from inactivation, on the other hand, was very voltage dependent, with marked delays for potentials more positive than -60 mV. In gating current experiments, there was a fraction of the transferred charge which depended on the holding potential resembling the voltage dependence of the inactivation process of the ionic currents. At the single channel level, it was possible to construct a single channel steady-state inactivation curve by taking the ratio of blank traces to the total number of pulses to the same potential from different holding potentials. In single channel voltage-jump experiments, the 20 pS channel (the main contributor to the delayed rectifier) inactivated with the same time course as the macroscopic currents. Supported by USPHS grant GM30376.

W-PM-A8

FACILITATION OF BACKGROUND POTASSIUM CURRENT IN HEART CELLS: NOVEL MECHANISM FOR REGULATION OF ACTION POTENTIAL DURATION? Peter H. Backx and Eduardo Marban. Dept. of Medicine, Johns Hopkins University, Baltimore MD 21205

We have identified an outward current in guinea-pig ventricular myocytes that represents the macroscopic correlate of $i_{K,p}$ (Pfluegers Arch. 413:127-133, 1988). The properties of this background current render it capable of modulating action potential duration (APD): it activates within 10 msec at positive potentials, does not inactivate, and deactivates very rapidly upon repolarization. The current is insensitive to Cl channel blockers, internal or external $[Cl^-]$, dihydropyridines and sulfonylureas, but is blocked completely by 0.5-1 mM Ba. It remains present when $[K^+]_o$ is reduced to 0mM, which eliminates I_{K1}. We measured this current at room temperature with whole-cell patch clamp in 5 mM $[K^+]_o$, 10 μM nitrendipine, 130 mM $[K^+]_i$ and 2 mM $[EGTA]_i$. From V_H = -40 mV, Ba-sensitive current density increased from 0.16 ± 0.04 pA/pF at 0 mV to 0.52 ± 0.21 pA/pF at +80 mV (n = 8, means ± SE). These and other features suggest that the background current $I_{K,p}$ is generated by K channels that are distinct from I_{K1} or the delayed rectifier I_K. Although essentially time-independent during a step, background outward current exhibits voltage-dependent facilitation: current magnitude roughly doubles when elicited from a holding potential of 0 mV (Figure). Facilitation is not mediated by changes in $[Ca^{2+}]_i$, given that it is observed with internal EGTA and with Ca channels blocked. In conclusion, we have identified a background component of K current in ventricular cells. Voltage-dependent facilitation of background K^+ current may underlie the frequency-dependent decrease in APD.

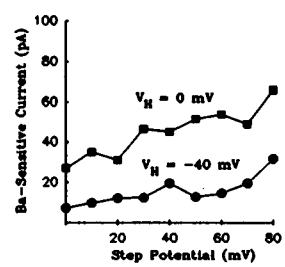

W-PM-A9

PHARMACOLOGIC SEPARATION OF FAST AND SLOW DELAYED RECTIFER K CURRENT COMPONENTS. Kevin Chinn, Searle, Skokie, IL 60077.

Guinea pig ventricular myocytes show delayed rectifier K tail currents whose decay is best fit by the sum of fast and slow exponentials. Whole cell data described here (.1 mM external Cd^{2+} used to block Ica, EGTA internal to buffer Cai, 22°C) show the effect of the benzenesulfonamide class III antiarrhythmic agent E-4031 (1 and 5 μM) on the amplitude of fast (IKf) and slow (IKs) potassium tail current components. IK was activated using voltage pulses from -40 mV to +40 mV and tail currents were examined at -40 mV. E-4031 abolished IKf irrespective of voltage pulse duration. IKs was blocked using short pulses (< about 0.5 s) but appeared to become unblocked using long pulses. In one cell IKs reached approximately 80% of control values using pulse durations of 2 - 8 s. Before exposure to E-4031 the ratio of IK tail/IK during the voltage pulse varied from > 1 using short (< 0.5 s) pulses, to < 1 for long (> 1 s) pulses. In addition, for pulses between 0.7 to 4 s this ratio decreased steadily to a plateau level at about 4 s. 4 s was the approximate time where with increasing pulse duration IKs also reached a plateau (IKf plateaus within 0.5 s). After drug exposure the ratio was unaffected by pulse duration indicating the presence of only one channel type during the pulse and the tail current. The ratio was always < 1 after drug exposure. This in addition to the fact that E-4031 abolished IKf at all pulse durations indicated that under drug free conditions conductance through IKf channels was greatly decreased during the stimulus pulse. This was easily observed in experiments using short pulses where IKf was often larger than IKs. In such cases, IK during the pulse was actually smaller than IKf observed in the tail current. In conclusion, IKf and IKs are pharmacologcially separable. The change in current characteristics after drug exposure indicates that the delayed rectifier in guinea pig ventricular myocytes is primarily formed from a combination of two different channel types.

W-PM-B1

EVIDENCE FOR 2 CALCIUM BINDING SITES IN CGMP-ACTIVATED CHANNELS **K. Su, R.E. Furman and J.C. Tanaka**
Dept of Biochemistry & Biophysics, Univ. of Pennsylvania, Philadelphia, Pa. 19104

The cGMP activated currents in excised inside-out patches from *Rana pipiens* photoreceptor membranes were recorded initially under symmetrical conditions with 120 mM NaCl and no divalent cations. Ca or Mg, 1 nM to 1 mM, was then added to the cytoplasmic side and cGMP-activated currents were recorded. At saturating [cGMP], divalent cations have small but reproducible effects on I_{Na} until ~1mM when block is apparent. At 10 mM divalent cation, the inward I_{Na} shows a voltage-dependent block, but block of the outward current is voltage independent consistent with the notion that divalent cations are permeant. A plot of ln (fraction block/fraction unblock) (fb/fub) vs V_m for inward currents was roughly linear in 10 mM Ca or Mg with slopes of 0.024 ± 0.006 and 0.02 ± 0.004, respectively. Fractional electrical distances for a divalent binding site were estimated to be 0.69 and 0.57 from the cytoplasmic side using a single-site model. Plots of ln (fb/fub) vs log [Ca], however, indicated a second high-affinity site of $\sim 10^{-8}$M Ca.

Additional evidence for this high affinity binding site is seen at low [cGMP]. At 20 μM cGMP, divalent ions block ~80% of the currents in both directions at $\sim 10^{-8}$ M. As the divalents are increased, the currents show some recovery but decrease again above 1 mM. The voltage-dependence of the inward and outward currents at 10 mM Ca is similar to that seen at saturating [cGMP], however, the ln(fb/ub) at 10^{-8}M Ca is voltage independent for both inward and outward currents.

Reversal potentials from bionic substitution with divalent cations could not be determined because the currents were too small. We therefore measured the shift in E_{Rev} with 10 mM Ca added to the 120 mM NaCl bath. The average shift of -10.8 mV corresponds to P_{Ca}/P_{Na} of 4.1 as determined from the GHK current equation. Several models will be considered which would predict these observations

W-PM-B2

THE EFFECT OF DIVALENT CATIONS ON THE SINGLE CHANNEL CURRENT OF cGMP-ACTIVATED CHANNELS OF ROD PHOTORECEPTORS

P.Salvani, T.D.Lamb+, M.Straforini and V.Torre (Intro. by L. Cervetto)
Dipartimento di Fisica, Universita' di Genova, Italy and
+Physiological Laboratory, University of Cambridge, U.K.

We have used the patch clamp technique in the excised inside-out configuration to study the properties of single channels activated by cyclic GMP(cGMP), in the outer segment plasma membrane of rods from the salamander (Ambystoma tigrinum). In the absence of divalent cations, addition of cGMP (1 or 2 μM) to the medium bathing the cytoplasmic surface of the membrane induced brief openings, which had an average open duration of about 0.1 ms at membrane voltages between -100 and 100 mV. Addition of 1 mM Ca^{2+} to the bathing medium drastically reduced the rate of occurrence of these openings. However, by raising the concentration of cyclic GMP to 3 μM with 1 mM Ca^{2+}, openings were induced which appeared very similar to those observed with 2 μM cGMP and zero divalent concentration, over the range -100 to +100 mV. Analysis of power spectra of the cGMP-induced current showed that the effect of Ca^{2+} is a simple scaling of the magnitude of the spectrum, independent of frequency.

In contrast Mg^{2+} induced an effect which was voltage- and frequency dependent. 200 μM Mg^{2+} in the bathing medium had little effect at the membrane voltages between -100 and -40 mV, but it markedly depressed the current between +40 and +100 mV. In addition, the components of the power spectrum at low frequencies (below 200 Hz) were reduced most prominently.

We conclude that single channels activated by cGMP can be observed in the presence of mM amounts of divalent cation bathing the cytoplasmic surface, and that Ca^{2+} and Mg^{2+} block the cGMP-activated channels in different ways.

W-PM-B3

GTPase ACTIVITY OF A PORTION OF TRANSDUCIN EQUIMOLAR TO PHOSPHODIESTERASE IS SUPPRESSED BY cGMP: A PUTATIVE FEEDBACK MECHANISM OF THE ROD PHOTORESPONSE. **Vadim Yu. Arshavsky*, Mark P. Gray-Keller@ & M. Deric Bownds*@#, Lab of Molecular Biology*, The Neuroscience Training Program@, and Dept. of Zoology#, University of Wisconsin, Madison, WI, 53706.**

We have found two pools of transducin (G_t) in frog rods that express different rates of light-dependent GTPase activity: 20% hydrolyzing GTP at >0.5 turnovers/sec ("fast") and 80% hydrolyzing GTP at ~0.05 turnovers/sec ("slow"). Fast GTPase activity is abolished by physiological concentrations of cGMP. Half-saturation of the inhibition occurs at ~2 μM cGMP. 8-Bromo-cGMP mimics cGMP, but neither cAMP nor GMP affect GTPase activity. We suggest that fast GTPase, regulated by cGMP, is a property of G_t which binds to and activates phosphodiesterase (PDE), while slow GTPase reflects G_t that has not bound to PDE. Such a model is supported by our finding that the lifetime of activated PDE is enhanced in the presence of μM cGMP using mM cAMP as substrate for hydrolysis. GTPase regulation by cGMP is not affected by Ca^{++} over the concentration range 5-500nM. The data suggest that cGMP is not only a messenger of excitation in rods but may also mediate negative feedback regulation of the primary transduction pathway at the level of PDE quench. The fact that cGMP-dependent suppression of GTPase activity is independent of Ca^{++} suggests a clear distinction from the previously described feedback mechanism based on Ca^{++}-dependent modulation of guanylate cyclase. **(Supported by NIH EY00463).**

W-PM-B4

SITE-SPECIFIC MUTAGENESIS OF THE INHIBITORY SUBUNIT OF THE RETINAL ROD CYCLIC GMP PHOSPHODIESTERASE R. L. Brown and L. Stryer, Department of Cell Biology, Stanford University School of Medicine, Stanford, CA 94305

The cGMP phosphodiesterase in retinal rod outer segments is activated following illumination by transducin, the visual G-protein. In the dark, PDE activity is held in check by its two inhibitory γ subunits which bind with very high affinity (K_d = 10 pM). γ is rapidly removed by activated transducin. How does this system maintain such strict inhibition and yet allow for activation on a millisecond time scale? We have chemically synthesized a gene for γ and expressed it in *E. coli*, yielding quantities sufficient for biochemical characterization. To date we have also expressed eight mutants of γ. The expression and mutagenEsis of γ in bacteria coupled with biophysical techniques have provided several insights. Three properties of each mutant were studied: What is its binding affinity for trypsin-activated PDE (tPDE)? Does it inhibit tPDE? if so, can transducin relieve the inhibition? The binding affinity of each mutant was assayed independent of inhibitory ability using changes in fluorescence emision anisotropy of fluorescein attached to the sole sulfhydryl of γ, cysteine 68. These studies have revealed that many regions of γ participate in binding. In contrast, the carboxy-terminal half of γ is more important than the amino-terminal half for inhibition. Mutation of three acidic residues D52, D53, and E58 to Q, or the truncation of the last five residues caused a total loss of inhibitory activity, while decreasing the binding affinity only 50-100 fold. These mutants bind competitively with wild type γ and actually activate the holoenzyme when added in excess. Each of the inhibitory mutants is capable of functional interaction with transducin, as shown by a reconstitution assay using membrane-bound PDE catalytic subunits formed by limited proteolysis with Arg-C protease. An inhibitory mutant that cannot interact with transducin is being sought.

W-PM-B5

LIGHT-INDUCED CHANGES IN cGMP BINDING IN ELECTROPERMEABILIZED TOAD ROD OUTER SEGMENTS. Rick H. Cote and Maura A. Brunnock, Dept. of Biochemistry, University of New Hampshire, Durham, NH 03824-3544.

Changes in the total intracellular cyclic GMP concentration of retinal rod photoreceptors during visual transduction do not correlate with the behavior of the ion channel believed to be directly regulated by changes in cytoplasmic cyclic GMP levels. One possible explanation is that the intracellular cyclic GMP concentration is buffered by binding to specific cyclic GMP binding sites in the rod outer segment.

High affinity cyclic GMP binding sites have been characterized in dark-adapted, highly disrupted rod outer segment preparations in which > 90% of the endogenous cyclic GMP has been removed by ultrafiltration. At low (< 1 μM cyclic GMP) concentrations, a single class of binding sites can be resolved by a filter binding assay with a $K_D = 59 \pm 21$ nM at 22° C; the maximum amount bound under these conditions was 0.005 ± 0.001 mol cyclic GMP per mol rhodopsin. Lower affinity cyclic GMP binding sites have also been detected. Illumination of this preparation did not result in a statistically significant change in cyclic GMP binding.

Purified toad rod outer segments have been electropermeabilized with six 2500 V/cm, 0.25 μFd electric discharges, resulting in morphologically intact cells of which > 85% are now permeable to exogenous nucleotides. Light-induced increases in the amount of [3H]cyclic GMP bound have been observed over the range of 10^2 to 10^6 rhodopsin bleached (R*) per rod in this preparation. At dim light intensities, the stoichiometry of light-induced cyclic GMP binding is 10^3 cyclic GMP molecules per R*. Changes in cyclic GMP binding may represent a high stoichiometry, non-enzymatic mechanism for regulating the cytoplasmic cyclic GMP concentration during visual transduction. Supported in part by NIH (EY05798) and Fight for Sight-Prevent Blindness (GA90097).

W-PM-B6

PHOTOCURRENT RECOVERY AND R* LIFETIME IN RETINAL RODS. DR Pepperberg[1], MC Cornwall[2], M Kahlert[3], KP Hofmann[3], J Jin[2], GJ Jones[2], and H Ripps[1]. [1]Dept. of Ophthalmology, Univ. of Illinois, Chicago, IL; [2]Dept. of Physiology, Boston Univ., Boston, MA; and [3]Institut für Biophysik, Albert-Ludwigs Univ., Freiburg, Fed. Rep. of Germany.

The membrane current response of retinal rod photoreceptors to bright flashes exhibits a delay in the recovery from the maximum, saturating amplitude. Responses to 100-ms saturating flashes were recorded from isolated, single rods of larval tiger salamander (A. tigrinum) (24-25° C). Waveforms were analyzed for the post-stimulus period (T_c) that preceded recovery of the photocurrent by a criterion value (3 pA). The flash-induced fractional bleach (R_o^*/R_{tot}) was compared with R_s^*/R_{tot} ($\simeq 7\times10^{-5}$), the bleaching level at which transducin activation (T* formation) is predicted to approach saturation.

T_c increased linearly with ln (R_o^*/R_{tot}) over a range ($R_o^*/R_{tot} \simeq 2\times10^{-6}$ - 6×10^{-3}) that included R_s^*/R_{tot}. Data obtained from 5 rods yielded 1.7 ± 0.2 s (mean ± SD) as the slope (τ_c) of the T_c function (i.e., $\tau_c = \Delta T_c + \Delta[\ln (R_o^*/R_{tot})]$). Background light reduced T_c measured at a given R_o^*/R_{tot} but did not alter τ_c. The intensity-dependence of T_c resembles that of a delay (T_d) which, in light-scattering studies, describes the period of T* saturation in bovine rods after a bright flash; the slope of the T_d function ($\Delta T_d + \Delta[\ln (R_o^*/R_{tot})]$) is thought to reflect the lifetime of photoactivated visual pigment (R*) (refs. 1-2). The present data suggest that the electrophysiological delay has a similar basis in the deactivation kinetics of R*, and that τ_c represents the lifetime of R* in the phototransduction process. (1) Pepperberg et al., Proc. Natl. Acad. Sci. USA 85, 5531 (1988). (2) Kahlert et al., Nature 345, 537 (1990).

W-PM-B7

RELIEF OF BLEACHING ADAPTATION AND INDUCTION OF WAVELENGTH DEPENDENT RESPONSE SHAPES BY 9-DESMETHYL RETINAL IN RODS.

D. Wesley Corson,[1,2] Fadila Derguini,[3] Koji. Nakanishi,[3] Rosalie K. Crouch,[2] Edward F. MacNichol,[4] & M. Carter Cornwall[4] Depts. of Pathology[1] and Ophthalmology,[2] Med. Univ. of S. Carolina, Dept. of Chemistry,[3] Columbia Univ. and Dept. of Physiology,[4] Boston Univ. School of Medicine

11-*cis*-9-Desmethyl retinal has been reported to form an active but inefficient photopigment with abnormal metarhodopsin states in biochemical preparations (Ganter *et al., Biochem. 28*:5954). We find that it forms a bleachable photopigment in *Ambystoma* rods with a peak absorbance near 475 nm, ~50 nm removed from the peak of the native pigment near 523 nm. This analogue partially restores sensitivity to isolated bleached rods (1.1±0.4 out of 2.2±.6 log units lost in bleaching; n=3). In this regard, its activity appears similar to that of 11-*cis*-locked analogues of retinal which partially restore sensitivity by efficiently relieving bleaching adaptation without restoring photosensitivity.

In addition, we observe that the shapes of flash responses elicited after resensitization vary with wavelength and are greatly prolonged for blue wavelengths relative to red. The spectral sensitivity measured at a point 10 seconds after the flash is shifted 54±5 nm (n=3) to the blue relative to that measured at the peak of the response. This result is most readily explained by the mixed contributions of a small amount of residual native pigment which produces normal responses and a component of 9-desmethyl retinal pigment which has a different absorption spectrum and produces prolonged or delayed responses.

We expect that further measurements with this and other retinal analogues will reveal the relations between the chromophore-protein interactions and the relief of bleaching desensitization. In addition, 9-desmethyl retinal appears to be a useful probe for the physiological activity of photoexcited states of rhodopsin.

Supported by NIH grants EY07543,EY04939,EY01157 & GM34509 and by a grant from the Medical University of South Carolina.

W-PM-B8

Recoverin: A 26 kD Calcium-sensitive Activator of Retinal Rod Guanylate Cyclase. S. Ray, A. Dizhoor, S. Kumar, M. Spencer, G. Niemi, K. Walsh, J. Hurley and L. Stryer.

In retinal rod cells, guanylate cyclase is markedly activated following illumination by the light-induced reduction of the cytosolic calcium level. Stimulation is mediated by a 26 kD protein, named recoverin because it promotes the restoration of the cyclic GMP concentration. The amino acid sequence of recoverin purified from bovine rod outer segments points to the presence of three Ca^{2+} binding sites (EF hands). This inference is supported by the finding that calcium shifts the tryptophan fluorescence emission spectrum of recoverin. Most significant, highly cooperative calcium-sensitive activation of guanylate cyclase is restored by the addition of recoverin to membranes stripped of the endogenous stimulatory protein. Activation of guanylate cyclase in native membranes can be blocked by an anti-recoverin antibody. Immunocytochemical labeling studies show that recoverin is located in both retinal rod and cone cells. The homology of recoverin to visinin, a chicken cone protein of hitherto unknown function, suggests that these proteins are members of a new family of calcium-sensitive regulators that act as switches at submicromolar levels.

W-PM-B9

MUTUAL INTERACTION BETWEEN Na/Ca,K-EXCHANGERS AND cGMP-GATED CHANNELS OF ROD PHOTORECEPTORS.

Paul J. Bauer, Inst. of Biol. Information Processing, KFA, D-5170 Jülich, FRG

In vertebrate photoreceptors, Ca enters the cell through the cGMP-gated channels, and it is pumped out by the Na/Ca,K-exchangers. Both protein species are only found in the plasma membrane, i.e. in a small membrane fraction of about 6% of the rod outer segment (ROS) membranes (Bauer 1988, J. Physiol. 401,309). Fusion of disk and plasma membranes induces a spread of these proteins over a 8-10 times larger membrane area (Bauer 1988, Biophys. J. 53, 473a). Do cGMP-gated channels and Na/Ca,K-exchanger spread out independently of each other?

Mild sonication of fused ROS membranes creates more vesicles than there are cGMP-gated channels, and the cGMP-gated channels show no tendency for aggregation (Bauer 1989, Biophys. J. 55, 62a). If the Na/Ca,K-exchangers diffuse also independently of the cGMP-gated channels, then they should essentially occur on different vesicle fractions in the fused ROS membranes. Consecutive activation of the cGMP-gated channel and the Na/Ca,K-exchanger yield about equal Ca-releases (cGMP/Na-competition); however, activation of the Na/Ca,K-exchanger prior to activation of the cGMP-gated channel yields a large Ca-release upon activation of the Na/Ca,K-exchangers, but only little Ca-release after activation of the cGMP-gated channels (Na/cGMP-competition). This finding suggests that most, if not all, cGMP-gated channels are associated with (at least) one Na/Ca,K-exchanger.

In order to separate these two protein species, the ROS membranes were solubilized in CHAPS and reconstituted in soybean phosphatidylcholine (PC). Surprisingly, even in these liposomes the cGMP-gated channels were again found to be associated with the Na/Ca,K-exchangers. For low lipid-to-protein ratios ($\leq$ 6mg PC/mg rhodopsin), cGMP/Na-competition yielded equal cGMP- and Na-induced Ca-releases, whereas for higher lipid-to-protein ratios, the Na-induced Ca-release generally exceeded the cGMP-induced Ca-release.

These experiments suggest that (a), the Na/Ca,K-exchangers have a strong tendency to interact with the cGMP-gated channels whereas, (b) the cGMP-gated channels show no tendency to aggregate, and (c), there are at least as much Na/Ca,K-exchangers as cGMP-gated channels in photoreceptors.

W-PM-C1

INTRAMOLECULAR DISULFIDE BOND FORMATION IN MUTANTS OF MYOSIN LIGHT CHAIN 2. V. Wolff, L.D. Saraswat, and S. Lowey, Rosenstiel Basic Medical Sciences Research Center, Brandeis University, Waltham, MA 02254-9110.

Cloned mutants of myosin light chain 2 (LC2) were recently prepared in which a third cysteine residue was engineered into a sequence already containing two endogenous cysteine residues at positions 126 and 155 (Saraswat and Lowey, Biophys. J. 57:330a, 1990). One mutant had a cysteine substituted for proline at position 2. Oxidation of this light chain resulted in the presence of two fast migrating bands on non-reducing SDS polyacrylamide gels. One band was ascribed to the formation of a disulfide bond between C126 and C155, and the other was tentatively assigned to a disulfide bond between C2 and one of the endogenous cysteines. The latter species suggests that the amino- and carboxyl-terminal ends of the free light chain can be in close proximity. To distinguish whether C126 or C155 was bonded to C2, oligonucleotide-directed mutagenesis was used to delete C126 or C155, while retaining C2. DTNB titration of the purified C2/C126 and C2/C155 mutants, followed by non-reducing SDS-PAGE, showed that each mutant formed an intramolecular disulfide species with a distinct electrophoretic mobility. From comigration experiments, it was concluded that C2 bonding to C155 was favored in mutants containing both C126 and C155. DTNB titration of myosin reconstituted with mutant LCs showed that disulfide bond formation can take place in the presence of the myosin heavy chain. The extent to which the oxidized LC remains bound to the heavy chain is being determined. The ability of mutant LCs to form the multiple disulfide bonds described here emphasizes the flexible, globular structure of the regulatory light chain, and its resemblance to other Ca/Mg binding proteins. This research was supported by grants from NIH, MDA and NSF.

W-PM-C2

ISOLATION OF THE TERNARY DNase I - G-ACTIN- MYOSIN HEAD COMPLEX

Patrick Chaussepied (Intro. by Andrzej A. Kasprzak)
CRBM du CNRS, INSERM U 249, University of Montpellier I, BP 5051 34033 Montpellier Cedex, France

A stable G-actin-myosin head (S1) complex can be obtained by using S1 isoenzyme carrying the A2 light chain subunit (Chaussepied, P. & Kasprzak, A.A., 1989, *Nature*, **342**, 950-953). Indeed, in contrast to the G-actin-S1 (A1) complex which rapidly polymerizes, the G-actin-S1 (A2) complex is stable in low ionic strength conditions. This later complex, however, is highly sensitive to the presence of salts, such as 500 μM $MgCl_2$ or 10 mM KCl, which induce its quasi-instantaneous polymerization.

In the presence of DNase I, known to stabilize actin in its monomeric form, neither S1 (A1) nor S1 (A2) isoenzyme induced actin polymerization in the absence or in the presence of salt (5 mM $MgCl_2$, 100 mM KCl). By measuring the S1-induced increase in fluorescence intensity of a pyrenyl group attached to residue Cys 374 of actin, it was found that the presence of DNase I only slightly diminishes the Ka of the G-actin-S1 complexes (with a 2 fold decrease). On the other hand, the absence of effect of S1 on the G-actin-induced inhibition of DNase I activity showed that S1 does not significantly influence the interaction of DNase I with G-actin. Additionally, the interaction between G-actin and S1 was found to be strongly sensitive to both ATP (or ADP) and ionic strength (complete dissociation was reached at i.s. = 100 mM) in the absence as in the presence of DNase I. Consequently, the ternary DNase I - G-actin- S1 complex could be isolated only after covalent linkage of the G-actin-S1 interaction by EDC-catalyzed crosslinking.

In summary, the isolation of the ternary DNase I - G-actin - S1 complex reveals the non-overlapping of the DNase I and myosin head binding sites on monomeric actin. Furthermore this ternary complex, stabilized by DNase I, provides the ideal material for further characterization of the G-actin - S1 interface either by conventional biochemical approaches or by crystallization and 3-D structure reconstitution of the complex.

W-PM-C3

MYOSIN SUBFRAGMENT-1 INTERACTS WITH 2 G-ACTIN MOLECULES IN THE ABSENCE OF ATP.

Catherine VALENTIN-RANC, Cécile COMBEAU and Marie-France CARLIER*
Laboratoire d'Enzymologie, C.N.R.S., 91198 Gif-sur-Yvette, France

The interaction between CaATP-G-actin and myosin subfragment-1 (S_1) has been monitored by pyrenyl-actin fluorescence and light scattering. In low ionic strength buffer and in the absence of ATP (G_0 buffer), a tight ternary complex of S_1 with two G-actin molecules, G_2S, is observed, in which pyrenyl-actin fluorescence is 3-fold higher than in G-actin. ATP bound to actin is not hydrolyzed in the G_2S complex. Formation of the G_2S complex takes place with either S_1A_1 and S_1A_2 isomers of S_1, and precedes S_1-induced polymerization of G-actin into F-acto-S_1 decorated filaments in which pyrenyl actin fluorescence is 6-fold higher than in G-actin. G_2S is also formed upon interaction of S_1A_1 and S_1A_2 with PLP-G-actin, which is unable to polymerize following covalent modification of Lys61 by PLP. The critical concentration for S_1A_2-induced polymerization of G-actin is at least ten-fold higher than for S_1A_1. ATP added to G_0 buffer (containing 100 μM $CaCl_2$) is rapidly hydrolyzed into ADP by S_1. Binding of ATP or CaATP or ADP to S_1 inhibits the formation of G_2S, ATP being a much more potent inhibitor than ADP. The possible structural similarity of the G_2S complex with the rigor F-actin-S_1 state is discussed.

W-PM-C4

ELECTRON CRYO-MICROSCOPY OF ACTOMYOSIN-S1 DURING STEADY STATE ATP HYDROLYSIS: John Trinick and Howard White, Dept. of Muscle Biology, AFRC Institute of Food Research, Langford, Bristol BS187DY, UK and Dept. of Biochemistry, Eastern Virginia Medical School, Norfolk, Va. 23501.

The primary force of muscle contraction is thought to originate from a change in the myosin head while attached to actin, with energy for this transition coming from ATP hydrolysis. The geometry of only one such attached acto-myosin state is known to moderate resolution (~3 nm). This is the stable or so called strongly attached state which occurs in the presence of ADP or in the absence of nucleotide. The structure(s) of other weakly attached states in the ATPase cycle have been difficult to study, because at low protein concentration the states are almost completely dissociated.

We have recently found conditions of low ionic-strength and moderate protein concentration where, without resorting to cross-linking, a high fraction of heads (S1) bind to actin during steady state ATP hydrolysis. The structure of this complex is being studied by electron cryo-microscopy of hydrated specimens. In the micrographs some S1 molecules are seen in the background, but we estimate from 90° light scattering experiments that approximately 70% of the S1 is bound to actin. During steady state ATP hydrolysis, the acto-myosin-S1 complex has an appearance distinct from images obtained in the absence of ATP(1) or actin filaments alone(2). Preliminary analysis of the images, and of Fourier transforms calculated from them, does not reveal strong evidence of preferred conformations. Rather the data suggest a variety of structures. Micrographs of similar preparations that had been allowed to completely hydrolyze ATP have the so-called arrowhead appearance characteristic of a 45° angle of binding. In future it may be possible to extend this approach to obtain details of the structure(s) of defined kinetic states in the ATPase cycle. This work was supported by research grants from AHA and MDA.

1. Milligan, R. & Flicker, P. (1987) J. Cell Biol. 105, 29.
2. Trinick, J., Cooper, J., Seymour, J. & Egelman, E. H. (1986) J. Microscopy, 141, 349.

W-PM-C5

EVIDENCE FOR THE EXISTENCE OF MULTIPLE INTERFACES BETWEEN ACTIN AND MYOSIN SUBFRAGMENT-1 Renné Chen Lu & Anna Wong, Dept. of Muscle Research, Boston Biomed. Res. Inst., Boston, MA 02114

Mornet et al. reported that both the 50K & 20K domains of myosin S1 can be crosslinked to actin with 1-ethyl-3-[3-dimethylaminopropyl] carbodiimide (EDC) and suggested that one S1 can bind two actins (Nature 292 306'81). Subsequent work by Sutoh (Bioch. 21 3654'82), Chen et al. (Bioch. 24 137'85) and others have demonstrated that the crosslinked species are 1:1 complexes of actin and S1. As part of the study of identifying the interface between actin and S1 under various conditions we used EDC in the presence of N-hydroxy-succinimide to improve the efficiency (Grabarek & Gergely, Anal. Bioch. 185 131'90). The products were examined on SDS-PAGE and showed that all of the S1 were complexed with actin by 15 min and appeared as a major band at 150K and a minor one at 200K. As the reaction proceeds, the intensity of the 200K band increases at the expense of the 150K one. Using fluorescently labeled actin we found the same stoichiometry between actin and S1 in two species, showing that the conversion of 150K to 200K was not due to the addition of a second actin. We also found no difference in the proteolytic digestion patterns of two products by various enzymes. Using S1 nicked at the 25/70 junction, two bands with mobility of 120K & 170K were obtained, indicating that the N-terminal 25K region of S1 was not involved in the crosslinking. Using S1 nicked with V8 protease, products show that actin can be crosslinked to the 50 or 20K fragments with similar efficiency. Thus it appears that the 200K product corresponds to a complex of one actin linked to one S1 via two interfaces, presumbly one at the 20K and the other at the 50K region. The anomalous mobility is attributable to the presence of a loop structure, a phenomenon previously observed in intramolecularly crosslinked S1 (Lu et al., PNAS 83 6392'86). Our study also showed that a higher actin to S1 molar ratio (4:1) enhanced the crosslinking via the second interface.

W-PM-C6

ELECTRIC CHARGE CHANGES AT THE ACTOMYOSIN INTERFACE FOR THE ADP,P TO ADP TRANSITION

S. Highsmith & A.J. Murphy, Department of Biochemistry, U. Pacific, S.F.,CA 94115.

The concentrations of free and actin-bound skeletal myosin S1 during MgATP hydrolysis were determined in solutions containing increasing concentrations of monovalent salt (KAc, LiAc, KCl). The ionic strength dependence of the apparent association constant (K) was analyzed using the theory of Pitzer (1973 J. Phys. Chem. 77, 268), which is accurate at high ionic strengths. The apparent association constants at 0 M and 0.2 M and the product of the effective net electric charges of the actin binding site on myosin (z_M) and myosin binding site on actin (z_A) are shown in the Table for ATP (ADP,P), along with the results for ADP.

Nucleotide	K(0 M),M^{-1}	K(0.2 M),M^{-1}	$\lvert z_M z_A \rvert$, esu^2
"ATP"	1.7×10^6	3×10^3	16
ADP	4×10^7	3×10^6	7

It can be shown that for the "ATP" case, K is an upper limit for [A·S1·ADP,P]/([A][S1·ADP,P]). With this in mind and using the K(0.2 M) results to approximate *in vivo* conditions, it is noteworthy that the 1000-fold increase in association constant for ATP→ADP is accompanied by a large decrease in the electric charge of the actin binding site on myosin. The values for z_M and z_A are not resolved, but presumably z_A is not changed by Pi dissociation from A·S1·ADP,P. These results suggest that the increase in actomyosin affinity that accompanies force generation is due to an increase in nonionic interactions between actin and the myosin nucleotide complex. **(NIH Grant AR37499).**

W-PM-C7

RABBIT SKELETAL MUSCLE MYOSIN : UNFOLDED CARBOXYL TERMINUS AND ITS ROLE IN MOLECULAR ASSEMBLY

Andrea Rösch, Hans-Robert Kalbitzer, Kayo Maeda, Yuichiro Maéda*, Wolfgang Beneicke, Kevin Leonard§ and Alfred Wittinghofer

Max-Planck-Institut für medizinische Forschung, Jahnstraße 29, W-6900 Heidelberg, § European Molecular Biology Laboratory, Meyerhofstraße 1, W-6900 Heidelberg, * European Molecular Biology Laboratory at DESY, Notkestraße 85, W-2000 Hamburg 52, Germany.
(Sponsored by Fumio.Matsumura).

In order to study the C-terminus structure of rabbit skeletal myosin and its possible role in myosin assembly, we have expressed in E. coli short LMM segments and compared physical properties of two different species, LMM-30 (263 a.a.) which includes the original C-terminus of MHC and LMM-30C′ which is devoid of 17 residues at the original C-terminus.
(1) Electron microscopy and small angle X-ray scattering showed that the expressed polypeptides form rods about 40 nm long and 2 nm thick, indicating that each molecule is a dimer of two identical polypeptides which are arranged parallel and in register, forming a two-stranded α-helical coiled-coil. (2) ^{1}H NMR spectra indicated that nine residues at the C-termini of LMM-30 and of intact myosin extracted from muscle are unfolded and freely mobile. (3) The low ionic solubility tests show that the unfolded C-terminus may be essential for molecular assembly of LMM-30 under particular conditions; at pH 8.0 LMM-30, but not LMM-30C′, formed aggregates upon decreasing the ionic strength. This implies that the molecular assembly of LMM may be caused by two types of interactions, the electrostatic interactions between the helical parts of LMM and a C-terminus-mediated interaction. At pH 7.5 or lower, the electro-static interactions would be strong enough to induce aggregation even without substantial contribution of the C-terminus-mediated interaction. (4) The assembly of LMM30 is a condensation process and the critical concentration (C_c) of LMM30 assembly is strongly pH dependent. This indicates that at least electrostatic interactions are responsible for the molecular assembly.

We are now trying to characterize separately the two types of interactions.

W-PM-C8

IONIC EFFECTS ON THE VANADATE-INDUCED PHOTOCLEAVAGE OF MYOSIN SUBFRAGMENT-1.

[1]Andras Muhlrad, [1]Y.Michael Peyser and [2]Israel Ringel
[1]Dept. of Oral Biology, Hadassah School of Dental Medicine and [2]Dept. of Pharmacology, Hadassah Medical School, Hebrew University, Jerusalem 91010, ISRAEL.

Myosin subfragment-1 (S1) is cleaved by near UV irradiation in the presence of vanadate at three sites located at 23kDa, 31kDa and 74kDa from the N-terminus. Since vanadate is considered to be a good structural analog of phosphate, it is assumed that the cleavage sites participate in forming the phosphate binding sites(s) of S1. The photocleavage takes place at all sites both in the presence or in the absence of divalent cations indicating that the presence of divalent cations is not essential for the cleavage. The sodium, potassium or ammonium salts of monovalent anions inhibit the photocleavage at 50 to 200 mM concentration range. The inhibition is more expressed at 74 kDa from the N-terminus than at the 23kDa and 31kDa sites. The inhibitory effect increases in the order acetate $\cong F^- < Cl^- < Br^- < I^- \cong SCN^-$. Since the order of the inhibitory effect is identical with the order of the known structure damaging effect of monovalent anions in the von Hippel series, it is assumed that the reason of decreased photocleavage is the local perturbation of structure specially at the 74kDa sites. It is improbable that the inhibition of the photocleavage is caused by a direct reaction of vanadate with the foregoing monovalent anions because ^{51}V NMR measurements did not indicate any reaction between vanadate and the ionic species added. Divalent anions, sulfate and thiosulfate, also inhibit photocleavage at the 2 to 10 mM concentration range without reacting with vanadate according to ^{51}V NMR. The inhibition is very pronounced at the 23kDa and 31 kDa sites, while the 74kDa site is almost not affected. Since the inhibition of the photocleavage at the 23kDa and 31kDa sites occurs simultaneously and independently from that of the 74kDa site, it is assumed that S1 has two distinct phosphate binding sites. Both the 23kDa and the 31kDa cleavage sites participate in the first binding site distinct from a second site located at 74kDa from the N-terminus.

W-PM-D1

COMPUTATIONAL STUDIES OF STRUCTURE-FUNCTION RELATIONS IN Ca^{2+}-BINDING PROTEINS: SIMULATIONS IN SOLUTION MODELS.
Harel Weinstein and **Ernest L. Mehler**, Department of Physiology and Biophysics, Mt. Sinai School of Medicine, CUNY, New York, NY 10029.
Computational simulations combining methods of quantum and statistical mechanics are used to investigate proteins that are active in Ca-dependent modulation of cellular functions, including troponin C (TNC) and calmodulin (CAM). The studies are designed to provide an understanding of their selectivity for Ca^{2+}, and to account for the role of ions in the regulatory functions of these proteins. A basis for the selectivity for Ca^{2+} over Mg^{2+} was found (F. Sussman & H. Weinstein, *PNAS* 86, 7880, 1989) to reside in the difference between the solvation energies of the competing ions in water. Recent experiments suggest that the Ca-bound (but not Mg-bound) structures of CAM and TNC in solution may be more compacted than those observed in the crystal, due to a kinking or bending of the helix linking the two domains. Molecular dynamics simulations served to investigate whether such global structural alterations due to changed environmental conditions can be accounted for by observations from computational approaches. The results were used to determine the structural consequences of compaction and its functional implications. All calculations were started from the available crystal structures. Different solvent models were tested by the exclusion or inclusion of crystallographic waters in combination with a constant, or a distance dependent dielectric permittivity, ε. Simulations with the solvent model which includes crystallographic waters and ε=r, resulted in compacted structures which conserve intradomain secondary and tertiary architecture. Compaction was also observed in computations with the less complete solvent models, but these exhibited concomitant loss of intradomain structure, and distortions in regions of secondary structure other than the central helix. The compaction appeared to be complete after about 150ps of dynamics, but the runs were continued for more than 300ps. Comparison of the Ca-bound C-terminal domains of CAM and TNC showed that their structures remained remarkably similar, although the dynamics were carried out completely independently. The changes in CAM's structure were greater than in TNC. The compacted CAM is somewhat **S** shaped, presenting to the environment two pockets containing several nonpolar residues, and an increased accessibility of some of the hydrophobic residues known from experiment to be involved in the complexation of CAM with cellular proteins. Initial modeling studies of interactions with trifluoperazine suggest that these hydrophobic patches could also be involved in the binding of CAM inhibitors.
SUPPORT: NIH Grant GM-41373, F33 fellowship GM-13103 (to ELM).

W-PM-D2

CO_2 Binding to Human Carbonic Anhydrase II

Kenneth M. Merz, Jr.

Department of Chemistry and
the Department of Molecular and Cell Biology
The Pennsylvania State University
University Park, Pennsylvania 16802

Abstract: We report molecular dynamics and free energy perturbation simulations aimed at studying the binding of CO_2 with human carbonic anhydrase II (HCAII). From our molecular dynamics simulations we have identified to CO_2 binding sites. The first binding pocket is about 3-4 Å away from the zinc ion (Zn···C distance) and is surrounded by Val 121,143,207, Trp 209, Leu 198, His 119, Thr 199 and the residue consisting of Zn-OH. The second pocket is about 5-6 Å away from zinc and is formed by His 64,94,96, Ala 65, Asn 244, Tyr7, Phe 93 and Thr 200. Further analysis of the MD trajectories yields information regarding the fluctuations of a CO_2 molecule bound in these two sites and insights into the function of the Glu 106-Thr 199-zinc-hydroxide hydrogen bond interaction. Using free energy perturbation techniques we have also evaluated the absolute free energies of binding for these two sites. The pocket closer to the zinc ion has a higher affinity for CO_2 than does the more remote site. The calculated binding energies are -3.4 ± 1.1 and -2.2 ± 0.8 kcal/mol, respectively. Our computed free energies of binding are in reasonable agreement with the experimental value (-2.2 kcal/mol), but importantly our computed values indicate that the closer of the two pockets has a higher affinity for CO_2. These observations as well as the proximity of CO_2 to the functionally important zinc ion suggests that the closer site is catalytically important, while the second site serves to increase the surface area by which a CO_2 molecule is recognized and bound by HCAII. By taking advantage of both molecular dynamics and free energy perturbation techniques new insights into the dynamics and energetics of protein-substrate interactions can be readily obtained.

W-PM-D3

ACTIVE SITE DYNAMICS AND REGIOSPECIFICITY OF CYTOCHROME $P450_{CAM}$ AS DETERMINED BY MOLECULAR DYNAMICS SIMULATIONS

Mark D. Paulsen, Michael B. Bass, Gregory E.Arnold, and Rick L. Ornstein, Molecular Science Research Center and Environmental Sciences Research Center, Pacific Northwest Laboratory*, Richland WA, 99352.

Molecular dynamics simulations of the enzyme cytochrome P450cam from *Pseudomonas putida*, the only member of the P450 superfamily for which 3-dimensional data is available, have been carried out for 200 psec. Simulations have been performed with both the native substrate camphor and a substrate analog, norcamphor, bound at the active site. Camphor bound at the active site shows very limited motions. In contrast norcamphor is able to rotate in the active site during the simulation. This observation is consistent with the decreased specificity seen for the hydroxylation of norcamphor by cytochrome $P450_{cam}$. As well as being able to rotate, the norcamphor is on average approximately 1 Å further from the heme than is the camphor. This motion may be the cause of the experimentally observed uncoupling of hydroxylation from electron transfer. In addition to the native enzyme, simulations have also been performed with active site mutants. Together, these simulations provide valuable insight into the molecular basis of substrate specificity, and are a first step in the rational redesign of this enzyme for enhanced bioremediation of recalcitrant DOE-site contaminants.
Pacific Northwest Laboratory is operated for the U.S. Department of Energy by Battelle Memorial Institute under contract DE-AC06-76RLO 1830. M. D. Paulsen, M. B. Bass, and G. E. Arnold are supported by the Northwest College and University Association for Science, in affiliation with Washington State University, under contract DE-AM06-76RLO 2225 with the Department of Energy, Office of Energy Research.

W-PM-D4

TITRATION OF MULTIPLE SITES IN A PROTEIN BY MONTE CARLO SAMPLING: APPLICATION TO THE REACTION CENTER FROM *RB. SPHAEROIDES**

P. Beroza, D. R. Fredkin, M. Okamura and G. Feher, Physics Dept., 9500 Gilman Dr., UCSD, La Jolla, CA., 92093-0319, USA.

A Monte Carlo method for treating electrostatic interactions among many titrating sites was developed and applied to the free energy change upon electron transfer from Q_A to Q_B in the photosynthetic reaction center (RC) in *Rb. sphaeroides*. Initial calculations give the electrostatic contribution to $\Delta G(Q_A^- Q_B \rightarrow Q_A Q_B^-)$ as –130 meV at pH 7, in qualitative agreement with the experimental value of –67 meV[1].

Electrostatic energies were calculated from a finite difference solution[2] to the linearized Poisson-Boltzmann equation for the RC crystal structure[3]. Correct energetics could only be obtained by allowing the protonation of all 174 protonatable residues in the RC to vary. The protonation of the various sites was determined by a Monte Carlo sampling of the 2^{174} protonation states, using the Metropolis algorithm[4]. However, for strongly coupled sites, a modified sampling technique allowing multiple site transitions was employed to search the configuration space more completely. Such sites were identified by strong cross correlations (which resulted in large statistical errors) in their titration curves.

The method agrees with exact calculations for small test systems for which the complete partition function can be calculated, e.g., lysozyme[2]. Previous schemes to treat multiple interacting sites were either inaccurate or unable to handle more than approximately 20 sites. The Monte Carlo technique is an accurate way to treat a large number of titrating residues. We believe that the discrepancy between theory and experiment in the electron transfer free energy results from errors in the electrostatic energy calculations.

[1] Kleinfeld, *et al.* (1984) Biochim. Biophys. Acta 776, 126-140.
[2] Bashford, D., Karplus, M., Biochemistry, in press.
[3] Allen, *et al.* (1988) Proc. Natl. Acad. Sci. USA 85, 8487-8491 and references therein.
[4] Metropolis, *et al.* (1953) J. Chem. Phys. 21, 1087-1092.

*Supported by NSF, NIH and NIH training grant 1T32 GM08326-01.

W-PM-D5

THE TRANSDUCTION OF ENZYME-LIGAND BINDING ENERGY INTO CATALYTIC DRIVING FORCE. Harvey F. Fisher and Narinder Singh, U. of Kansas Medical Center and VA Medical Center, 4801 Linwood, Kansas City, MO 64128.

We propose a testable general mechanism by which ligand binding energy can be used to drive a catalytic step in an enzyme catalyzed reaction. One element of this theory is based on our finding of the wide spread occurrence of ligand binding-induced protein macrostate interconversions having large invariant $\Delta H°$'s accompanied by small but highly variable $\Delta G°$'s. This phenomenon, which can be recognized by the large $\Delta Cp°$'s it generates, can provide the necessary energy input step but is in itself insufficient to constitute a workable transduction mechanism. A viable mechanism requires the additional presence of a "locking step" and a properly connected "power stroke." In the model we propose here, these additional steps are provided by a sequence of two-state enzyme forms in which the interconversions of certain forms are blocked by high energetic barriers. We provide evidence supporting the existence of these additional mechanistic components and more indirect evidence that certain enzyme reactions are indeed driven by just such machinery. We also propose experimental criteria by which the validity of this transduction model can be tested for individual cases.

Supported by Veterans Administration and NIH (GM15188).

W-PM-D6

ENERGETICS OF THROMBIN CATALYTIC ACTIVITY AND MODULATION BY ALLOSTERIC EFFECTORS

Raimondo De Cristofaro, Diane J. Albright and Enrico Di Cera
Department of Biochemistry and Molecular Biophysics, Washington University School of Medicine, Box 8231, St. Louis, MO 63110.

A general thermodynamic scheme has been developed for the description of the linkage between catalytic activity and effector binding to human α-thrombin [1]. The scheme is cast in terms of detailed partition functions for each enzyme intermediate involved in the catalytic cycle and opens the way to application of the thermodynamic theory of site-specific energetics [2,3] to the analysis of steady state kinetics. Application of the linkage scheme to the analysis of the effects of protons on human α-thrombin amidase activity has revealed the existence of multiple catalytic forms that are accessed at different pH values, as well as the apparent pK values of the ionizable groups linked to catalytic and binding events [1]. Analysis of the effects of adenosine nucleotides on human α-thrombin amidase activity has pointed out the energetic aspects underlying the biphasic modulation observed with these important physiological effectors [4]. Further investigation shows that this biphasic effect can be split into its activatory and inhibitory components under suitable experimental conditions. This allows for a complete thermodynamic dissection of the biphasic modulation in terms of the detailed energetics of individual allosteric sites. The results suggest that adenosine nucleotides may play an important role in the *in vivo* modulation of thrombin activity during the early stages of blood clotting.

1. De Cristofaro, R. & Di Cera, E. (1990) *J. Mol. Biol.*, in press.
2. Di Cera, E. (1989) *J. Theor. Biol.* **136**, 467-474.
3. Di Cera, E. (1990) *Biophys. Chem.* **37**, 147-164.
4. De Cristofaro, R., Landolfi, R. & Di Cera, E. (1990) *Biophys. Chem.* **36**, 77-84.

W-PM-D7

COMPUTER SIMULATION OF THE ENZYME REACTION IN TRIOSEPHOSPHATE ISOMERASE

Paul A. Bash, Martin Field, Robert Davenport, Dagmar Ringe, Gregory Petsko, and Martin Karplus
Departments of Chemistry
Florida State University, Boston University, Brandeis University, and Harvard University

A structural and energetic analysis of the key events in the enzymatic reaction of triosephosphate isomerase (TIM) is carried out using a hybrid computational method that combines quantum and molecular mechanics techniques. Energy profiles for each proton transfer are determined for two hypothesized mechanisms of the reaction using a structure of an enzyme-inhibitor complex determined by x-ray crystallography (Davenport et. al.) as a starting point for all simulations. The key questions addressed are the effect specific amino acids have on the reduction of the energy barrier for the isomerization reaction, and the protonation state of His-95 which is thought to facilitate one of the proton transfers. We show that Lys-12, which is within hydrogen bonding distance of the substrate, has the most significant effect on energy barrier reduction, but other residues not in close proximity to the substrate can also have stabilizing/destabilizing effects. This result can be tested with site-specific mutagenesis. Simulations utilizing both singly and doubly protonated His-95 suggest that a neutral imidazole is the most likely state for the His-95 proton transfers. Recent NMR experiments (Knowles et. al.) have determined that His-95 is singly protonated in the enzyme.

W-PM-E1

STRUCTURE OF DUPLEX OLIGODEOXYNUCLEOTIDES USING NON-RADIATIVE FLUORESCENCE RESONANCE ENERGY TRANSFER. Richard A. Cardullo, Sudhir Agrawal, Jeffrey Yoder, and David E. Wolf. Worcester Foundation for Experimental Biology, Shrewsbury, MA 01545.

We have previously reported that Non-Radiative Fluorescence Resonance Energy Transfer (FRET) can be used to detect hybridization of two fluorescently labeled oligodeoxynucleotides (ODNTs) using a number of different configurations (Cardullo *et al.*, 1988, Proc. Natl. Acad. Sci., 85:8490-8494). In these studies fluorescein and rhodamine were attached to the 3′ and 5′ ends of ODNTs using a hexyl spacer and donor quenching was found to occur by both a Förster mechanism as well as a non-Förster mechanism which accounted for 26% of the quenching observed. In this study, fluorescent probes were attached to the 5′ ends of complementary ODNTs using either an ethyl, hexyl, or dodecyl spacer group. The resultant energy transfer between donor (fluorescein) and acceptor (rhodamine) groups was a complex function of ODNT length and spacer length. In general, fluorescence quenching of donor in the absence of acceptor was greatest for the ethyl spacer for short ODNT lengths (>90%) but decreased to 25% for ODNTs longer than 12 base pairs. When hexyl and dodecyl spacers were used, non-Förster quenching was found to be independent of ODNT length (26%). In the presence of acceptor, fluorescent ODNT data using ethyl spacers was corrected for non-Förster quenching and transfer efficiencies were calculated. The transfer efficiency varied with ODNT length and showed cyclicity similar to that expected from a helix. However, these data could not be fit to any simple model suggesting that the relative orientation of the donor dipole to the acceptor dipole, κ^2, varies with position along the helical axis. In addition, temperature spectra showed that the ethyl spacer raised the melting temperature, Tm, an average of 4°C for all ODNTs between 6 and 20 nucleotides. These data, taken together, suggest that the spacer groups play an important role in the stability of the ODNT duplex and that calculation of end-to-end distances of hybrid ODNTs depends strongly on the relative orientation of donor and acceptor fluorophores.

W-PM-E2

TORSIONAL RIGIDITY OF POSITIVELY AND NEGATIVELY SUPERCOILED DNA

Paul R. Selvin, David N. Cook, Ning G. Pon, Melvin P. Klein, John E. Hearst: University of California, Berkeley, and Lawrence Berkeley Laboratory:

We have used Time Correlated Single Photon Counting of intercalated Ethidium Bromide to measure the torsional constant of positive, relaxed, and negative supercoiled pBR322 DNA, ranging in superhelical density from +0.042 to -0.123. At physiological salt concentration, the torsional constant monotonically increases from 1.76×10^{-19} erg-cm for the most positively supercoiled DNA to 2.28×10^{-19} erg-cm for the most negatively supercoiled DNA. At low salt concentration, the torsional constant rapidly increases from positively supercoiled (1.91×10^{-19}erg-cm) to relaxed DNA (2.42×10^{-19}erg-cm), and then levels off at negative superhelical densities (≈2.3×10^{-19}erg-cm). These results indicate that the DNA behaves as a non-linear torsional pendulum under superhelical stress and that the anharmonic term in the Hamiltonian is approximately 15%. The torsional constants were found by fitting the data using the Barkley-Zimm theory, a harmonic approximation that nevertheless fits the data well. These conclusions may be relevant to an understanding of supercoiled domains generated during transcription. At the level of secondary structure, we find that positively supercoiled is significantly more flexible than negatively supercoiled DNA . We also believe that the torsional rigidity of DNA strongly constrains the available conformations of closed-circular DNA, which is important for topoisomer separation in gel electrophoresis.

W-PM-E3

CHARACTERIZATION OF ROTATIONAL DIFFUSION CONSTANTS OF DNA OLIGOMERS USING THE OPTICAL KERR EFFECT.
Don Eden[1] and Richard H. Shafer[2], [1]Dept. of Chemistry and Biochemistry, San Francisco State University, San Francisco, CA 94132 and [2]Dept. of Pharmaceutical Chemistry, University of California, San Francisco, CA 94143.

We have used the optical Kerr effect to characterize the rotational diffusion constant of the synthetic oligomer, $d(GCGAATTCGC)_2$ in aqueous buffers with ionic strength >100 mM. Measurements have been performed as a function of temperature and concentration to examine the interaction of oligomers and to explore the sensitivity of the technique. Unlike the technique of transient electric birefringence, in which an electric field is directly applied to a solution, the optical Kerr effect produces molecular orientation with the intense electric field of a pulsed laser. Since there is negligible sample heating, macromolecules in arbitrarily high ionic strength solutions may be investigated as long as the solution does not exhibit absorption at the laser wavelengths. In the experiments reported the birefringence was induced by an eight nsec FWHM wide Q-switched 10 mJ unfocused YAG laser pulse that is collinear with the probe beam of an argon ion laser. This geometry permits measurements to be made in small volumes, typically 100 μl. The birefringence signal is recorded with a 1.3 giga-sample/sec averaging transient digitizer and analyzed using standard approaches. Although the resulting rotational diffusion constants for solutions of moderate concentration are consistent with those expected from hydrodynamic models, solutions with a concentration of 35 mg/ml exhibit decreased rotational diffusion constants. The optical Kerr effect should be very useful in selectively studying the internal bending and flexing dynamics in a wide variety of nucleic acid and protein systems. We gratefully acknowledge Corey Levenson of Cetus Corporation for the donation of the oligomers. Supported by NIH Grant GM44281 to DE.

W-PM-E4

STRINGENCY CLAMPING DNA TRIPLE HELIX FORMATION Richard W. Roberts and Donald M. Crothers, Department of Chemistry, Yale University, New Haven, CT 06511-8118

It has been demonstrated that DNA oligos can bind to duplex DNA in a sequence specific manner through triple helix formation. Specificity of binding is dependent on finding stringent conditions where only the perfectly matched complexes form ($\Delta G_{f,perfect} < 0$) and defect complexes do not ($\Delta G_{f,defect} > 0$). Stringent conditions exist in a window with dimensions of pH, salt, DNA concentration, and temperature. UV melting curves and gel competitions were used to examine the width of the stringency window provided by a number of simple defects in third strand binding. The width of the window is proportional to the the specificity of triplex formation.

Using this information, we have found it is possbile to maintian specific, saturating binding under conditions far from the stringency window. We refer to this phenomenon as "stringency clamping." To do this, one need only provide for the formation of some competing 2° structure, involving the third strand, with stability in-between the defect and perfect complexes (i.e. $K_{f,perfect} < K_{f,clamp} < K_{f,defect}$). There are several possible 2° structures, one of which is the Watson-Crick (WC) duplex containing the third strand. This duplex is less stable at pH 5.0 than the third strand bound to its triplex site. Intra-molecular clamps may be made by adding sequence to one end of the third strand to give either WC or non-WC base paired hairpins. The utility of stringency clamping is threefold: 1) It avoids stringency searching to obtain sequence specific conditions. 2) The concept is general to all the different triplexes demonstrated up to now (α-anomers, 5-Me C, 5-Br U, non-canonical base triplets, and 3rd strand polarity switches) as long as structures of intermediate stability can be found. 3) It allows maintenance of specificity under condtions where third strand binding is very robust. Using these stable complexes, we demonstrate purification of desired sites using affinity methods.

W-PM-E5

TRIPLEX FORMATION OF OLIGONUCLEOTIDES CONTAINING 2'-O-METHYLPSEUDOISOCYTIDINE IN SUBSTITUTION OF 2'-DEOXYCYTIDINE. Akira Ono, Paul O. P. Ts'o, and Lou-sing Kan, Department of Biochemistry, School of Public Health, The Johns Hopkins University, 615 N. Wolfe Street, Baltimore, Maryland 21205.

In order to investigate a new approach for oligonucleotide directed triplex formation in neutral and basic conditions, a new type of oligonucleotide analog was designed. 2'-O-methyl-pseudoisocytidine (1) which may form two hydrogen bonds with 2'-deoxyguanosine in a Hoogsteen type base pairing at neutral pH (as shown in the figure), was incorporated into an octamer TT1TTT1TT (a). Triplex formation of a with an undecameric duplex 5'd(AAGAAGAAGAA)3'-5'(TTCTTCTTCTT)3', (d) was indicated as follows: A mixture of a and the duplex d in a buffer at neutral pH showed a transition (Tm= 12°C) which was attributable to the dissociation of the third strand a from duplex d. A negative band at 215 nm, which is representative of triplex formation, was observed in the circular dichroism spectrum of the mixture at neutral pH at 3 °C. (Supported in part by DOE and NIH)

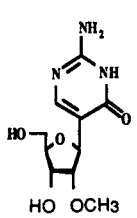

1

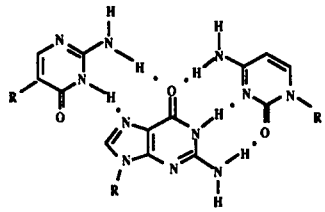

1/G·C

W-PM-E6

STRUCTURAL AND THERMODYNAMIC ANALYSES OF OLIGODEOXYNUCLEOTIDE TRIPLE HELICES. **Daniel S. Pilch[1] and Richard H. Shafer[1,2], [1]Graduate Group in Biophysics and [2]Department of Pharmaceutical Chemistry, University of California, San Francisco, CA 94143.**

The solution structures of the $d(A)_{10}\cdot 2d(T)_{10}$ and $d(C^+{}_3T_4C^+{}_3)\cdot d(G_3A_4G_3)\cdot d(C_3T_4C_3)$ triple helices were analyzed by UV absorption, circular dichroism (CD) and ^{1}H-NMR. Both triplexes were stabilized by either Na^+, Mg^{2+} or spermine^{4+} cations and/or low pH. At suitable cationic concentrations and/or levels of pH, UV mixing curves have points of maximum hypochromicity corresponding to 1:2 stoichiometries of purine to pyrimidine strand. The CD spectra of both triplexes have similar features in the 200-240 nm region, suggesting that this spectral region may provide a circular dichroic signature for triplex formation irrespective of base sequence. Imino proton NMR experiments show that triplex formation in both the $d(A)_{10}$ + $d(T)_{10}$ and $d(G_3A_4G_3)$ + $d(C_3T_4C_3)$ systems is accompanied by the induction of novel imino proton resonances. Two-dimensional nuclear Overhauser effect spectroscopy (NOESY) experiments demonstrate connectivities between these novel resonances and those of the aromatic H8 protons of either adenine or guanine. These connectivities indicate that these novel resonances correspond to Hoogsteen (HG) base paired imino protons. The thermodynamics of triplex formation were evaluated by analysis of thermal denaturation profiles at varying oligomer concentrations. For both oligomer systems, the helix-coil transitions of the Mg^{2+}-stabilized triplexes are biphasic. The first phase reflects separation of the third strand from the duplex (HG phase) and the second phase reflects denaturation of the duplex (W-C phase). However, the melting profile of the Na^+-stabilized $d(A)_{10}\cdot 2d(T)_{10}$ triplex in monophasic, while that of the $d(C^+{}_3T_4C^+{}_3)\cdot d(G_3A_4G_3)\cdot d(C_3T_4C_3)$ triplex is biphasic under identical conditions. The single phase in the melting profile of the Na^+-stabilized $d(A)_{10}\cdot 2d(T)_{10}$ triplex corresponds to a triplex=coil equilibrium. HG base pairs are 0.22-0.69 kcal/mole base pair less stable than the corresponding W-C base pairs depending on the cationic conditions and the base sequence. When formed in the presence of either Na^+ or Mg^{2+} ions in low pH, both T·A and C^+·G HG base pairs have similar stabilities, differing by only 0.02-0.06 kcal/mole base pair. The results of studies on triplexes stabilized by spermine^{4+} will also be discussed.

W-PM-E7

BINDING OF ETHIDIUM BROMIDE TO THE POLY(dA)•2POLY(dT) TRIPLE HELIX: EVIDENCE FOR INTERCALATION. P.V. Scaria and R.H. Shafer, Department of Pharmaceutical Chemistry, University of California, San Francisco, CA 94143.

Binding of ethidium bromide to the double helical forms of DNA and synthetic polynucleotides has been studied extensively. There have been a few reports in the literature on the binding of ethidium to triple helical forms of RNA. According to these studies, ethidium has a higher affinity for the double helix compared to the corresponding triple helix. Also, the binding preferentially stabilizes the double helix. None of these studies addressed the mode of interaction of ethidium with the triplex. We have made a comparative study of the binding of ethidium to the double and triple helical forms of poly(dA) and poly(dT), using a variety of spectroscopic and hydrodynamic techniques. Fluorescence studies show that the fluorescence increase for ethidium in the presence of the triplex is larger than that in the presence of the duplex. Binding studies, using absorbance measurements, yield a binding constant to the triplex about 30 times larger than to the duplex. Furthermore, while the binding to the duplex shows positive cooperativity, binding to the triplex is non-cooperative. Thermal denaturation experiments demonstrate that ethidium stabilizes the triple helix. Appearance of induced CD bands in the visible absorption region of ethidium in the presence of both duplex and the triplex along with the results of fluorescence energy transfer and quenching studies provide evidence of intercalation of ethidium in both duplex and triplex complexes. Binding of ethidium leads to an initial decrease in viscosity for both duplex and triplex structures, followed by an increase which is greater for the duplex. These results strongly suggest that ethidium binds to the poly(dA)•2poly(dT) triplex via an intercalative mechanism. This research was supported by grant CA27343 awarded by the National Cancer Institute, DHHS.

W-PM-E8

EFFECT OF G-T AND I-T MISMATCHES ON LOCAL STABILITY IN B-DNAS. **A. Wishnia, J.-L. Leroy and M. Guéron, Dept. of Chemistry, SUNY at Stony Brook, and Groupe de Biophysique, Ecole Polytechnique, Palaiseau, France.**

The self-complementary oligonucleotides CGCGXTCGCG (X=G,I,A) each form Watson-Crick base-paired duplexes at 15°C in 0.1M NaCl. The ^{1}H NMR peaks of the G1,G2, G3,G4,G5,I5 and T6=T5 hydrogen-bonded imino protons are resolved and have been assigned. From the kinetics of proton exchange as a function of pH and NH_3 exchange catalyst concentration (see Leroy et al., *J. Mol. Biol.*, 200, 223-238 (1988)) the thermodynamic dissociation constant, K_D, and the first-order rate constant, $1/\tau_o$, for opening each base pair are obtained.

Bases in the G-T or I-T wobble pairs appear to open out together, not individually: to within experimental error, exchange of both imino protons is governed by the same parameters. The G5-T5 and I5-T5 pairs are at least 4 kcal less stable than A5-T5 (K_D, 7×10^{-3} or 3×10^{-2} vs. 6×10^{-6}), and also have lower free energies of activation for opening out (τ_o, 0±1 ms or 0.4±0.1 ms vs. 4 ms). (Parallel reduction in thermodynamic and kinetic stability is not a general rule: at least in other G-C, A-T systems, there is not a straightforward correlation between K_D and τ_o.) In these complexes, the kinetic instability (ease of opening) is propagated to both the nearest-neighbor G4-C4 and next-neighbor G3-C3 pairs: for X=G,I vs. A, τ_o is 4 or 1 ms vs. 16 ms (G4) and 0±1 or 1±1 ms vs. 9 ms (G3). The thermodynamic stability of the G4-C4 pairs is reduced by 2 kcal (K_D, $14,11\times10^{-6}$ vs. 0.4×10^{-6}), while that of G3-C3 is unchanged (~0.7×10^{-6} for all three). Adjacent base pairs are indeed perturbed by the relatively unstable nonstandard G-T or I-T pairs, but the effect is rapidly attenuated.

W-PM-E9

SUBSTITUENT EFFECTS ON Z-DNA STABILITY: A SOLVATION FREE ENERGY ANALYSIS. K. Tseng, T.F. Kagawa, G.W. Zhou, and P.S. Ho, Department of Biochemistry and Biophysics, Oregon State University, Corvallis, OR. 97331.

In our attempt to understand the effect of water interactions on macromolecular structure, we have applied the method of calculating solvation free energies (SFE) from solvent accessible surfaces to nucleotide sequences in the B- and in the Z-conformations of DNA. For alternating purine and pyrimidine sequences, the difference in the SFE between the B- and Z-conformations (ΔSFE(Z-B) in kcal/mol/dn, where dn is the dinucleotide repeat) showed that sequences with a higher propensity to adopting left-handed Z-DNA are more negative than those which are less stable as the Z-form. The ΔSFE(Z-B) values of four well studied sequences were -0.44 for d(m^{5}CG), 0.14 for d(CG), 0.17 for d(CA)-(TG), and 0.67 for d(TA) dinucleotides. The relationship between the calculated ΔSFE(Z-B) and the experimentally determined B- to Z-DNA transition free energies for these dinucleotides has a slope of 0.36 and y-intercept of -0.23, showing that the ΔSFE(Z-B) values follow the trend and are of the same order of magnitude as the experimentally determined differences in stabilization free energy.

This analysis has been extended to study the effects of each base substituent group on the ΔSFE(Z-B) and their subsequent effect on Z-DNA stability. We found that the methyl group at the C5 position of thymine destablizes Z-DNA by 0.24 kcal/mol/dn, contrary to that of methylated cytosine. Removing the N2 amino group from the minor groove of guanine destabilizes Z-DNA by 0.6 kcal/mol/dn, while adding an amino group to adenine has a stabilizing effect of -0.6 kcal/mol/dn. By inference, mutation of the O6 keto oxygen of guanine to the amino group of adenine stabilizes Z-DNA by 0.08 kcal/mol/dn. These calculations have lead to a model for substituent effects on Z-DNA crystallization and subsequently to a predictive method for crystallizing hexamer sequences in the Z-DNA lattice. The crystal structures of various substituted Z-DNA sequences have provided molecular models for the predicted effects on substituent groups on solvent interactions with Z-DNA.

W-Pos1

RELAXATION OF SINGLE FROG FIBRES UPON PHOTOLYSIS OF THE CAGED CALCIUM-CHELATOR, DIAZO-2, IS SLOWED BY ADP

R.E. Palmer, I.P. Mulligan, S.J. Simnett and C.C. Ashley
University Laboratory of Physiology, Oxford OX1 3PT

Diazo-2 is a photolabile calcium chelator which upon photolysis rapidly (rate 2000 s^{-1}) changes from a chelator of low Ca^{2+} affinity (K_d 2.2 μM) to a chelator of higher affinity (K_d 0.073 μm) for Ca^{2+} (Adams *et al.*, 1989 *J. Am. Chem. Soc.* *111*, 7957-7968). We have used Diazo-2 to lower Ca^{2+} rapidly within single skinned fibres from the semitendinosus muscle of the frog, *Rana temporaria*, and investigate the effect of a high ADP concentration upon the rate of relaxation. A concentration of 6.4 mM free ADP led to an increase in the half time of relaxation from 73.5 ±5.9 ms (n=6) with no ADP, to 122.9 ±8.3 ms (n=7) ($P<0.05$, Student's t test). The size of the relaxation expressed as a percentage of P_{max} was the same in the two groups. The force transients were analyzed using a non-linear least squares regression technique (N.A.G. routine EO4FDF). This indicated that the curves consisted of two exponential phases.

Free [ADP] (mM)	Fast rate (s^{-1})	Slow rate (s^{-1})
0	11.0±0.31	0.53±0.07
6.4	7.9±0.45	0.54±0.08

The relative contribution of the two phases to the size of the relaxation was the same in the two groups.

These results suggest that ADP has a direct action on the contractile proteins prolonging relaxation in muscle, slowing the fast phase of relaxation by decreasing the rate of transition of crossbridges from a strongly-bound force generating state to a non force-generating state.

Supported by BHF, MDA and SERC. We are grateful to Drs. S.R. Adams and R.Y. Tsien for supplies of Diazo-2.

W-Pos2

KINETICS OF CARDIAC MUSCLE RELAXATION FROM RIGOR INITIATED BY LASER PHOTOLYSIS OF CAGED-ATP.

H. Martin and R.J. Barsotti, Bockus Research Institute, The Graduate Hospital, Philadelphia, PA 19146

Barsotti & Ferenczi (1988, J.Biol.Chem. 263:16750) reported the apparent rate constant for ATP-induced cross-bridge detachment in triton-skinned ventricular trabeculae of the guinea-pig to be 1 x 10^3 $M^{-1}s^{-1}$. This estimate was 2-3 orders of magnitude slower than that reported for similar experiments on skeletal muscle fibers (Goldman et al., 1984, J.Physiol. 354:577) and on cardiac acto-S1 (Seimankowski & White, 1984, J. Biol.Chem. 259:5045). In order to investigate the basis for this discrepancy skinned trabeculae were first incubated in a solution containing no ATP (I=200mM, pH 7.1, 23°C) to induce rigor tension and transferred into a solution containing 10mM caged ATP, 30 mM EGTA and < 2uM contaminating ADP. A pulse of light (347nm, 100mJ, 50ns) on average, released 0.9 mM ATP and resulted in the tension response shown in the figure below. After a 10ms lag, tension increased transiently before declining to the relaxed level, similar to the results reported previously by Barsotti & Ferenczi (1988). Treatment of the tissue with apyrase (20ug/ml) in a rigor solution for 30 min prior to photolysis of caged-ATP eliminated the transient rise in tension and significantly increased the final relaxation rate. The estimate of the apparent second order rate constant for ATP-induced cross-bridge detachment, following apyrase treatment was 2-5 x 10^4 $M^{-1}s^{-1}$ (n=13). These results indicate that in the absence of enzymatic treatment, a significant population of cross-bridges are in the AM·ADP state in cardiac trabeculae in rigor. These cross-bridges act to prolong the decrease in tension following the release of ATP.

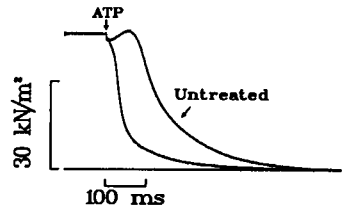

Supported by NIH grant HL40953 and AHA 88-09960.

W-Pos3

SHORTENING OF GLYCERINATED SKELETAL MUSCLE FIBERS INDUCED BY LASER FLASH PHOTOLYSIS OF CAGED ATP.

T. Yamada, O. Abe[1] and H. Sugi. Dept.of Physiol., Sch. of Med., Teikyo Univ., Itabashi-ku, 173 Tokyo, and [1]Zool. Inst., Fac. of Sci., Tokyo Univ., Bunkyo-ku, 113 Tokyo, JAPAN.

To study myofilament sliding coupled with ATP hydrolysis, we recorded shortening of single glycerinated rabbit psoas muscle fibers induced by photolysis of caged ATP. The relation between the amount of released ATP and the intensity of laser flash (10 ns, Nd:YAG laser, Spectra Physics) was determined chromatographically. The fiber was mounted between two glass rods. One rod was rigid while the other was very compliant, so that the fiber could shorten under a very small load (less than 1% of P_0). The fiber was first immersed in a rigor solution containing 2 mM caged ATP and 0.1 mM Ca^{2+}, and then the external solution was replaced by silicone oil to prevent diffusion of released ATP out of the fiber. The initial sarcomere length was adjusted to 2.4 μm. Muscle fiber shortening was recorded with a high speed video system (200 frames/s).

In response to a laser flash, the fiber shortening started after a delay (about 20 ms), reflecting the time for breaking of rigor linkages by the released ATP, and eventually stopped when ATP was used up for myofilament sliding. Video records showed that the fiber shortening was uniform along the entire length. Both the velocity and the distance of the ATP-induced shortening decreased with decreasing the amount of released ATP. The minimum uniform fiber shortening (2-4%) was observed with 50-100 μM ATP. Since the concentration of myosin head in the fiber is about 150 μM, this result suggests that myofilament sliding distance per hydrolysis of one ATP molecule might be 20-50 nm, if some cooperativity between the two myosin heads is taken into consideration.

W-Pos4

EFFECTS OF Ca^{2+} AND P_i ON TENSION TRANSIENTS INDUCED BY PHOTOGENERATION OF ADP IN SKINNED RABBIT PSOAS FIBERS.

Z. Lu, J.W. Walker and R.L. Moss, Department of Physiology, University of Wisconsin, Madison, WI 53706.

We have investigated the kinetic properties of the MgADP induced increase in isometric tension by photolysis of caged ADP (P^2-1(2-nitrophenyl)ethyl ADP) in skinned fibers from rabbit psoas muscle. Photogeneration of 500 μM MgADP increased active tension at all levels of Ca^{2+}, but the tension increase was greater at low Ca^{2+} (0.2 P_o, pCa 6.3) than at maximal Ca^{2+} (0.05 P_o, pCa 4.5). This is consistent with the effects of 500 μM MgADP on the steady state tension-pCa relationship (i.e., reduced steepness, 0.2 unit increase in pCa_{50}). The time course of the tension increase was approximately exponential with a rate constant, k_{ADP}, of 9.0 ± 0.3 s^{-1} (I=0.18 M, SL=2.5 μm, 15°C). k_{ADP} was not significantly different when the final [MgADP] was 200 μM, 500 μM or 5 mM. At submaximal Ca^{2+}, tension increases were more adequately fit by double exponentials and the response was dominated by the faster phase. The rate constant of the fast phase, k_{ADP}, decreased steadily from 9.0 ± 0.3 s^{-1} to 1.6 ± 0.2 s^{-1} as pCa was varied from 4.5 to 6.4. The rate constant of the slow phase was 1-2 s^{-1} at all pCa values. k_{ADP} was similar in rate and Ca^{2+} sensitivity to the rate constant of tension re-development, k_{tr}, measured under the same conditions by a rapid release and re-stretch procedure. Both k_{ADP} and k_{tr} increased 2-fold in the presence of 10 mM P_i when Ca^{2+} was either maximal or submaximal. Photolysis of caged ADP in fibers in rigor resulted in tension transients with very different properties. MgADP at 200 uM caused an exponential decline in rigor tension with a rate constant that was at least an order of magnitude greater than k_{ADP}, and that increased at higher [MgADP]. The results are consistent with the suggestion that MgADP increases isometric force by accumulation of actomyosin-ADP states resulting from ATP hydrolysis, rather than by reversal of the ADP dissociation process (Lacktis & Homsher, Biophys. J. 51:475a, 1987). The results further suggest that accumulation and/or recuitment of cross-bridges into force generating states occur via steps that are Ca^{2+} and P_i sensitive.

W-Pos5

THIN FILAMENT MODULATION OF CROSS-BRIDGE TRANSITIONS MEASURED BY PHOTOGENERATION OF P_i IN SKELETAL MUSCLE FIBERS. J.W. Walker, Z. Lu, D.R. Swartz and R.L. Moss, Department of Physiology, University of Wisconsin, Madison, WI 53706.

Steps in the cross-bridge cycle closely associated with P_i release were investigated by photolysis of caged P_i within skinned single fibers from rabbit psoas muscle. R and S isomers of 1(2-nitrophenyl)ethyl phosphate and a new compound, α-carboxy-2-nitrobenzyl phosphate, were used to address possible side effects of caged P_i. Photogeneration of P_i from all precursors caused a decline in active tension with an observed rate constant, k_{pi}, that depended on the final $[P_i]$. k_{pi} increased hyperbolically from 30 s^{-1} to 120 s^{-1} as P_i was increased from 0.8 mM to 12 mM. The effects of P_i are consistent with reversal of the P_i release step and with the suggestion that coupling between P_i release and force generation involves at least two steps (Millar & Homsher, Biophys. J. 57:397a, 1990). Variations in $[Ca^{2+}]$ had two effects on the P_i transient. k_{pi} decreased from 45 $\pm$ 3 s^{-1} to 17 $\pm$ 1 s^{-1} as Ca^{2+} activated tension was lowered from P_o to $0.1P_o$. Most of the decrease in k_{pi} occurred below $0.3P_o$ and could be detected only at $[P_i] < 1$ mM. The amplitude of the P_i transient decreased only 3-fold as Ca^{2+} activated tension was reduced from P_o to $0.1P_o$. For comparison, the rate constant of tension re-development (k_{tr}) was measured just after the P_i transient. k_{tr} was more influenced by Ca^{2+} than was k_{pi}, decreasing about 10-fold as Ca^{2+} activated tension was lowered from P_o to $0.1P_o$. P_i accelerated k_{tr} at both maximal and submaximal Ca^{2+}. At pCa 4.5, k_{tr} increased from 12 s^{-1} (0.5 mM P_i) to 20 s^{-1} (10 mM P_i), while at pCa 6.0, k_{tr} increased from 5 s^{-1} (0.5 mM P_i) to 9 s^{-1} (10 mM P_i) (see also, Metzger and Moss, 1991, this volume). The effects of Ca^{2+} on both k_{pi} and k_{tr} were significantly reduced following incubation of the fiber with 14 μM N-ethylmaleimide modified myosin S-1 for 10 min. This treatment is thought to increase the level of thin filament activation at low Ca^{2+} (Swartz and Moss, 1991, this volume). The results will be discussed in terms of a kinetic model in which steps associated with P_i dissociation from the actomyosin complex are influenced by the thin filament regulatory system.

W-Pos6

Phosphate and the kinetics of force generation in skinned skeletal muscle fibers. Joseph M. Metzger and Richard L. Moss. Dept. of Physiology, University of Wisconsin, Madison, WI. 53706. We investigated the basis of the Ca^{2+}-sensitivity of the rate constant of tension redevelopment (k_{tr}; Brenner, PNAS 85: 3265-3269, 1988) following release and re-extension of length in steadily Ca^{2+} activated skinned fibers obtained from rabbit fast psoas and rat fast s. vastus lateralis and slow soleus muscles. k_{tr} is thought to be a manifestation of the transition of cross-bridges from detached and/or weakly attached states to the strongly bound, force generating state in the actin-myosin ATP hydrolysis reaction. Previous findings suggest that the force generating step is closely associated with the release of phosphate from the actin-myosin complex (Hibberd et al. Science, 228: 1317, 1985). Thus, we examined effects on the Ca^{2+}-sensitivity of k_{tr} due to variations in the concentration of phosphate between 0.2 mM and 30 mM. Increased concentration of phosphate 1) depressed maximum tension and the Ca^{2+} sensitivity of tension and 2) increased k_{tr} at both maximal and submaximal levels of Ca^{2+} activation. In psoas fibers at pCa 4.5, k_{tr} was 16.6±0.6 s^{-1} in zero added phosphate and 55.8±3.6 s^{-1} (n = 5) in 30 mM phosphate. At pCa 6.0, k_{tr} increased from 10.8±0.6 s^{-1} in zero added phosphate to 27.9±3.8 s^{-1} (n = 5) in 30 mM phosphate. At each pCa, the increase in k_{tr} was not linear with phosphate concentration but showed saturation at 30 mM phosphate. Half-maximal acceleration of k_{tr} was observed at about 5 mM added phosphate. Similar results were obtained from rat fast and slow fibers although k_{tr} values were 8-10 fold smaller in slow fibers. These results indicate that k_{tr} is coupled to the phosphate release step at both maximal and submaximal concentrations of Ca^{2+} and support the hypothesis that one or more of the steps in the transition of cross-bridges to the force generating state are Ca^{2+} sensitive. The saturation phenomenon observed at high concentrations of phosphate suggests that force generation may be more closely associated with isomerization steps rather than phosphate dissociation from the cross-bridge.

W-Pos7

Velocity of shortening and phosphate in single skeletal muscle fibers and isolated ventricular myocytes. Joseph M. Metzger and Richard L. Moss. Department of Physiology, University of Wisconsin, Madison WI 53706.

The influence of increased concentration of phosphate upon velocity of shortening was examined in rabbit psoas skinned single skeletal muscle fibers and ventricular myocytes isolated from the rat. In psoas fibers activated at maximal Ca^{2+} (180 mM ionic strength; 4 mM MgATP; 1 mM free Mg^{2+}; 20 mM imidazole; 14.5 mM creatine phosphate; pH 7.00; temperature 15°C), added phosphate (10 to 30 mM) had no effect on unloaded shortening velocity as determined by the slack test technique. In psoas fibers and ventricular myocytes, force-velocity data obtained during isotonic releases indicated there was a slight increase in V_{max} in the presence of added phosphate. In psoas fibers activated at submaximal concentrations of Ca^{2+} in the absence of added phosphate, plots of slack length versus duration of unloaded shortening were biphasic consisting of an initial high velocity phase of shortening and subsequent low velocity phase as described previously (Moss, J. Physiol. 377:487, 1986). The appearance of a length dependent decrease in velocity is hypothesized to result from an abrupt increase in internal load due to cross-bridges that bear a compressive or negative load which impedes filament sliding. Interestingly, in the presence of added phosphate biphasic slack tests were no longer evident. This result was obtained in control psoas fibers over a range of submaximal Ca^{2+} concentrations and in maximally Ca^{2+} activated fibers which were first treated to partially extract troponin C. Thus, under various conditions which favor the appearance of biphasic shortening, added phosphate abolished the low velocity component. Our findings may be explained if phosphate binds to cross-bridges in a strain-dependent manner, which reverses formation of highly strained, compressed cross-bridges.

W-Pos8

EFFECT OF MgADP ON PRESSURE-INDUCED TENSION TRANSIENTS IN SKINNED RABBIT PSOAS FIBRES. N.S. Fortune, M.A. Geeves[#] & K.W. Ranatunga. (Intr. by H. Gutfreund) [#]Departments of Biochemistry & Physiology, University of Bristol, Bristol, UK.

ADP has been shown to increase maximally Ca-activated isometric tension in rabbit psoas fibres by upto 30% (Cooke & Pate Biophys.J.58 p789, 1985). We have previously reported that increased hydrostatic pressure (upto 10 MPa) results in an 8% reversible reduction in active tension. The magnitude of this tension depression is lowered by the presence of 11 mM MgADP (6% Fortune et al. J.Musc.Res.Cell.Motil. 10 p113, 1989). A rapid reduction in pressure (<1 ms) results in a 3 phase tension response; phase I is a decrease in tension in phase with pressure release, phase II is a quick recovery of tension at $17s^{-1}$ and phase III is a slower recovery at $3s^{-1}$. The addition of 11 mM MgADP had little effect on phase I, but reduced phase II by 15% and phase III by 30%.

A pressure-induced increase in rigor tension has been fully reported by Ranatunga et al. (Biophys.J. 58 p1,1990). A single step decrease in tension, similar to the first recovery event seen in the active fibre, was observed following pressure release. The addition of 2mM MgADP to a rigor fibre (in the presence of hexokinase/glucose to remove contaminating ATP) caused a 10% decrease in tension which was fully recoverable on removal of nucleotide. The presence of MgADP had no effect on the mechanical response of the fibre

W-Pos9

THE INTERACTION OF WILD TYPE AND MUTANT DROSOPHILA ACTIN WITH RABBIT MYOSIN SUBFRAGMENT 1 IN SOLUTION. M.A. Geeves[#] D.R. Drummond[*], E.S. Hennessey[*] & J.C.Sparrow[*].(Intr. by J.J. Holbrook) [#]Department of Biochemistry, University of Bristol, Bristol, UK., and [*]Department of Biology, University of York, York, UK.

An actin mutant, G368E, of Drosophila flight muscle produces normal myofibrillar structure. G368E flies are only partially flighted and mechanical measurement of skinned fibres show a reduced rate constant for delayed tension generation. Actin was purified from the flight muscles of wild type G368E flies and their interaction with rabbit myosin subfragment 1 was investigated in vitro and compared to rabbit actin. The dissociation constant (K_d) was measured in a titration experiment. A stopped flow apparatus was used to measure the rate of association of actin with S1 (k_{on}); the rate of actin displacement from the acto.S1 complex by an excess of fluorescently labelled rabbit actin (k_{off}); the rate of ATP induced dissociation of acto.S1 (k_{ATP}) and the affinity of ADP for acto.S1 by competition with ATP binding(K_{ADP}). The results are summarized below.

EXPT	RABBIT	WILD TYPE	G368E
k_{on} ($\mu M^{-1}s^{-1}$)	2.64	1.77	1.54
k_{off} (s^{-1})	0.098	0.11	0.27
K_d (μM)	0.037	0.11	0.17
k_{ATP} ($\mu M^{-1}s^{-1}$)	2.77	2.80	2.61
K_{ADP} (μM)	178	152	179

This work supported by The Royal Society (MG) and SERC (DRD, ESH, JCS).

W-Pos10

MYOSIN HEAD ORIENTATION IN NEGATIVELY STRAINED CROSSBRIDGES. AN EPR STUDY.

Piotr G. Fajer, Paul Johnson and David D. Thomas, Institute of Molecular Biophysics, Florida State University. Tallahassee, and Biochemistry, University of Minnesota, Mpls.

We have examined the orientation of spin labelled myosin heads in rabbit psoas fibers under mechanical stress. The muscle fibers were labeled with maleimide and iodoacetamide spin labels and their perdeuterated derivatives, in order to increase orientational resolution. Pulling on a bundle of fibers in rigor with forces of 0.1-0.3 kg/cm^2 did not change the orientation of the deuterated or protonated spin labels (IASL, MSL, d-IASL and d-MSL) as was found before by Cooke (1981) for IASL. In order to change the direction of applied force we have used the protocol developed by Goldman *et al.* (1988). The compressive force was generated by stretching passive elastic components of muscle in the presence of ATP. Removal of ATP results in attachment of crossbridges in the positions of least strain. The fiber bundles were then slackened to about 20% of the original resting tension, putting compressive tension on the rigor crossbridge. The crossbridges resisted the compression without being torne off as shown by steady and persisting levels of tension and sarcomere length. The EPR spectra recorded before and after the slack were virtually indistinguishable for both IASL and MSL. Since EPR is sensitive to rotation of spin label about any axis, this result is inconsistent with significant changes in fluorescence polarization of muscle fibers labeled with iodoacetemide rhodamine as observed by Burghardt and Ajtai (1989). We confirmed our result at seven-fold higher compressive forces by stretching to long sarcomere lengths (3.4 μm). In order to increase the sensitivity of the EPR to the orientational distribution we used deuterated spin labels, which have narrower linewidths and thus any changes are more easily observed. However, as before there was no difference between the spectra of resting and negatively strained rigor crossbridges. We conclude that the orientation of spin labels attached rigidly to the myosin head does not vary with either positive or negative force by more than 5°.

W-Pos11

FORCE-VELOCITY RELATIONSHIPS IN SINGLE VENTRICULAR MYOCYTES: EFFECT OF ß ADRENERGIC STIMULATION.

Nancy K. Sweitzer and Richard L. Moss. Department of Physiology, University of Wisconsin, Madison WI.

Stimulation of cardiac muscle by ß adrenergic agonists has been shown to increase cross-bridge cycling rate (Hoh et al. Circ Res 62:452, 1988). We have developed a single ventricular cell preparation with intact, coupled receptors, allowing us to determine the effect of ß stimulation on the force-velocity relationship. Enzymatically isolated rat ventricular myocytes were permeabilized using α hemolysin (a.k.a. α toxin), a staphylococcal toxin which acts by self-associating into pentameric "pores" in foreign cell membranes. While detergent skinning has been shown to uncouple receptors from their intracellular effectors, α hemolysin permeabilized cells contain functional receptors (Kitazawa et al. JBC 264:5339 1989). Force was clamped at a level below maximal within 5 ms using a diode switching network. Following ß stimulation of single myocytes by isoproterenol, shortening velocity is increased at all loads (see figure), a response which is reversed by propranolol. The increase in cycling rate may thus be attributed, at least in part, to an increase in the rate of detachment of cross-bridges. Second messengers involved in the increase in velocity, as well as its dependence on the myosin isozyme composition of the myocyte, will also be discussed.

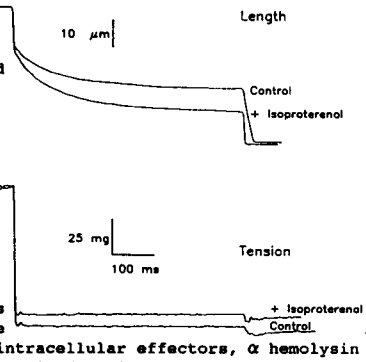

W-Pos12

THE APPARENT RATE CONSTANT FOR THE DISSOCIATION OF FORCE GENERATING MYOSIN CROSSBRIDGES FROM ACTIN DECREASES DURING Ca^{2+} ACTIVATION OF SKINNED CARDIAC MUSCLE FIBERS. Mei Z. Zhang[*], Michael Sama[#], Gang Wang[#], Phyllis E. Hoar[#], and W. Glenn L. Kerrick[*#] Depts. of [*]Mol. & Cell. Pharm. and [#]Physiol. & Biophys., Univ. of Miami Sch. of Med., Miami, FL.

The effect of Ca^{2+} activation on the apparent rate constant governing the dissociation of force generating myosin cross-bridges was studied in skinned rat ventricular muscle at 21 ± 1 °C. Simultaneous measurements of Ca^{2+}-activated isometric force and ATPase activity where conducted. The Ca^{2+} activation of isometric force occurred at approximately two times higher Ca^{2+} concentration than did actomyosin ATPase activity at 2.0 mM MgATP. According to the model of Huxley (1957) and assuming the hydrolysis of one molecule of ATP per cycle of the cross-bridge, the apparent rate constant g_{app} for the dissociation of force generating myosin cross-bridges is proportional to the actomyosin ATPase/isometric force ratio. This measure of g_{app} shows greater than a 5 fold decrease during Ca^{2+} activation of isometric force. This change in g_{app} is responsible for separation of the Ca^{2+} sensitivity of the normalized ATPase activity and isometric force curves. If the MgATP concentration is reduced to 0.5 mM, the change in g_{app} is reduced and consequently the difference in Ca^{2+} sensitivity between normalized steady state ATPase and force is also reduced.

Supported by the American Heart Association (Florida Affiliate) and the Muscular Dystrophy Association.

W-Pos13

THE SENSITIVITY OF THE MYOFILAMENTS TO CALCIUM CORRELATES WITH THE RELATIVE PROPORTIONS OF TROPONIN T ISOFORMS IN RABBIT MYOCARDIUM, Page A.W. Anderson, Rashid Nassar, Nadia N. Malouf*, Michael B. Kelly and Annette E. Oakeley, Departments of Pediatrics and Cell Biology, Duke University, Durham, NC 27710, *Department of Pathology, University of North Carolina at Chapel Hill, NC, 27514

We have previously demonstrated that in rabbit myocardium several isoforms of troponin T are expressed (TnT1 - TnT5) and that their proportions change with development. In this study we measured the force-calcium relationship and the troponin T isoform content from 11 ventricular strands of rabbits 2 to 5 days old. The preparations were skinned with Triton-X and the force developed was measured at pCa 4.5 - 9 at a sarcomere length of 2 to 2.4 μm. The data from each strand were fitted with the Hill equation using non-linear regression and the pCa_{50} and Hill coefficient were determined. The proteins from each strand were separated, using SDS-PAGE. The TnT isoforms were identified on Western blots using a cardiac-specific monoclonal antibody Mab 13-11. The proportions of each TnT isoform were calculated from densitometric scans in terms of the total TnT content. The slope of the pCa_{50} vs. %TnT2 least squares regression line was .02 pCa units/%TnT2 ($p < .02$). These results suggest that the sensitivity of the myofilaments to calcium is related to the TnT isoforms in the myofilaments. Moreover, they suggest that structural differences in TnT domains, which may exist among TnT isoforms, should be identified and their functional effects tested more directly.

W-Pos14

COMPARISON OF SARCOMERE LENGTH AND MYOCARDIAL STRAIN IN RAT TRABECULAE. *Tusha S. Hoskere, Pieter P. de Tombe, William C. Hunter. Department of Biomedical Engineering, The Johns Hopkins University.*

We compared sarcomere length (SL) measured by the laser diffraction technique (LD) to that estimated from myocardial tissue strain (MS), measured by motion of internal markers. The markers were 9 μm diameter microspheres, which were injected into the perfusion line of an excised rat heart and subsequently lodged in the capillaries. Thin trabeculae were then dissected and mounted in a chamber perfused with a modified Krebs-Henseleit solution. Images of a marked trabecula obtained via video microscopy were input to a tracking system, which determined the spatial coordinates of any marker. At different stretches, we compared the positions of three markers (forming a triangle ≈100 μm on a side) to their positions in a reference state, to obtain the strain tensors describing each state of stretch. Using the strain in the fiber direction and the SL measured by laser in the reference state (2 μm), we obtained the SL predicted by the myocardial strain.

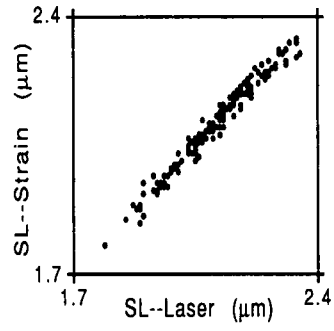

The figure compares the strain-derived SL to that measured simultaneously by laser diffraction for nine passive trabeculae. The linear relationship between the two fell on the line of identity (SL_{MS}= .99 SL_{LD} + .01; R^2 = .97). The agreement between these independent techniques supports the use of myocardial strain to estimate in-vivo sarcomere lengths in other preparations which are too thick for laser diffraction.

W-Pos15

FORCE YIELD IN ACTIVE SOLEUS MUSCLES AND SKINNED SOLEUS FIBERS AND PAPILLARY MUSCLES IN THE CAT AND RAT.

J.G. Malamud, R.R. Lee, P.J. Nichols and T.R. Nichols, Department of Physiology, Emory University, Atlanta, GA 30322.

Force yield is a sudden decline in the stiffness of a contracting muscle during a lengthening contraction such that during further stretch the force stops increasing or even decreases. This phenomenon has been observed in the electrically stimulated cat soleus muscle (Joyce, et al., J.Physiol. 204, 461-474 (1969)), which is composed largely of type S muscle fibers.

We have observed force yield in stimulated rat and cat solei for initial lengths, stimulation rates and stretch velocities spanning the physiological range of these variables. However, active gastrocnemius muscles, which are heterogeneous in fiber type, exhibited a modest reduction in stiffness during stretch but not a force yield. To investigate the cellular mechanisms underlying force yield, we delivered stretches to chemically skinned fibers from the following muscles: soleus and gastrocnemius (superficial part) of the cat and rat, and rabbit psoas. Parallel studies were performed on chemically skinned rat papillary muscles. Among the skeletal fibers, force yield was observed only in the soleus muscle and occurred over a wide range of calcium levels, initial lengths and velocities of stretch. We conclude that force yield results from nonlinear properties of the contractile apparatus rather than from architectural features of whole muscle or from the excitation-contraction coupling mechanism, and that it is present over a wide range of physiologically relevant operating conditions.

The responses of skinned papillary muscles were dominated by a large "passive," elastic response, but the subtraction of this passive component revealed a force yield in the active component of the responses. While force yield in the soleus muscle is compensated in the intact animal by spinal reflex mechanisms, it is masked by "passive" mechanical properties in cardiac muscle. We are currently testing whether yield is present in identified type S fibers of gastrocnemius muscles.

(supported by NS20855, the Georgia Heart Association and the University Research Fund of Emory University)

W-Pos16

LOAD DEPENDENCE OF RELAXATION IN RAT MYOCARDIUM IS ATTENUATED BY NIFEDIPINE Michael R. Berman[1,2] and Lynn E. Dobrunz[2], Departments of Anesthesiology/Critical Care Medicine[1] and Biomedical Engineering[2], Johns Hopkins University, Baltimore MD 21205.

A dose dependent and reversible attenuation of load dependence of relaxation by volatile anesthetics (VA) has been demonstrated in mammalian cardiac muscle (Anesth 69:464, 1988). This raises the possibility that VA may directly effect sarcoplasmic reticulum (SR) function. However, care need be taken to distinguish a direct effect of VA on SR from the effect on SR of reduced $[Ca^{2+}]_i$ alone (Pflug Arch 401:368, 1984). We examined the effect of $[Ca^{2+}]_i$ on SR function by measuring its effect on load dependence of relaxation. Rat right ventricular papillary muscles (n = 6) were placed in a muscle chamber superfused with a solution at 37° C consisting of (in mM) NaCl 108, KCl 5, $MgCl_2$ 1, $CaCl_2$ 2.5, $C_2H_3NaO_2$ 20, HEPES 5, and dextrose 10, at pH 7.4, bubbled with 100% O_2. Muscles were stimulated (0.2 PPS) to contract isometrically during initial equilibration; length was set to maximize twitch force while maintaining the total to diastolic force ratio > 4. Load clamps of 90% to 10% of active force were applied with ≥ 5 isometric twitches interposed between each clamp. Load dependence of relaxation was analyzed as described by Housmans and Murat (Anesth 69:464, 1988). Load clamps were repeated after the sarcolemmal calcium channel blocker nifedipine (0.01-10 μM in 7-10 steps) was added to the superfusate to reduce $[Ca^{2+}]_i$ while exerting no known direct effect on SR. Nifedipine reduced twitch force and load dependence of relaxation in a dose dependent manner. Twitch force was reduced by 50% and load dependence of relaxation was virtually obliterated by ≈ 1 μM nifedipine. Load dependence of relaxation is an indicator of SR function; its attenuation suggests derangement of SR function. Since nifedipine only reduces $[Ca^{2+}]_i$, we conclude that a reduced $[Ca^{2+}]_i$ by itself deranges SR function. A major action of VA is to reduce $[Ca^{2+}]_i$; we suggest that some or all of the reported effect of VA on load dependence of relaxation reflects lowered $[Ca^{2+}]_i$ rather than a direct effect of VA on SR function.

Supported by USPHS grant HL 38488 to MRB.

W-Pos17

IS THE TIME COURSE OF LIGHTLY LOADED SHORTENING OF CARDIAC MYOCYTES SIMILAR TO THAT OF ISOMETRIC FORCE DURING TWITCH CONTRACTIONS? Sanjay Parikh and Leslie Tung, Department of Biomedical Engineering, The Johns Hopkins University, Baltimore, MD 21205.

Indices of cardiac contraction at the cellular level have been limited primarily to unloaded shortening, which is used as a measure of contractile force. However, a comparison of the unloaded shortening and isometric force in the *same* cell has not yet been made. In this study we have approximated unloaded shortening by lightly loaded shortening and compared it to isometric force in the same cell. Cardiac myocytes were obtained by enzymatic dissociation of frog ventricle and mounted on an optical fiber force probe. By adding piezoelectric actuators, we have devised a method whereby the mechanical load presented to the cell can be controlled electronically. A ten-fold drop in the cell force amplitude can by achieved by allowing the cell to shorten by ~12% of its resting length. The figure below shows that for twitch contractions, the time course of cell shortening under near zero load conditions is similar to that of cell force under isometric conditions. These results suggest that the internal load of frog cardiac myocytes is elastic and are consistent with data from studies of whole muscle which indicate that the rate of relaxation in the frog heart is independent of load and is determined by the kinetics of Ca^{2+} uptake.

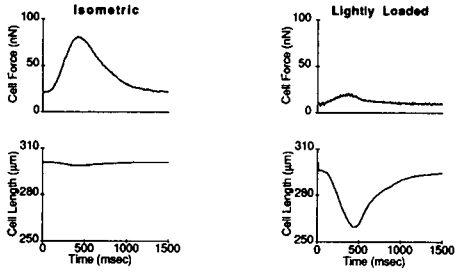

W-Pos18

CARDIAC MYOCYTES DRIVEN IN A PHYSIOLOGICAL LOADING SEQUENCE - THE CELLULAR EQUIVALENT OF A PRESSURE-VOLUME LOOP. Sanjay Parikh and Leslie Tung, Department of Biomedical Engineering, The Johns Hopkins University, Baltimore, MD 21205.

Myocardial contractility has been studied in isolated muscle preparations with loading patterns which mimic those normally experienced *in situ* in the whole heart. However, studies of contraction in isolated cardiac myocytes have been limited to one of 3 external loading conditions: zero load (unloaded shortening), auxotonic, or isometric. We have developed a system that allows us to sequence different loading conditions over the course of a single beat. The force of contraction of the cell is monitored using an optical fiber cantilever, while the shortening pattern of the cell is controlled by piezoelectric bimorph actuators. This system allows us to drive the myocyte through a physiological cycle of contraction: (1) At the start of contraction the cell is held "isometric" (cell shortening ≤1%) at its end diastolic length (↔ isovolumic contraction in the whole heart). (2) When force reaches a set level of afterload, the cell is allowed to shorten isotonically or auxotonically (↔ cardiac ejection). (3) Starting at the instant of peak shortening, the cell is held isometric at the shortened length until contractile force has decayed (↔ isovolumic relaxation). (4) Finally, the cell is stretched back to its original end diastolic length (↔ diastolic filling). A typical force-length loop obtained with this loading sequence is shown for a frog ventricular myocyte and resembles the pressure-volume loop measured in the intact ventricle. The straight line on the right corresponds to an isometric contraction obtained in the same cell at the same end-diastolic length.

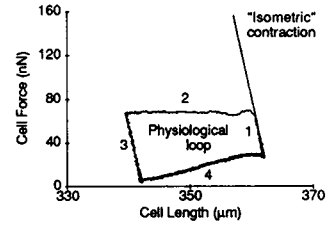

W-Pos19

EFFECTS OF CALCIUM AND 2,3-BUTANEDIONE MONOXIME ON NON-WORK-RELATED OXYGEN CONSUMPTION IN ISOLATED HEARTS.

Pieter P. de Tombe, Daniel Burkhoff, William C. Hunter. Department of Biomedical Engineering, The Johns Hopkins University, Baltimore, Maryland.

For all inotropic agents tested to date, there has been a direct relationship between the level of contractility and the oxygen consumption of unloaded hearts that are not generating pressure. Thus, negative inotropic agents "save" oxygen (i.e., they reduce the non-work-related oxygen consumption), presumably as a result of decreased calcium cycling. 2,3-Butanedione monoxime (BDM), on the other hand, has been shown to reduce myofilament force developement in isolated cardiac muscle even when intracellular calcium levels were maintained. It would therefore be expected that BDM could reduce contractility without reducing the non-work-related oxygen consumption. We tested this hypothesis by measuring non-work-related oxygen consumption in 5 isolated, blood-perfused canine hearts. Contractility was increased by infusing calcium chloride and subsequently reduced by BDM infusion (1-10 mM). At each contractile state we measured non-work-related oxygen consumption and contractility, which was expressed as the isovolumic pressure developed at a fixed volume. Unexpectedly, the relationship between non-work-related oxygen consumption and contractility was similar for both calcium chloride and BDM infusion. (A similar result was also observed in crystalloid perfused rat hearts.) These results suggest that the primary effect of BDM in the intact heart is to reduce intracellular calcium levels, rather than to reduce the calcium sensitivity of the myofilaments.

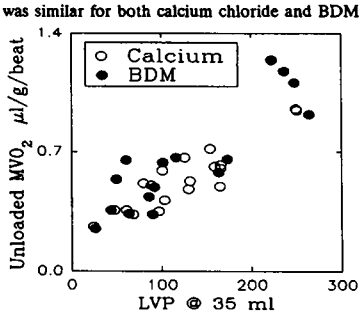

Supported by the Maryland Heart Association

W-Pos20

THE TIME COURSE OF MECHANICAL EFFICIENCY DURING AFTERLOADED CONTRACTIONS IN ISOLATED CARDIAC MUSCLE. Jon N. Peterson and Norman R. Alpert, Dept. of Physiology & Biophysics, The Univ. of Vermont College of Medicine, Burlington, Vermont 05405.

Previous studies of mechanical efficiency in cardiac muscle have yielded a single value for each twitch. This value, generally obtained by dividing peak work by the total enthalpy (work + heat) developed during a twitch, does not provide insight into how efficiency evolves as a function of time during a single contraction as the muscle performs work. By using a high speed, vacuum deposited metal film thermopile, we are in a position to consider the time course of heat evolution during a single twitch. The present study examines the time course of mechanical efficiency during working contractions in rabbit papillary muscle at 21°C, where efficiency is computed as the ratio of time resolved muscle work and enthalpy. Enthalpy as a function of time is computed as the sum of initial heat evolved and muscle work. Efficiency is found to remain relatively constant during the working portion of the twitch, where the muscle is contracting against a constant load. As afterload was decreased, efficiency increased to 65 ± 11% (mean ± SEM, n = 3) at 10% P_0 (P_0 = peak isometric force). This is in contrast to muscle work, which reached a peak of 3.0 ± 0.3 mJ/g (n = 6) at 50% P_0. This 65% efficiency represents the lower limit of cross-bridge (X-Br) efficiency, since our value of work underestimates X-Br work and initial heat overestimates X-Br heat by including non X-Br related processes. (Support: PHS T32-07647)

W-Pos21

THE LIMIT OF REVERSIBLE EXTENSION IN RESTING ISOLATED CARDIAC MUSCLE CELLS.

Kenneth P. Roos, Hans Poggemeyer, Allan J. Brady
Cardiovascular Research Lab, Department of Physiology, UCLA School of Medicine, Los Angeles, CA. 90024-1760.

In general, stretch of cardiac muscle much past the plateau of the length-tension relation results in structural damage. We have reevaluated this characteristic finding of multicellular preparations in single cells enzymatically isolated from adult rats. Detergent skinned myocytes in relaxing solution are attached to a perturbator and force transducer with double barrelled glass pipettes. A 70Hz index of oscillatory stiffness is measured and sarcomere length (SL) is concurrently monitored to assess striation pattern uniformity with a 240Hz video system (Roos & Parker, Proc. SPIE 1205:134, 1990). Attached cells are slowly stretched above slack length in small steps determined by the magnitude of stiffness increase and the half time of stress relaxation. From slack length (SL $\simeq$ 1.90μm) to SL $\simeq$ 2.40μm, oscillatory stiffness and the half time of stress relaxation increase rapidly for small step increases in length. In this range, the standard deviation of SL (striation pattern uniformity) is largely maintained. The half times of stress relaxation and the step increases in stiffness peak at a SL $\simeq$ 2.40μm, then rapidly decline to a stable level near that of slack length. When cells are stretched beyond SL's $\simeq$ 2.40μm, the standard deviation of sarcomere lengths dramatically increases with regional distortions in the striation pattern uniformity. These data suggest 1) that there is a significant cellular component to cardiac muscle's resistance to overextension, and 2) that this longitudinal component is probably irreversibly damaged when the cell is stretched beyond $\simeq$ 2.40μm.

Supported by NIH HL-29671 (KPR).

W-Pos22

EVIDENCE FOR THE EXISTENCE OF ENDOTHELIAL FACTORS REGULATING CONTRACTILITY IN RAT HEART

G. McClellan, A. Weisberg and S. Winegrad, Dept. of Physiology, University of Pennsylvania, Phila., PA

Force developed by isolated papillary muscles or trabeculae taken from the endocardial surface of mammalian hearts decreases as the cross-sectional area increases. The basis for this decline in force is not clear but diffusion of oxygen into the relatively thin bundles should not be limiting. Similar observations of the decline of maximum Ca-activated force with increasing cross-sectional area of detergent skinned trabeculae or papillary muscles have been attributed to the accumulation of inorganic phosphate, a known depressant of force development, in the center of the bundle of cells. The limitation of diffusion of oxygen into the intact bundle and the limitation of diffusion of P_i outward in the skinned bundle would result in the lowest level of activity being in the center of the bundle. We have used quantitative histochemistry to measure Ca- and actin-activated myosin ATPase activity in cryostatic sections of rapidly frozen trabeculae to determine if this occurs. The technique is very sensitive and has sufficient spatial resolution to resolve individual myofibrils. Trabeculae were isolated from the endocardial surface of the right ventricle of young rats (containing > 90% alpha myosin heavy chain) and suspended with continuous measurement of force. At different times after dissection, the trabeculae were quickly frozen, transversely sectioned and Ca- and actin-activated myosin ATPase measured in serial sections both without and with 1 uM cAMP in the assay solution. In every one of over 40 trabeculae studied, there was a gradient of actin-activated ATPase activity of myosin from the center outward, and the most superficial cells had very low enzymatic activity. Cyclic AMP markedly decreased the gradient by raising the enzymatic activity of the more superficial cells. Ca-activated myosin ATPase was always uniform across the transverse section. These observations are incompatible with a limitation of diffusion of oxygen into the trabeculae or of an inhibitory factor out of the trabeculae. The results are, however, consistent with the production of a regulatory factor that inhibits cross-bridge attachment to the thin filament by endothelial cells lining the endocardial surface of the trabeculae. Endocardial regulation of contractility has been proposed by Brutsaert and co-workers. (Supported by NIH grant HL-33294)

W-Pos23

MECHANISM OF CARDIAC INOTROPY BY PHENAMIL, AN AMILORIDE DERIVATIVE. Guia, A., T. Chau, E. J. Cragoe Jr., R. Bose, and D. Bose, Depts. of Pharmacology, Internal Medicine & Anesthesia, Univ. of Manitoba, Winnipeg, Manitoba, Canada R3E 0W3.

Amiloride, a potassium-sparing diuretic, has multiple cellular actions, such as blockade of Na channels, Na-Ca exchange, and Na-K ATPase. Amiloride has a potent relaxant effect on smooth muscle, and a positive inotropic effect on cardiac muscle. Through the use of several analogues of amiloride with more specific actions, it has been postulated that amiloride relaxes smooth muscle mostly through Na channel blockade, while in cardiac muscle, Na-Ca exchange blockade results in positive inotropy. Phenamil, an analogue with greater specificity for Na channel blockade, is the most potent smooth muscle relaxant among the amiloride analogues, yet paradoxically it produces positive inotropy in the heart. This study was intended to elucidate the mechanism by which phenamil produces positive inotropy. Thin canine ventricular trabeculae (< 1 mm diam.) were isometrically suspended in Krebs Henseleit solution (37°C; pH 7.3) and stimulated at 0.5 Hz by field stimulation at a voltage 50% above threshold. Phenamil had an appreciable positive inotropic effect only at concentrations greater than 30 μM. This differs from smooth muscle where a concentration of 30 μM produces pronounced relaxation. 60 μM phenamil increased steady state contractions to 227% of control. In biphasic contractions, obtained by replacing 90% of external Ca^{2+} with Sr^{2+}, P2, the second phase of contraction, reflects trans-sarcolemmal divalent cation influx, and P1, the first component, indicates the sarcoplasmic reticular release of Ca^{2+}. Since phenamil (60 μM) increased P2 whereas β agonists preferentially increase P1, phenamil's effect does not match a β adrenergic agonistic profile. Furthermore the potentiation of post-rest contractions seen in untreated tissues, was reduced by phenamil. The above pharmacological effects are also shared by Na pump inhibitors, such as ouabagenin. Relaxation by restoring K+ in K+-deprived canine portal vein is an indicator of Na pump activity and can be blocked by ouabagenin. Phenamil (60 μM) did not inhibit the Na pump in this system. Furthermore, a high concentration of phenamil (120 μM) did not cause an increase in baseline tension of the isolated canine trabeculae, whereas ouabagenin produced aftercontractions, often associated with an increase in diastolic tension. In conclusion, the positive inotropic actions of phenamil are different from those of β adrenoceptor agonists or of Na pump inhibitors. (Supported by MHRC and MRC of Canada)

W-Pos24

CARDIAC HYPERTROPHY MODIFIES POST-REST CONTRACTILITY OF FERRET VENTRICULAR MUSCLE. S. Baudet, J. Noireaud & C. Léoty. Lab. Gen. Physiol, URA CNRS 1340, Nat. Vet. Sch., 44087 NANTES CEDEX 03, France (intr. by M. M. REDDY).

In mammalian ventricular muscle, the amplitude of the first contraction after a period of quiescence (post-rest contraction (PRC)) is thought to be relatively dependent on the sarcoplasmic reticulum (SR) calcium (Ca) load (Bers, Am. J. Physiol. 248: H366-H381, 1985). As intracellular Ca regulation is modified during cardiac hypertrophy, post-rest contractility studies in control (C) and hypertrophied (H) ventricular muscle may be useful to localize the site(s) involved in defective Ca handling. At a stimulation frequency of 0.1 Hz, in 3 mM external [Ca] and at room temperature, steady-state (SS) twitch amplitude of ferret right ventricular, pressure-overloaded papillary muscles (n=4) was decreased compared to C (n=5) (3.5±1.5 mN/mm² *vs* 17.8±2.4 mN/mm²; mean±SD, respectively; P<0.001). The figure shows that for rest periods >10s, PRC amplitude was potentiated compared to SS contractions in C and H muscles. Maximal twitch amplitude was 21.6±1.2 mN/mm² and 6.8±3.1 mN/mm² and occured at 60s and 120s of quiescence in C and H muscles respectively. However, relative to SS contractions, PRC amplitude potentiation was greater in the H group compared to the C: maximal potentiation was 74±35% in H *vs* 19±19% in C (P<0.001). In both groups, after peak potentiation has occured, PRC amplitude decayed exponentially. However, the time constant of PRC decline was increased in H muscles (1203±99s) than in C (550±55s; P<0.001). Assuming that twitch force is indicative of SR Ca content, then the depressed SS force in H may be partly due to a decreased SR Ca load and/or a lower fraction of Ca release. However, during rest, the H SR may accumulate and maintain a greater fraction of Ca in the SR. The higher relative potentiation and the slower rest decay may be indicative of a decreased SR Ca leak or depressed Ca extrusion through the sarcolemmal sodium/calcium exchanger.

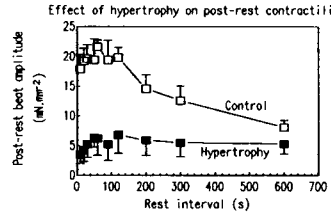

W-Pos25

HISTOLOGICAL AND IMMUNOCYTOCHEMICAL ASSESSMENT OF WHOLE MUSCLE TRANSPLANTS IN A MURINE MODEL FOR MUSCULAR DYSTROPHY.

Cheri Mechalchuk, Joy Wee, William Ovalle and Bernard Bressler, Department of Anatomy, University of British Columbia, Vancouver, B.C., Canada.

The mdx mouse mutant, an animal model for x-linked Duchenne Muscular Dystrophy lacks the sub-sarcolemmal protein, dystrophin. The extent to which muscle environment influences dystrophin expression was assessed through a series of extensor digitorum longus (EDL) transplants in 4-week-old mdx mice and their normal controls. Orthotopically (EDL replaced into the same animal) and heterotopically (EDL muscles exchanged between mdx and normal mice) transplanted muscles were initially immersed in marcaine for 20 minutes to destroy mature muscle fibers, while leaving an intact myoblast population. Regenerating muscles and their left hindlimb controls were processed through conventional histological, histochemical and immunocytochemical staining (for dystrophin and neonatal myosin) at different stages of recovery.

Two-week transplants exhibited a high degree of neonatal staining and little differentiation between fiber types. Older regenerates demonstrated progressively less neonatal staining with increasing cell size and fiber-type differentiation. Dystrophin staining was positive in muscle fibers of all normal regenerates, while it was not seen in the mdx regenerates. Of particular note was the sustained presence of dystrophin at the 20-week post-surgical stage in normal EDL transplanted into an mdx host. Further experiments are to be conducted to determine whether long-term survival of dystrophin-producing fibers occurs within a dystrophic host. (Supported by MDAC)

W-Pos26

STRUCTURAL CHARACTERIZATION OF DYSTROPHIN USING MONOCLONAL AND POLYCLONAL ANTIBODIES

Steven D. Kahl, James M. Ervasti, Kay Ohlendieck, Suzanne W. Northrup and Kevin P. Campbell. Howard Hughes Medical Institute and Department of Physiology and Biophysics, University of Iowa College of Medicine, Iowa City, Iowa 52242.

Dystrophin is the ~400,000 Da protein product of the human Duchenne muscular dystrophy (DMD) gene that is localized to the cytoplasmic surface of the sarcolemma. We have prepared polyclonal antibodies to three distinct regions (amino acid positions 1-15, 3265-3280 and 3676-3685) derived from the known cDNA sequence of human dystrophin. Antibodies were affinity purified using either isolated dystrophin or a conjugate of the peptide with bovine serum albumin. Indirect immunofluorescence with antibodies to the C-terminal showed specific labeling of the sarcolemma in skeletal muscle of normal humans and mice but did not show labeling in patients with DMD or in *mdx* mice. This confirms that the antibodies identify dystrophin and not dystrophin-related proteins (Love, D.R. et al. *Nature* 339:55-58, 1989) which are not missing in DMD or *mdx* muscle (T.S. Khurana et al. *JBC* 265:16717-16720, 1990). Antibodies to the C-terminal of dystrophin preferentially recognized the major high molecular weight form of dystrophin, whereas antibodies to the N-terminal of dystrophin recognized both isoforms of dystrophin demonstrating that dystrophin is completely intact in isolated membranes. Immunoblot staining of cardiac membranes revealed that the C-terminal of dystrophin has not been modified in cardiac muscle. Monoclonal antibodies were also generated against dystrophin using isolated dystrophin-glycoprotein complex (J.M. Ervasti et al. *Nature* 345:315-319, 1990) as immunogen. Monoclonal antibodies to dystrophin and polyclonal antibodies to the N and C-terminal of dystrophin immunoprecipitated ^{125}I-labeled dystrophin-glycoprotein complex. Immunoblot staining of wheat-germ agglutinin immunoprecipitates of solubilized skeletal and cardiac membranes indicate the presence of the dystrophin-glycoprotein complex in cardiac muscle. Antibody staining following limited proteolysis of isolated sarcolemma, dystrophin-glycoprotein complex and purified dystrophin has identified unique dystrophin peptide epitopes for the various antibodies. We are currently using these antibodies to determine the domain of dystrophin that is responsible for interaction with the associated sarcolemma glycoproteins. K.P. Campbell is an Investigator of the Howard Hughes Medical Institute. J.M. Ervasti is an MDA postdoctoral fellow. This work was also supported by a grant from MDA.

W-Pos27

SOME PROPERTIES OF SKELETAL MUSCLE FIBERS FROM YOUNG AND MATURE DYSTROPHIC (MDX) MICE.

Stewart I. Head, Anthony J. Bakker, David A. Williams* and D. George Stephenson. Department of Zoology, La Trobe University, Melbourne, Australia and *Department of Physiology Melbourne University, Melbourne, Australia.

Mdx mice have a similar genetic defect and lack the same protein "dystrophin" as boys suffering from Duchenne muscular dystrophy.

In our study we enzymatically isolated single skeletal muscle fibers from mdx mice (age 3-84 weeks) in order to study their morphology and cytosolic Ca^{2+} concentrations. We have shown that as the mdx mice mature the skeletal muscle fibers develop morphological abnormalities which range from simple branching of the fiber to complex multiple splitting [3-15wks soleus(n=9) <5%, EDL(n=11) <5%, FDB(n=4) <5%; 15-17wks soleus(n=4) 40%, EDL(n=4), 20%; 26-84wks Soleus(n=4) 88%, EDL(n=5) 90%, FDB(n=5) 30%; percentages are the average number of deformed fibers from each muscle, n = number of muscles, abbreviations: EDL =extensor digitorum longus; FDB =flexor digitorum brevis]. These abnormalities were not evident in any fibers isolated from phenotypically normal mice(3-65wks). A laser scanning confocal microscope was used to examine single fibers *in situ*, as they lay within the muscle. These images showed that the malformed fibres were normally aligned within the muscle. In the mature group of muscle fibers (26-84wks) the average resting cytosolic Ca^{2+} was 94 nM, when the fiber was electrically stimulated this rose to 3.36μM.

This study suggests that one of the consequences of the absence of "dystrophin" in dystrophic animals is the formation of abnormal skeletal muscle fibers.

W-Pos28

EFFECT OF TEMPERATURE ON TRIGGERED PROPAGATED CONTRACTIONS IN RAT RIGHT VENTRICULAR TRABECULAE

Marcel C.G. Daniels and Henk E.D.J. ter Keurs, University of Calgary, Canada

Spontaneous activity in cardiac muscle preparations is facilitated at low temperature. At 21 C, triggered contractions (TPCs) can be induced in rat cardiac trabeculae that start in a region of damage and propagate along the muscle. We studied the temperature dependence of triggering and propagation of TPCs, compared this with the effects of changing $[Ca^{++}]_o$, and assessed whether TPCs can be elicited at body temperature.

TPCs were induced by stimulation in trains of 15 stimuli (2 Hz; 15 s intervals) at 21 C and $[Ca^{++}]_o$ 1.0 mM in the superfusate. Subsequently, temperature of the superfusate or $[Ca^{++}]_o$ was varied. Force was measured with a silicon strain gauge; length and shortening of sarcomeres were measured at two sites of the muscle using laser diffraction techniques.

Force produced by the last stimulated twitch (Ft) and propagation velocity of TPCs (Vprop) increased linearly between 15 and 23 C by a factor of 3.3 and 14.5 respectively. In contrast, latency of TPCs decreased 2.2 fold and force produced by TPCs (Fpc) decreased by 18±5% per degree C increase in temperature. With increasing $[Ca^{++}]_o$ at constant temperature, Ft, Fpc, and Vprop increased, while latency decreased. Latency and Vprop changed less with temperature than with a change in $[Ca^{++}]_o$ for a comparable change in Ft (which was assumed to reflect sarcoplasmic reticular calcium content). At 37 C, TPCs and triggered arrhythmias could be induced at $[Ca^{++}]_o$ 3.0-4.0 mM.

We conclude that both triggering and propagation of TPCs are facilitated with increasing temperature; this can not be attributed to an increase in calcium content of the sarcoplasmic reticulum with increasing temperature alone and most likely results from temperature dependence of calcium release from the sarcoplasmic reticulum. Moreover, TPCs can be elicited at body temperature if $[Ca^{++}]_o$ is elevated sufficiently.

W-Pos29

EFFECT OF CALYCULIN-A ON SMOOTH MUSCLE CONTRACTILE RESPONSES. James T. Stull, Yasutaka Kubota, Kristine E. Kamm, Masatoshi Hori* and Hideaki Karaki*. Dept Physiol, Univ Tx Southwestern Med Ctr, Dallas, Tx, and *Dept Vet Pharmacol, Univ Tokyo, Tokyo, Japan.

Calyculin-A (CLA), an inhibitor of protein phosphatases, induces smooth muscle contraction without an increase in cytosolic Ca^{2+} concentrations (Ishihara *et al.*, *J Pharmacol Exp Ther* 250:388, 1989). The effects of CLA on myosin light chain (MLC) phosphorylation were examined in bovine tracheal smooth muscle. Carbachol (0.1 μM) alone resulted in contraction (1.0 fractional force) and 50% monophosphorylated MLC by 10 min with ^{32}P in the serine site phosphorylated by myosin light chain kinase. CLA (1 μM) increased fractional force at 2 min to 0.20 without an increase in MLC phosphorylation (2%) or cytosolic Ca^{2+} concentrations. These results show that smooth muscle contracts rapidly in the presence of CLA without MLC phosphorylation.

The addition of CLA for 10 min increased fractional force to 1.45 and total MLC phosphorylation to 49%. MLC was 15% monophosphorylated and 34% diphosphorylated with ^{32}P in the serine and threonine sites phosphorylated by myosin light chain kinase. The responses to CLA were not associated with increases in cytosolic Ca^{2+} concentrations and were not altered in Ca^{2+}-depleted tissues. In addition, CLA induced a Ca^{2+}-independent, ATP-dependent contraction and MLC phosphorylation in skinned tracheal smooth muscle. These results reveal the existence of multiple cellular mechanisms regulating smooth muscle contractile elements. Supported in part by HL23990.

W-Pos30

A NOVEL PHOSPHATASE INHIBITOR, TAUTOMYCIN: EFFECTS ON SMOOTH MUSCLE. Hideaki Karaki and Masatoshi Hori. Department of Veterinary Pharmacology, Faculty of Agriculture, The University of Tokyo, Bunkyo-ku, Tokyo 113, Japan.

Tautomycin (TM) is an antibiotic isolated from Streptomyces spiroverticillatus (1,2). TM induces shape change and activates protein kinase C in leukemia cells (3) which may be due to inhibition of phosphatase (Magae, J: personal commun). We have examined the effects of TM on smooth muscle. In isolated rat aorta, 100nM-30μM TM induced sustained contraction with little increase in cytosolic Ca^{2+} measured with fura-2. The contractile effect was not inhibited by removal of external Ca^{2+} (with 4 mM EGTA). Cumulative addition of TM during sustained contraction due to high K^+ or norepinephrine induced additional increase in muscle tension. In permeabilized chicken gizzard and rabbit mesenteric artery, TM (10nM-30 μM) induced contraction in the absence of Ca^{2+} (pCa^{2+} <1nM). TM increased 20kDa myosin light chain (MLC) phosphorylation and myosin ATPase activity in the absence of Ca^{2+} in chicken gizzard preparation. TM inhibited the dephosphorylation of phosphorylated MLC due to removal of Ca^{2+} and ATP. These results suggest that TM is a phosphatase inhibitor with different characteristics from okadaic acid which inhibits contraction at lower concentrations and induces contraction at higher concentrations (4).

1) Cheng et al: J Antibiot 40, 907, 1987 2) Ubukata et al: J Chem Soc Chem Commun 244, 1990 3) Magae et al: J Antibiot 41, 932, 1988 4) Karaki et al: Br J Pharmacol 98, 590, 1989

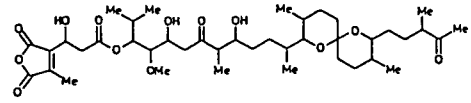

W-Pos31

Ca^{2+} INDEPENDENT CHANGES IN MYOSIN LIGHT CHAIN PHOSPHORYLATION DURING PROSTAGLANDIN $F_{2\alpha}$ CONTRACTIONS IN VASCULAR SMOOTH MUSCLE. Eiichi Suematsu, Moira Resnick, and Kathleen G. Morgan. Harvard Medical School, Beth Israel Hospital, Boston, MA 02215

The mechanism of contraction of vascular smooth muscle by prostaglandin $F_{2\alpha}$ ($PGF_{2\alpha}$) and the degree of Ca^{2+}-dependence of that mechanism are controversial. In order to clarify these points, intracellular Ca^{2+} levels ($[Ca^{2+}]_i$), force and phosphorylation of the myosin light chain (MLC) were measured in ferret aorta during the contraction induced by $PGF_{2\alpha}$. In physiologic Ca^{2+} solutions, $PGF_{2\alpha}$ (10^{-5}M) produced a tonic contraction with a transient spike in $[Ca^{2+}]_i$, followed by a relatively small sustained increase in $[Ca^{2+}]_i$ ($2.32x10^{-7}\pm0.07x10^{-7}$M to $2.72x10^{-7}\pm0.05x10^{-7}$M (n=16)). In a Ca^{2+}-free bathing media, $PGF_{2\alpha}$ also produced a tonic contraction with a small spike in $[Ca^{2+}]_i$, indicating a release of Ca^{2+} from intracellular store sites, followed by no significant increase in $[Ca^{2+}]_i$. Calcium-force curves were constructed by plotting the calibrated aequorin light signal against the resulting force. The control curve was significantly shifted to the left by $PGF_{2\alpha}$. $PGF_{2\alpha}$ shifted the Ca^{2+}-phosphorylation curve to the left. We conclude that $PGF_{2\alpha}$ causes contraction by both elevating $[Ca^{2+}]_i$ and increasing the Ca^{2+} sensitivity of MLC phosphorylation. These results are consistent with a mechanism where either there is an increase in activity of MLC kinase or a decrease in phosphatase activity. (Support: NIH HL-31704 to KGM and AHA MA Affiliate to ES)

W-Pos32

INTRACELLULAR CALCIUM, MYOSIN LIGHT CHAIN PHOSPHORYLATION AND ISOMETRIC FORCE OF GUINEA PIG AORTIC SMOOTH MUSCLE. Meei Jyh Jiang and Chin-Feng Chan. Institute of Biomedical Sciences, Academia Sinica, Taipei 11529, Taiwan, R.O.C.

We investigated the relationship of $[Ca^{2+}]_i$, myosin light chain phosphorylation and isometric force of guinea pig aortic strips during contractions activated by a thromboxane A_2 analogue, U46619. Isometric force and $[Ca^{2+}]_i$ were measured simultaneously using preloaded aequorin as an intracellular Ca^{2+} indicator. Myosin light chain phosphorylation levels were determined by two dimensional polyacrylamide gel electrophoresis in parallel preparations. U46619 (100 nM) induced a contraction which is 135% of contractions activated by a maximal dose of alpha-adrenergic agonist, phenylephrine. Force development rate of U46619-induced contractions, estimated by time to reach half peak force, was significantly lower than that of phenylephrine-induced contractions (2.19+0.26 min vs 0.40+0.06 min, respectively). An aequorin spike occurred in 6 out of 10 aortic strips and did not seem to correlate with force development rate. The steady state $[Ca^{2+}]_i$ increased 20% from the resting levels of 196+14.6 nM (n=15). Myosin light chain phosphorylation levels increased significantly at 1.5 min and remained higher than resting levels during a 15 min period. These results suggest that $[Ca^{2+}]_i$ and myosin light chain phosphorylation levels correlate well with isometric force in U46619-induced contractions of guinea pig aortic smooth muscle. Supported by Academia Sinica and the National Science Council of Republic of China.

W-Pos33

AGONIST-INDUCED MYOSIN PHOSPHORYLATION DURING UNLOADED SHORTENING AND ISOMETRIC CONTRACTION IN AIRWAY SMOOTH MUSCLE. Chi-Ming Hai and Beatrice Szeto. Section of Physiology, Division of Biology and Medicine, Brown University, Providence, RI 02912

Phosphorylation of the 20,000 dalton myosin light chain is an important regulatory mechanism of smooth muscle contraction. We measured myosin phosphorylation during unloaded shortening and isometric contraction induced by K^+-depolarization, carbachol, histamine, phorbol dibutyrate (PDB), and electrical stimulation in bovine tracheal smooth muscle. Peak and steady-state myosin phosphorylation induced by 109 mM K^+, 1 uM carbachol, and 1 uM histamine during unloaded shortening were lower than those during isometric contraction by 42%. To distinguish the effects of shortening and changing tissue length, tissues were pre-shortened by K^+-depolarization and unloaded shortening for 30 min, allowed to relax without external load for 60 min before a second stimulation. Peak and steady-state myosin phosphorylation were reduced further during the second unloaded shortening, indicating that the lower myosin phosphorylation during unloaded shortening was a length-dependent effect. Peak and steady-state myosin phosphorylation induced by electrical stimulation during the first and second unloaded shortening were similarly reduced, indicating that the lower myosin phosphorylation was not due to change in diffusion distance. In contrast, steady-state myosin phosphorylation induced by 100 uM histamine and 1 uM PDB (an activator of protein kinase C) during unloaded shortening and isometric contraction were not significantly different. Since steady-state myosin phosphorylation is maintained by Ca^{2+} influx, these results suggest two mechanisms for the activation of calcium channels in the smooth muscle cell membrane. A length-sensitive mechanism is activated at lower agonist concentration, whereas a length-insensitive mechanism, possibly calcium channel phosphorylation by protein kinase C, is activated at higher agonist concentration. (Supported by National Science Foundation)

W-Pos34

THE MECHANICAL PROPERTIES OF SINGLE ISOLATED HOG CAROTID ARTERIAL CELLS. Frank V. Brozovich, Bockus Research Institute, Graduate Hospital, Philadelphia, PA 19146.

The mechanical properties of cells isolated from the hog carotid artery were studied. Cells were isolated in Ca^{2+} free Hanks solution containing elastase, collagenase and trypsin inhibitor. After isolation, the cells were plated onto glass coverslips and stored on ice at 4°C until experiments were performed. Prior to experimentation, calcium was adjusted to 1 mM. The coverslips were transferred to the stage of an inverted microscope where experiments were performed. The single isolated cells were long (150±28 μm; x±sd, n=97) and relaxed. Cells maintained their pharmacological responsiveness; when stimulated with a maximal dose (10^{-3} M) of histamine, the cells would rapidly shorten from their initial length to a final length of 50-60 μm. Cell shortening was not graded; after stimulation, all cells would shorten from their initial length to the final cell length and develop membrane blebs. Relaxed single cells could also be attached to glass microelectrodes, one of which was connected to a Cambridge model 406A force transducer (sensitivity, 20 mv/μN). After maximal histamine stimulation, force rapidly increased to an average of 3.3±1.2 μN (n=8). Thus, single isolated arterial cells appear to be an excellent model for studies of the contractile regulation of smooth muscle. Supported by a grant from the NIH HL44181.

W-Pos35

MECHANISM OF ALPHA AGONIST-INDUCED FORCE GENERATION IN SKINNED SINGLE VASCULAR CELLS.
Elizabeth M. Collins, Michael P. Walsh and Kathleen G. Morgan. Harvard Medical School, Beth Israel Hospital, Boston, MA 02215

We have previously reported that skinned single cells retain responsiveness to alpha agonists even though $[Ca^{2+}]_i$ is clamped at resting levels by Ca buffers. The present study was undertaken to characterize the mechanism of the response to phenylephrine (PE). Ferret aorta cells were isolated in a collagenase-elastase trypsin inhibitor solution and made hyperpermeable in a pCa 9 buffer by exposure for 5-8 min to 30 μg/cc of saponin. Force was recorded by techniques previously described (Brozovich, Walsh & Morgan, Pflugers Arch, 1990). We have reported that the control Ca-force curve begins to rise at pCa 7.5 and reaches a maximum (about 440 μg) at a pCa of 6.5. The increment in force on addition of PE at various $[Ca^{2+}]_i$ showed little Ca dependence. There was no significant difference between the force generated by PE at pCa 8.0 (215±102 μg) and pCa 7.0 (202±44 μg). The PE induced increment dropped to 88±30 μg at pCa 6.6 possibly because the cell had developed significant force by exposure to pCa 6.6 alone. To examine the involvement of protein kinase-C (PKC) in the PE contraction, we compared the magnitude of the PE contraction to that of the constitutively active PKC fragment (PKM). 5 μg/ml PKM in pCa 7 produced an increase of 254±98 μg. This was of interest in comparison to reports in other tissues of inhibitory responses to PKM as well as suggestions that contraction to phorbol esters may be due to non-specific actions. To further test the idea that the PE contraction at constant $[Ca^{2+}]_i$ involved PKC activation, we tested the effect of the pseudosubstrate inhibitor peptide (PSIP) on the PE contraction. Addition of 3 μM PSIP to a maximally effective PE contraction resulted in a significant decrease in force. Together these results suggest that the PE contraction that occurs in the skinned cells at constant $[Ca^{2+}]_i$ is the result of activation of a relatively Ca-independent isomer of PKC. Support: HL-31704 and HL-42293.

W-Pos36

NITROGLYCERIN-INDUCED cGMP ELEVATION RELAXES HISTAMINE STIMULATED SWINE CAROTID MEDIA WITHOUT REDUCTION IN MYOPLASMIC $[Ca^{2+}]$ OR CROSS-BRIDGE PHOSPHORYLATION.
Nancy L. McDaniel, Christopher M. Rembold and Richard A. Murphy. University of Virginia Health Sciences Center, Charlottesville, VA 22908 USA

We tested the hypothesis that cGMP elevation relaxes smooth muscle by reducing $[Ca^{2+}]$-dependent myosin phosphorylation. $[Ca^{2+}]$ (nM) as measured by aequorin, myosin light chain phosphorylation (mole P_i/mol MLC by 2D gel electrophoresis), [cGMP] (pM/mg wet tissue weight by radioimmunoassay), and stress (x 10^3 N/m^2) were measured in swine carotid medial tissues at 37° C. Ten uM histamine induced $[Ca^{2+}]$ and phosphorylation transients associated with rapid stress development. After 10 minutes, $[Ca^{2+}]$ and phosphorylation had decreased to lower but suprabasal levels with stress maintained near peak values. No change in [cGMP] was produced by histamine addition. Nitroglycerin (NTG, 100 uM) added 10 min after histamine produced half maximal relaxation associated with two-fourfold increases in [cGMP]. Minor reductions in $[Ca^{2+}]$ and phosphorylation could be detected one min after addition of NTG but levels returned to suprabasal values indistinguishable from the histamine control by 5 min. Relaxation was maintained with $[Ca^{2+}]$ and phosphorylation levels no different from the histamine contracted arteries. The steady state relationship dependence of stress on phosphorylation was therefore shifted to the right.

In conclusion, cGMP elevation did not appear to relax the swine carotid media by reducing myoplasmic $[Ca^{2+}]$ or myosin phosphorylation. Possible explanation for the NTG-induced relaxation despite high $[Ca^{2+}]$ and phosphorylation include 1) unrecognized metabolic effects of NTG and 2) unknown cGMP mediated effect on the contractile apparatus (possibly phosphorylation at a different site on the light chain). Supported by AHA Virginia Affiliate 90-G-6, NIH HL19242 & HL38918, and the Markey Trust.

W-Pos37

HIGH STEADY-STATE VALUES OF CROSSBRIDGE PHOSPHORYLATION IN ARTERIAL SMOOTH MUSCLE DO NOT INCREASE STEADY-STATE STRESS: A TEST OF THE LATCHBRIDGE HYPOTHESIS. Patrizia DiBlasi, Christopher M. Rembold, and Richard A. Murphy. Dept. of Physiology, University of Virginia Health Sciences Center, Charlottesville, VA 22908.

The 4-state crossbridge model incorporating a "latchbridge" (an attached, dephosphorylated crossbridge with a slowed detachment rate) proposed for smooth muscle by Hai and Murphy (Am. J. Physiol. 254: C99-C106, 1988, and 255: C86-C94, 1988) predicts that steady-state active stress would be highly dependent on small increases in myosin regulatory light chain phosphorylation up to some 30%. The model also predicts that stress will not rise appreciably with further increases in phosphorylation. The model's predictions were verified in prior studies with the swine carotid, but no individual stimulus induced steady-state phosphorylation levels much above 40%. In this work we tested the model's prediction that stress would be almost independent of phosphorylation above 40%. Our approach was to combine stimulation (e.g., histamine, depolarization, endothelin, and/or ionomycin) with various treatments to inhibit mechanisms acting to sequester or remove Ca^{2+} from the myoplasm (e.g., removal of extracellular Na^+ to block Na^+/Ca^{2+} exchange). The various protocols extended the attainable steady-state levels of phosphorylation to almost 60%. The results fitted the model's predictions that very high levels of phosphorylation will not enhance steady-state stress generation. Supported by PHS grant 5 PO1 HL19242, HL 38918 and the Lucille P. Markey Charitable Trust.

W-Pos38

$[Ca^{2+}]$-SENSITIVITY IN VASCULAR SMOOTH MUSCLE: A COMBINED AEQUORIN AND FURA 2 STUDY. Elizabeth K. Gilbert and Christopher M. Rembold (introduced by Bruce Gaylinn). Division of Cardiology, Department of Internal Medicine, University of Virginia Health Sciences Center, Charlottesville, VA 22908 USA

Stimulation of smooth muscle with contractile agonists (e.g. histamine) was associated with a high $[Ca^{2+}]$-sensitivity of myosin light chain phosphorylation when $[Ca^{2+}]$ was measured with aequorin (Circ Res 63:593, 1988). In contrast, depolarization was associated with a lower $[Ca^{2+}]$-sensitivity of phosphorylation. In this study, we evaluated whether artifacts in measuring $[Ca^{2+}]$ with aequorin were responsible for these differences in the $[Ca^{2+}]$-sensitivity of phosphorylation. We measured myoplasmic $[Ca^{2+}]$ with Fura 2 (loaded intracellularly by incubation of swine carotid medial tissues in Fura 2 AM as described by Himpens and Somlyo, J Physiol 395:507, 1988). In tissue loaded with aequorin or Fura 2, 109 mM KCl depolarization or 10 uM histamine stimulation induced rapid contractions and stress was maintained near peak values for 10 min. Depolarization induced large monotonic increases in $[Ca^{2+}]$ as detected with either aequorin or Fura 2. Histamine stimulation induced large transient increases in $[Ca^{2+}]$ as detected with both indicators. After 10 min of histamine stimulation, aequorin-estimated $[Ca^{2+}]$ decreased by approximately 50 % while Fura 2-estimated $[Ca^{2+}]$ remained near peak values. This difference may be caused by the Fura 2 loading procedure since myosin phosphorylation levels after 10 min of histamine stimulation were higher in Fura 2 loaded tissues than in controls. The $[Ca^{2+}]$-sensitivity of phosphorylation was higher with histamine stimulation regardless of whether the $[Ca^{2+}]$ indicator was aequorin or Fura 2. These results suggest that the stimulus-specific differences in the $[Ca^{2+}]$-sensitivity of phosphorylation is not an artifact of aequorin measurements. Supported by an AHA Medical student fellowship to E.G., NIH HL38918, and the Markey Trust.

W-Pos39

DO WE THROW OUT THE LATCHBRIDGE MODEL BECAUSE OF SOME ENERGETICS EXPERIMENTS ?
Steven P. Driska, Physiology Department, Temple University School of Medicine, Philadelphia, PA 19140

Kinetic models of smooth muscle can predict the time courses of force and myosin light chain phosphorylation during contraction and relaxation, and can approximate the steady-state relationship of force and phosphorylation. Using the best estimates of rate constants obtained from our laboratory, this relationship is nonlinear as shown in Figure 1. However, these models do not predict the observed linear dependence of ATP consumption on isometric force (Figure 2). For this reason, it has been suggested that latchbridges do not remain attached any longer than phosphorylated crossbridges (Paul, R.J. 1990, *Am. J. Physiol.* 258:C369-C375), but Paul's alternative model predicts a nearly linear force-phosphorylation relationship, which is not observed. However, during the long contractions necessary for steady-state energetics measurements in this tissue, phosphorylation would have declined to lower values, typically about 30%. Examination of the ATPase-force relationship in Figure 2 shows the curve is fairly linear in the region where the energetics measurements were probably made (0-30% phosphorylation). Thus, within experimental error, the model may be able to explain the linear ATPase-force relationship. Supported by NIH HL24881.

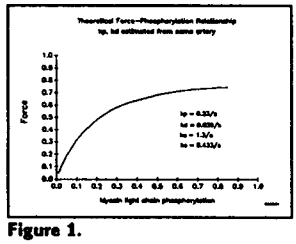

Figure 1.

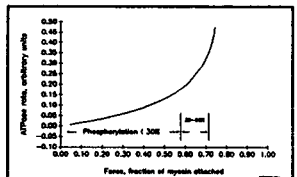

Figure 2.

W-Pos40

COOPERATIVE ACTIVATION OF MYOSIN: A DUAL ROLE FOR MYOSIN LIGHT CHAIN PHOSPHORYLATION IN THE REGULATION OF SMOOTH MUSCLE. T.M. Butler, M.J. Siegman, T. Vyas, S.U. Mooers, S.R. Narayan and C.S. Owen#. Departments of Physiology and Biochemistry and Molecular Biology#, Jefferson Medical College, Philadelphia, PA 19107

The purpose of this study was to determine the quantitative relationship between phosphorylation of the myosin light chain and the fraction of myosin molecules that increase their rate of ATPase activity during contraction of permeabilized rabbit portal vein. Formycin triphosphate (FTP), an analog of ATP which shows enhanced fluorescence on binding to myosin, was used in single turnover experiments in which either surface fluorescence of the muscle or FDP content was measured. Under resting conditions, incubation in FTP followed by a chase in both FTP and ATP resulted in a similar biphasic decrease in both the fluorescence enhancement and FDP content which was complete in about 30 minutes. The bound FDP is replaced with bound ADP during the chase, and based on previous results, we conclude that we are monitoring nucleotide diphosphate release from myosin. We then determined how the extent of myosin light chain phosphorylation controls the fraction of myosin which has released the bound FDP at two minutes of chase. Thiophosphorylation of less than 20% of the total myosin light chain caused the maximum FDP release. This shows that phosphorylation of a single myosin head cooperatively activates the ATPase activity of other unphosphorylated myosin heads. There is also a significant relationship between FDP released at 2 minutes of chase and force (r=0.8, n=40). Interestingly, there remains a significant dependence of ATPase on thiophosphorylation of the light chain at levels which exceed that required for maximum force and for the maximum effect on nucleotide diphosphate release. We conclude that a small degree of myosin light chain phosphorylation cooperatively turns on all of the myosin, and that a higher degree of phosphorylation makes the myosin cycle faster. Such a dual mechanism may allow the single process of myosin light chain phosphorylation to control both force output and maximum shortening velocity independently. (Supported by HL 15835 to the Pennsylvania Muscle Institute)

W-Pos41

STAPHYLOCOCCAL ALPHA-TOXIN PERMEABILIZED SMOOTH MUSCLE: RELATIONSHIP BETWEEN INTRACELLULAR Ca^{2+}, ATP HYDROLYSIS AND ISOMETRIC FORCE. Phyllis E. Hoar#, Steve Tjoe-Fat#, Gang Wang#, and W. Glenn L. Kerrick*#, Depts. of *Mol. & Cell. Pharm. and #Physiol. & Biophys., Univ. of Miami Sch. of Med., Miami, FL.

Treatment of smooth muscle fiber bundles with staphylococcal alpha-toxin, is thought to form pores 2-3 nm in diameter in the cell membrane thus allowing the equilibration of small molecules such as ATP, ATPγS and Ca^{2+} inside and outside the cell. The purpose of this study is to characterize the membrane permeability of α-toxin treated smooth muscle cells to the CaEGTA complex, ATP, Fura-2 and creatine phosphate (CP) in order to elucidate the advantages and disadvantages of using α-toxin permeabilized smooth muscle preparations. Intracellular [Ca^{2+}] (340/380 Fura-2 fluorescence), ATPase activity, and force measurements in α-toxin treated smooth muscle were used evaluate the overall effects of the permeabilization by α-toxin. Intact smooth muscle preparations were incubated with the ester Fura-2 AM for 3 hours in order to diffuse this dye into the intact cells prior to α-toxin treatment. Results show that α-toxin treated smooth muscle cells are not permeable to Fura-2 whereas cells skinned with Triton X-100 are freely permeable to Fura-2. The method used to measure ATPase activity (Guth and Wojciechowski, 1986) involves a PEP/pyruvate kinase regenerating system for ATP that can be monitored by NADH fluorescence changes. The ATPase activity of α-toxin treated smooth muscle is approximately twice the magnitude of ATPase activity associated with actomyosin. Intracellular Ca^{2+} measurements in intact and α-toxin treated smooth muscle cells show that the cell membranes are only partially permeable to CaEGTA and that GTPγS makes the contractile system more sensitive to Ca^{2+}.

Supported by grants from the American Heart Assn. (National & Florida Affiliate), the Muscular Dystrophy Assn., and NIH (RO1-AR37447).

W-Pos42

IONIC STRENGTH DIFFERENTIALLY AFFECTS THE Mg^{2+} MODULATION OF STRESS AND MYOSIN PHOSPHORYLATION IN PERMEABILIZED SWINE CAROTID ARTERY.
Jacqueline Cilea and Robert S. Moreland. Bockus Research Institute, Graduate Hospital, Philadelphia, PA 19146.

Although Ca^{2+} dependent myosin light chain (MLC) phosphorylation is important for contraction of smooth muscle, there is evidence to suggest that a second Ca^{2+} dependent (MLC phosphorylation independent) regulatory system may also play a prominent role. The goal of this study was to further examine the properties of the MLC phosphorylation independent regulatory system. Mg^{2+} has been shown to modulate Ca^{2+} and MLC phosphorylation dependent stress and initiate MLC phosphorylation independent stress. Ionic strength (μ) was varied to determine if these effects of Mg^{2+} on stress can be separated. Thin medial strips of swine carotid artery were mounted for isometric force recording and permeabilized with Triton X-100. Steady state force and MLC phosphorylation levels were measured during Ca^{2+} dependent contractions (0.01-10 μM) in the presence of varying [Mg^{2+}] (0.1-6 mM) and μ (20-120 mM). At "normal μ" (120 mM), [Mg^{2+}] > 3 mM decreased maximal levels of stress and MLC phosphorylation. Decreasing the μ lowered the threshold [Mg^{2+}] necessary to produce this inhibition. Increasing the [Mg^{2+}] at any μ had no effect on the Ca^{2+} sensitivity of stress, but decreased the Ca^{2+} sensitivity of MLC phosphorylation. The relationship between MLC phosphorylation and stress was linear in all conditions. The slope of a regression line of this relationship provided an index of the magnitude of the stress developed as a function of the level of MLC phosphorylation. Varying [Mg^{2+}] had no effect on this relationship. Decreasing μ, at all [Mg^{2+}], caused a generalized depression of contractile activity, but did not effect the Ca^{2+} sensitivity of either stress or MLC phosphorylation. However, lowering μ decreased the ratio of stress/MLC phosphorylation. The finding that Mg^{2+} did not alter the relationship between stress and MLC phosphorylation but decreased the Ca^{2+} sensitivity of MLC phosphorylation, suggests that Mg^{2+} dependent but MLC phosphorylation independent activation contributed to the stress developed. This MLC phosphorylation independent activation of stress development was more sensitive to changes in μ than was MLC phosphorylation dependent stress development. This study was supported, in part, by funds from NIH HL 37956.

W-Pos43

EXPRESSION OF THE CALPAIN-CALPASTATIN SYSTEM IN VASCULAR SMOOTH MUSCLE. P. McClelland and D.R. Hathaway, Krannert Institute of Cardiology, Indiana University School of Medicine, Indianapolis, IN 46202.

Vascular smooth muscle (VSM) contains large amounts of the Ca^{2+}-dependent thiol protease, calpain II. In this study, we surveyed the contractile and modulated phenotypes of VSM for the presence of calpains I and II and the specific inhibitor protein of the calpains, calpastatin. Following DEAE-Sephacel column chromatography of an extract of bovine aortic (BA) smooth muscle, calpain II was identified by specific elution at 0.3 M NaCl, and confirmed by Western blotting of column fractions using an antiserum specific for the 76 kDa catalytic subunit of the enzyme. No calpain I or calpastatin was detected by activity measurements or by Western blots using monoclonal antibodies specific for these proteins. Furthermore, Northern blots of BA poly A^+ RNA were negative using cDNA probes for calpain I and calpastatin but positive for calpain II. When cultured BA cells (ie. the modulated phenotype of VSM) were used as the starting material, calpain II and calpastatin were identified by activity measurements, immunoblotting, and Northern blots of RNA. However, cultured BA cells were devoid of calpain I by all detection methods. Our results show that: 1) irrespective of phenotype, VSM contains only calpain II and 2) calpastatin is expressed only in the modulated phenotype of VSM. We conclude that VSM is the only tissue identified to date that contains calpain II as the exclusive isoform of calpain. Moreover, factors which induce the modulated phenotype of VSM must also induce calpastatin expression in this tissue.

W-Pos44

INTRACELLULAR DISTRIBUTION OF FLUORESCENT DERIVATIVES OF PHORBOL ESTER IN SMOOTH MUSCLE. G.A. Meininger, R.M. Lynch, E.F. Etter, and F.S. Fay. Dept. of Physiol., Univ. Mass. Med. Center, Worcester, MA 01655 and Dept. of Med. Physiol., College of Medicine, Texas A. & M. Univ., Coll. Stn., TX 77843.

Tumor promoting phorbol esters bind to protein kinase C and cause activation of this enzyme. The binding of phorbol esters to protein kinase C is thought to be a specific process making them a potentially useful probe for studying the cellular localization of protein kinase C. The intracellular distribution of two fluorescent derivatives of phorbol ester, BODIPY-3-Phorbol acetate and BODIPY-12-Phorbol acetate (Molecular Probes) were investigated in stomach smooth muscle cells of Bufo marinus and in a cultured vascular smooth muscle cell line (A7R5). Cells were incubated with concentrations of the fluorescent phorbol ester ranging from .01 to 1 μM for 10 to 60 min. Fluorescently labelled cells were studied using a digital imaging microscopy system. Images of individual cells were acquired as a series of images representing different focal planes along the Z axis. These image series were used to reconstruct three-dimensional representations of the intracellular distribution of the fluorescently labelled phorbol ester. Analysis of the images indicated that the fluorescent phorbol derivatives label patches on the cell membrane, the nucleus, and small punctate regions within the cytosol. Preliminary immunocytochemical studies using antibodies to protein kinase C (Gibco-BRL) coupled to fluorescent secondary antibodies have demonstrated similarities in the intracellular distribution of the fluorescent labelling. Thus, these studies suggest that fluorescently labelled phorbol esters may provide a useful means of revealing the intracellular distribution of protein kinase C. (Supp. by CIBA-Geigy Est. Invest. Awd. and NIH HL 33324 to G.A.M. and by HL 14523 to F.S.F.).

W-Pos45

THE EFFECTS OF INNERVATION ON VASCULAR SMOOTH MUSCLES: SYNAPTIC TRANSMISSION AND NEURO-PEPTIDE Y (NPY) RECEPTOR EXPRESSION. S.A. LEWIS, R.Y.K. PUN, A. BALASUBRAMANIAM* AND D.G. FERGUSON. Dept. of Physiology and Biophysics, *Dept. of Surgery, Univ. of Cincinnati, Cincinnati, OH, 45267-0576

The influence of innervation on vascular smooth muscles (VSM) has not been established. We have used co-cultures of dissociated superior cervical ganglia with mesenteric VSM to examine the interactions between sympathetic neurons and VSM. Electrophysiological experiments were performed on VSM cells using whole-cell "tight seal" recording technique with EGTA-buffered K-aspartate solution in the pipette. Under voltage-clamp, outward currents predominated in the first several days of culture. By day 4, a small inward current which peaked at about +10 mV was evident in these cells. In co-cultures, excitatory junctional potentials 1-5 mV in amplitude were elicited in about 30% of the VSM cells following stimulation of the neurons by passage of depolarizing currents delivered through conventional sharp-tipped pipettes. On one occasion, action potentials were generated in the VSM. Our results demonstrate the existence of functional synapses between sympathetic neurons and mesenteric VSM.

Cultures were examined further using electron microscopy. Neurons were injected with horse radish peroxidase, fixed, reacted with diaminobenzidine, and prepared for transmission electron microscopy. Micrographs of the co-cultures indicate the presence of structural synapses with small secretory granules localized in the nerve terminals. Based on vesicular size and density we predicted that many of these are peptidergic granules. NPY could be contained in some of the secretory granules since it has been established that NPY is a neurotransmitter in sympathetic neurons. To determine if innervation influences transmitter-receptor expression in VSM cells we performed immunocytochemical staining with biotinylated NPY in VSM obtained from neonate, and VSM from neonate co-cultures. VSM alone stains negative for the NPY receptor, whereas neonatal co-cultures display a faint cytoplasmic staining. Our data indicate that innervation may have an effect upon NPY receptor expression in mesenteric VSM in culture.

W-Pos46

IMAGING OF DISTRIBUTION AND TRANSLOCATION OF ACTIVATED PROTEIN KINASE C IN VASCULAR SMOOTH MUSCLE CELLS. Raouf A. Khalil and Kathleen G. Morgan. Harvard Medical School, Boston, MA.

The subcellular distribution of protein kinase C (PKC) was imaged in intact freshly isolated cells from ferret portal vein with the use of the fluorescent PKC probe 12-(1,3,5,7-tetramethylBODIPY-2-propionyl)phorbol-13-acetate and digital imaging microscopy. In preliminary contraction experiments, the probe induced cell shortening indicating PKC activity. The probe rapidly localized mainly in the perinuclear area and to a lesser extent in the cytosol and the plasma membrane. The labelling of the three cellular compartments was displaced by the nonfluorescent phorbol ester DPBA. A membrane marker with similar lipophilicity and no PKC activity labelled primarily the surface membrane and over a longer time and to a lesser extent the perinuclear area. We measured the ratio between the PKC probe intensity at the surface membrane and that in the cytosol (R) as well as the degree of cell shortening at each point in time. In the presence of extracellular Ca^{2+}, the time to peak R was 128 sec and the time to peak shortening was 133 sec. The peak R and shortening were 2.08 and 65%, respectively. In Ca^{2+}-free solution, no significant degree of translocation of the probe could be detected with time and the time to peak shortening was delayed to 414 sec. The peak R and shortening were decreased significantly to 1.13 and 40%, respectively. The relatively specific PKC inhibitor H-7 significantly reduced the magnitude of shortening and delayed the time to peak shortening but did not alter the distribution of the PKC probe. This study introduces a method to study the distribution and the translocation of PKC in living smooth muscle cells. The study also suggests that: 1) the majority of PKC is located in the perinuclear area where it may modulate the sarcoplasmic reticulum Ca^{2+} and/or influence gene regulation, 2) PKC moves from the cytosol to the plasma membrane during smooth muscle contraction. The latter events are Ca^{2+}-dependent. (Support: NIH HL-31704 & HL-42293)

W-Pos47

THROMBIN PRODUCES BOVINE PULMONARY ARTERY ENDOTHELIAL CELL BARRIER DYSFUNCTION VIA PROTEIN KINASE C-DEPENDENT ACTIVATION OF THE CONTRACTILE APPARATUS. Joe G.N. Garcia, Jerome S. Stasek, Caroline E. Patterson. (Introduced by Susan Gunst). Department of Medicine, Indiana University, Indianapolis, IN.

We have demonstrated α-thrombin to increase vascular permeability in vivo and in vitro in association with morphologic alterations indicative of endothelial cell contraction. Furthermore, thrombin was noted to activate G protein-coupled, phosphoinositol-specific phospholipase C and phosphatidylcholine-specific phospholipase D resulting in increased levels of the protein kinase C (PKC) activation agent, diacylglycerol. We hypothesized that PKC may be an important effector in producing bovine pulmonary artery endothelial cell (BPAEC) barrier dysfunction. Both α-thrombin and the PKC activating agent, phorbol myristate acetate (PMA), resulted in dose-dependent increases (> 4 fold increases each agent) in the flux of Evans blue-albumin across confluent BPAEC monolayers indicative of barrier dysfunction. Thrombin (1 μM) produce rapid (beginning at 1 min) time-dependent translocation of PKC activity from the cytosol to the membrane as detected by the Ca^{++}-, phosphatidylserine-dependent phosphorylation of H_1 histone. Thrombin stimulation resulted in prominent redistribution of several cytoskeletal proteins from the triton-soluble to the triton-insoluble fractions indicating activation of the contractile apparatus. To examine whether the actin binding protein caldesmon (Mr 77kd) and the intermediate filament vimentin (55kd) were substrates for thrombin-induced phosphorylation, BPAEC monolayers prelabeled with ^{32}Pi were challenged with either α-thrombin (1 μM) or PMA (0.1 μM) and the SDS solubilized proteins used for immunoprecipitation using antisera to Cal_{150} and Vim_{55}. Both agonists produced time-dependent (0-15 min) generation of $phosphocal_{77}$ and $phosphovim_{55}$. PKC purified from BPAEC by threonine-sepharose chromatography was utilized for in vitro Cal_{77} and Vim_{55} phosphorylation confirmed by Western blot and immunoprecipitation techniques. These studies suggest that thrombin-induced PKC activation may be a critical event in activation of the BPAEC contractile apparatus and subsequent barrier dysfunction.

W-Pos48

STRUCTURE OF THE ACTIN-MYOSIN HEAD COMPLEX IN THE PRESENCE OF ATP. Ling-Ling Frado and Roger Craig, Dept. of Cell Biology, U. Mass. Medical School, Worcester, MA 01655. Intro. by P. Vibert.

The structure of the actin-myosin head complex at different stages of the ATPase cycle is unknown. The A.M.ATP and A.M.ADP.Pi states have been shown by electron microscopic studies of crosslinked acto-S1 to have a disordered appearance of attached heads, different from the regular, 45° angled A.M (rigor) state (Craig et al, PNAS 82, 3247, 1985; Applegate and Flicker, J. Biol. Chem. 262, 6856, 1987). However, it is possible that the structures observed were heads tethered by the crosslinker rather than specifically attached by noncovalent bonds (cf. Zot et al, Biophys. J. 57, 410a, 1990). Here we describe the structure of the acto-HMM complex studied by negative staining in the presence of ATP without the use of cross-linkers. Actin filaments, decorated in solution with HMM, were applied to an electron microscope grid; the grid was then rinsed with a rigor solution or the same solution containing 0.2-1 mM ATP and rapidly stained (within 0.1 s). Control grids (no ATP) showed many filaments exhibiting the typical arrowhead appearance of fully decorated actin. In the presence of ATP, many filaments were still decorated, but the level of decoration was less and its nature different from that in rigor: 1. Many attached HMM's had a fuzzy appearance which did not reveal the detailed structure of the molecule. 2. When the attached HMM's were distinct, a variety of angles of attachment were seen, different from the rigor angle. 3. Often only one of the two heads appeared to be attached. These results are consistent with those obtained from the studies with crosslinked acto-S1 and with the conclusion from those studies that the structures of the A.M.ATP and A.M.ADP.Pi states are different from the A.M state. Supported by NIH.

W-Pos49

LINEAR DICHROISM OF ACRYLODAN-LABELED TROPOMYOSIN (ACTm) AND MYOSIN SUBFRAGMENT 1 (ACS1) BOUND TO ACTIN IN MYOFIBRILS. Danuta Szczesna and Sherwin S. Lehrer. Department of Muscle Research, Boston Biomedical Research Institute, 20 Staniford Street, Boston, MA 02114

Previous studies of ACTm bound to actin in solution indicated a movement of Tm relative to actin associated with S1 binding (Lehrer & Ishii, Biochemistry 27, 5899, 1988). Further information about this movement was obtained with fluorescence detected linear dichroism (LD) of AC$\alpha\alpha$Tm bound to oriented ghost myofibrils attached to a coverslip on the rotating stage of a fluorescence microscope. Light from 50W Hg lamp was polarized relative to the fibril axis and a Zeiss dichroic filter assembly selected the excitation and emission. The fluorescence from 2-3 sarcomeres was selected with a 100x/1.3 oil neofluar objective and aperture, and measured by photon counting. The dichroic ratio, R(0°/90°) for excitation parallel/perpendicular to the fibril was obtained. The probe polar angle, Θ, was calculated with $R=2\cot^2\Theta$ (Borejdo et al., J. Mol. Biol. 158, 391, 1982) with the assumption of no static or dynamic disorder. A control study with rhodamine-labeled S1 bound to actin in fibrils indicated that MgADP changed R from 0.68 to 1.42, corresponding to $\Theta \approx 60°$ and $\Theta \approx 49°$, respectively, in reasonable agreement with previous fiber LD studies (Burghardt et al., Proc. Natl. Acad. Sci. USA 80, 7515, 1983). Similar measurements with ACS1, however, gave $R=0.60\pm0.05$ (-ADP) and 0.68 ± 0.05 (+ADP) indicating, $\Theta=60°$ without much effect of ADP. For ACTm bound to actin in fibrils, in the absence of S1, $R=1.21\pm0.09$ (n=93); in the presence of S1, $R=1.22\pm0.11$ (n=82); in the presence of S1-ADP, $R=1.11\pm0.06$ (n=77), showing that $\Theta \approx 52.5°$ without much S1-effect. These studies indicate that S1-induced movement of Tm on actin does not change the angle between the AC probe on Cys 190 of Tm and the actin axis. Supported by NSF and NIH.

W-Pos50

STOICHIOMETRY OF BINDING OF MYOSIN SUBFRAGMENT-1 TO F-ACTIN MEASURED BY FLUORESCENCE POLARIZATION.

Oleg A. Andreev and Julian Borejdo, Baylor Research Foundation, Baylor University Medical Center, 3812 Elm St., Dallas, TX, 75226.

We reexamined the question of stoichiometry of binding of myosin subfragment-1 (S-1) to F-actin. S-1 was labeled at SH_1 with fluorescent probes 5-IAF, 1,5-IAEDANS or IATR and the fluorescence anisotropy measurements were made using SLM-500C spectrofluorometer. All experiments were perfomed in 50mM KCl, 10mM Tris-HCl, pH 7.5, at 23°C. The fluorescence anisotropy of S-1 labeled with any of the three fluorophores increased upon binding to F-actin. The fluorescence anisotropies of 5-IAF*S-1 and 1,5-IAEDANS*S-1 were affected more by F-actin then that of IATR*S-1. When increasing amounts of F-actin were added to a fixed concentration of labeled S-1, the increase of fluorescence anisotropy reached maximum at a molar ratio of actin to S-1 of 1:1. When increasing amounts of labeled S-1 were added to a fixed concentration of F-actin anisotropy reached maximum at molar ratio of actin to S-1 of 2:1. The effect induced by binding of F-actin was removed upon addition of ATP. The addition of PP_i to a complex of labeled S-1 and F-actin caused small decrease of fluorescence anisotropy. In contrast, no effect of ADP, or AMP-PNP on fluorescence anisotropy of labeled S-1 alone or bound with F-actin was observed. These results indicate that depending on the mode of titration, one S-1 molecule may bind to one or to two monomers of F-actin. Supported by NIH BRSG S07 RR 0590605.

W-Pos51

SYNTHETIC PEPTIDES OF THE N-TERMINAL REGION OF ACTIN INTERACT WITH MYOSIN. J.E. Van Eyk and R.S. Hodges, (Intro. by C.M. Kay), Dept. of Biochemistry, University of Alberta, Edmonton, Alberta, Canada T6G 2H7

The induction of muscle contraction occurs by regulation of the actin and myosin interaction by the regulatory protein complex (Tn-TM). Previous work from numerous laboratories, have strongly indicated that the N-terminal region of actin contains one of the binding sites between actin and myosin. A peptide of skeletal actin residues 1-28 was synthesized by solid-phase peptide synthesis. The formation of a complex between the synthetic actin peptide residues 1-28 and myosin subfragment 1 (S1) and HMM was demonstrated by high performance size exclusion chromatography (pH 6.8). At higher pH (pH 7.2 to 8.2), the actin peptide 1-28 precipitated S1 but not HMM. However, the actin peptide activated both the S1 and HMM ATPase activity by up to 155% and 170%, respectively.

A series of shorter actin analogs were synthesized, in order to delineate the critical residues within this region of actin that are required for binding to the myosin fragments. The actin peptide 1-28 was the most effective analog, and hence is the minimum sequence required for biological activity. Deletion of residues from the N or C terminus of actin 1-28 decreased the S1, acto-S1 and HMM ATPase activity, indicating that these regions are essential for biological activity. Two non-overlapping peptides, actin 1-14 and 18-28 induced the equivalent level of ATPase activity. This suggests that there are two independent binding sites, however, the presence of both the N and C terminal regions results in the most effective response in the ATPase assays. These results clearly indicate that the N-terminal region of actin, residues 1-28, contain an important biological binding site for myosin.

W-Pos52

A STOCHASTIC ANALYSIS OF THE TRANSLOCATION OF FILAMENTS BY IMMOBILIZED MOTORS. E. Pate and R. Cooke. Depts. Math., Wash. St. Univ. & Biochemistry, Univ.Calif. San Francisco.

Recently developed techniques have allowed observations of the translocation of actin or tubulin filaments by myosin or kinesin motors immobilized on a fixed substrate. In order to better understand these data, we have used the Huxley (1957) cross-bridge model to investigate filament translation velocity as a function of substrate concentration and motor number. At physiological substrate concentration, velocity is observed experimentally to increase with increasing cross-bridge density in the actomyosin assay (Uyeda et al, JMB, 1990). Microtubule translation velocity, on the other hand, is independent of kinesin density at high [ATP], while decreasing with increasing motor density at low [ATP] (Howard et al, Nature, 1989). We show that translation velocities can vary with cross-bridge density. One motor translates a filament slower (faster) than many motors if the attachment rate at the beginning of the powerstroke is less than (greater than) the detachment rate at the end of the powerstroke (x less than 0). The velocity generated by a single motor will equal that of many motors if the two above rates are equal to each other. Analytical expressions are provided to quantitate this relationship for the important, limiting cases of one motor and an infinite number of motors. These expressions also allow one to explain variation in sliding velocity with respect to ATP concentration. For all of the above cases the ATPase activity decreases as the density of motors increases from one to infinity. Taken together, these results allow one to better interpret experimental data from in vitro assays in terms of models for motor function. Supported by USPHS grants HL32145 (RC), AR39643 (EP), and the Muscular Dystrophy Association (RC). EP is an American Heart Association Established Investigator.

W-Pos53

RELATION BETWEEN THE AMOUNT OF WORK DONE BY ACTIN-MYOSIN SLIDING AND THE AMOUNT OF IONTOPHORETICALLY APPLIED ATP STUDIED USING AN IN VITRO ASSAY SYSTEM CONTAINING GLUCOSE AND HEXOKINASE.
K. Oiwa, S. Chaen, and H. Sugi. Dep. of Physiol., Sch. of Med., Teikyo Univ., Tokyo 173, Japan.

To study the nature of actin-myosin sliding coupled with ATP hydrolysis, we combined our in vitro force-movement assay system (Chaen et al. Proc. Natl. Acad. Sci. USA 86: 1510-1514, 1989) with the technique of iontophoretic ATP application. A glass microneedle coated with rabbit skeletal muscle myosin was made to slide on actin cables in the internodal cell of an alga (Nitellopsis obtusa) by iontophoretic application of ATP from the ATP electrode placed 20-30μm distant from the needle. The needle was made rigid, so that the maximum needle movement, recorded photoelectrically, was limited to 1μm. To prevent accumulation of released ATP in the experimental chamber after repeated application of ATP, the surrounding medium contained 50Unit/ml hexokinase and 2mM glucose. As the myosin on the needle formed rigor linkages with actin cables in the absence of ATP, we could change the baseline force before ATP application with the mechanical stage carrying the chamber. For a given baseline force, the distance of needle movement on actin cables increased almost linearly with increasing amount of iontophoretically applied ATP. The slope of the movement versus ATP relation increased with increasing baseline force from zero to 0.5-0.6P_o, indicating an increase in apparent efficiency of actin-myosin sliding in utilizing ATP for work production. If the movement versus ATP relation at zero baseline force was extrapolated the movement axis at about 30nm. Since only 250-750 myosin heads are involved in the ATP-induced needle movement, the value may correspond to the distance of actin-myosin sliding per hydrolysis of one ATP molecule under unloaded conditions.

W-Pos54

EFFECT OF PARTIAL INACTIVATION OF MYOSIN HEADS ON THE ATP-DEPENDENT ACTIN-MYOSIN SLIDING.
S. Chaen, A. Muraoka and H. Sugi. Dept. Physiol., Sch. Med., Teikyo Univ., Itabashi-ku, Tokyo 173, Japan

To investigate possible cooperative interaction of two myosin heads in muscle contraction, the sliding velocity of fluorescenctly labelled F-actin on heavy meromyosin(HMM) fixed to a nitrocellulose film was measured after partial inactivation of myosin heads with p-phenylenedimaleimide (PDM), n-ethylmaleimide (NEM) or p-nitrophenylmaleinide (NPM). Two different kinds of HMM samples were used; one kind of samples were mixtures of native and totally inactivated HMM, while the other kind of samples were made by partial modification of HMM and consisted of HMM with zero, one and two inactivated heads. EDTA-ATPase activity was also measured for each HMM sample.

Analysis of the relation between the proportion of inactivated heads (determined by EDTA-ATPase activity) in the PDM-inactivated HMM samples and the F-actin sliding velocity on the HMM sample showed that the F-actin sliding velocity may be produced only by the HMM with two native heads. This implies that , if one head of HMM is inactivated with PDM, the other heads can still hydrolyze ATP but can not participate in the F-actin sliding. In the NEM- or NPM-inactivated HMM samples, on the other hand, the F-actin sliding was shown to be produced by all native heads irrespective of whether the other head of HMM was native or inactivated. The above difference in the inactivating effect between PDM and NEM and NPM may result from that the former is bifunctional while the other two are monofunctional. When the PDM-inactivated HMM was digested to S-1, the F-actin sliding was produced by all native S-1. These results indicate that one PDM-inactivated head suppresses the activity of the other native head of HMM in producing the F-actin sliding, while each native head has potential ability to cause F-actin sliding. It remains to be determined whether the two myosin heads in each myosin molecule in a cooperative manner or not in the physiological contraction.

W-Pos55

DIVERSITY OF SPEEDS OF MOVEMENT OF ACTIN FILAMENTS BY MYOSIN IN AN IN VITRO MOTILITY ASSAY
G.Cuda, D.Li[#], P.D. Chantler[#], E.Homsher[+] and J.R. Sellers, NHLBI, NIH, Bethesda, MD, [+]Dept. Physiol., UCLA, Los Angeles, CA and [#]Dept. Anat., Med. Coll. Penn., Philadelphia, PA.

The sliding actin *in vitro* motility assay is a quick and quantitative method for determining the relative sliding rates of actin and myosin which correlates with the unloaded shortening velocity of muscle fibers. We used this assay on myosins isolated from various muscles and cell types and have observed, under identical ionic conditions of low ionic strength and 25°C, a wide range of sliding speeds. The slowest myosin measured thus far is bovine brain myosin II. It moves actin filaments at less than 0.02 um/s which is significantly less than the rate of 0.04 um/s for myosin II from human platelet or chicken intestinal epithelial brush border. There are at least two isoforms of nonmuscle myosin II, termed A and B by Kawamoto and Adelstein (J.Cell Biol. in press). Brain myosin appears to be about 80% B whereas brush border (and probably platelet) are almost 100% A. The bovine brain myosin has K^+EDTA, MgATPase and actin-activated MgATPase activities similar to published brain myosin preparations. Bovine aorta smooth muscle myosin moves actin at 0.13 um/s while that from turkey gizzard moves actin at 0.2 um/s. Dog cardiac myosin moves actin at 0.53 um/s (see abstract by Margossian et al.). Rabbit slow skeletal muscle (purified from soleus) translocates actin filaments at 0.54 um/s whereas that from fast muscle moves at 3.9 um/s. Myosin from the catch muscle of the clam *Mercenaria mercenaria* moves actin at 2 um/s while that of the adductor muscle moves at 6 um/s. The fastest motion we measured is from extracts of the alga *Nitella axillaris* which move actin filaments at rates from 30-60 um/s (Rivolta et al. Biophys. J. 57:535a, 1990). The mechanism responsible for this diverse range of velocities is currently being studied. (Supported in part by NIAMSD grant #AR32858 to PDC and AR 30988 to EH).

W-Pos56

INVOLVEMENT OF CARDIAC MYOSIN HINGE REGION AND LC1 IN CONTRACTILE SHORTENING AND MOTILITY.

S.S. Margossian[*], J.W. Krueger[‡], J.R. Sellers[§], G. Cuda[§] and H.S. Slayter[+]. [*]Montefiore Med. Ctr. and [‡]Albert Einstein Col. Med., Bronx, N.Y.; [§]Lab. of Mol. Cardiol., NIH, Bethesda, MD and [+]Dana-Farber Cancer Inst. and Harvard Med. Sch., Boston, MA.

We have used cardiac myocytes and myosin to investigate the participation of the hinge in active unloaded shortening and motion. A polyclonal antibody was raised to a synthetic peptide 20 amino acids long flanking the S2/LMM junction (Kavinsky et al., JBC 259, 2775, 1984). The specificity of the hinge antibody was tested by RIA inhibition studies using affinity purified anti-hinge IgG competing with ^{125}I-hinge peptide. Also six myosins including human normal and myopathic, dog and rat cardiac myosins as well as turkey gizzard and rabbit skeletal muscle myosins were competed in this assay system. All of the cardiac myosins exhibited strong inhibition. The specificity of the antibody for skeletal myosin was somewhat less, while turkey gizzard myosin essentially did not interact. Immunoelectron microscopy of platinum-shadowed complexes of cardiac myosin demonstrated that the antibody binding site was about 55nm from the the S1/S2 junction which, when the size of the IgG was considered, was well within the expected hinge site on the myosin tail. In functional studies, the antibody to hinge peptide did not interfere with myofibrillar Ca^{++}-activated MgATPase. However, the movement of fluorescently-labeled actin by myosin bound to a glass surface was almost completely inhibited in the presence of the antibody. Anti-LC1 also inhibited the motility and the Ca^{++}-activated MgATPase of the myofibrils. Furthermore, when triton-permealyzed rat heart myocytes were incubated with the antibody, the extent of sarcomere shortening decreased by half relative to both the control and myocytes incubated in the presence of nonimmune IgG. In several instances shortening was fully suppressed. Our observations, conducted under very low resistance to shortening, suggest a modification at the hinge is transmitted along S2 but the mechanism of this communication and its influence upon acto-S1 interaction remain to be clarified.

W-Pos57

ACTOMYOSIN COMPLEXES, BINDING SITES, AND ATPase ACTIVITY.

Mike Mynt, Carl Miller, Theresa Chen, and Emil Reisler. Molecular Biology Institute, and the Department of Chemistry and Biochemistry, UCLA, Los Angeles, CA. 90024.

The superactivation of acto-S1 ATPase activity in cross-linked acto-S1 was examined by using acto-S1 cross-linked with two different reagents, DMS and EDC. Both types of cross-linked complexes exhibited similar salt-sensitivity in their ATPase activities, analogous to the SH_1 modified S1. The relationship between the N-terminus of actin and the superactivation of cross-linked complexes was examined by using anti-actin N-terminus antibodies. The antibodies inhibited the ATPase activities of both cross-linked complexes by about 50-60%. This was in contrast to the 100% inhibition achieved in reversible acto-S1 complexes (DasGupta and Reisler, JMB 207: 833, 1989). This results is consistent with the essential role of the N-terminus of actin in acto-S1 ATPase reaction and shows that the binding of Fab does not completely block the interaction between S1 and the N-terminus of actin in the cross-linked complexes.

The environment of the SH_1 site in acto-S1 complex was examined in the presence and absence of MgADP. Quenching experiment of fluorescein attached to the SH_1 site of S1 by both anti-fluorescein Fab and nitromethane verified that the probe was more protected in acto-S1 than in the free S1. Addition of MgADP reversed that protection to a large extent without significant dissociation of S1 from actin. Thus, the fluorescein probe reported a specific MgADP-induced conformational change in the SH_1 site of acto-S1.

W-Pos58

SIMPLE EXPRESSIONS FOR THE SINGLE HEADED INTERACTION OF HMM WITH ACTIN IN THE PRESENCE OF ATP.

LEONARD A. STEIN, LABORATORY OF MOLECULAR CARDIOLOGY, SUNY AT STONY BROOK MEDICAL CENTER.

PRIOR DETAILED ANALYSIS OF THE BINDING OF HMM TO ACTIN IN THE ABSENCE OF ATP HAVE COME TO THE CONCLUSION THAT HMM BINDING IS MUCH WEAKER THAN EXPECTED(1,2). THIS IMPLIES THAT SIGNIFICANT HEAD-HEAD INTERACTIONS ARE OCCURRING IN THE HMM MOLECULE DURING TWO HEADED BINDING. IN THE PRESENCE OF ATP THE BINDING OF EACH MYOSIN HEAD TO ACTIN IS GREATLY REDUCED, AND CONSIDERING THE SIGNIFICANT HEAD-HEAD INTERACTIONS PRESENT, THIS SUGGESTS THE POSSIBILITY THAT HMM BINDS WITH ONLY ONE HEAD AT A TIME IN THE PRESENCE OF ATP. IF IT IS ASSUMED THAT HMM CONSISTS OF TWO IDENTICAL S-1 MOLECULES WITH KNOWN KINETIC CONSTANTS, AND THAT ONLY ONE HMM HEAD CAN BIND ACTIN AT A TIME, THEN SIMPLE EXPRESSIONS FOR THE KINETIC PARAMETERS FOR HMM CAN BE DERIVED FROM A PROBABILITY ARGUMENT; AND THESE EXPRESSIONS ARE AS FOLLOWS:

1. K^{HMM}(DISSOCIATION) = (K^{S-1}(DISSOCIATION))/2

LET K^{S-1}(DISSOCIATION)/K^{S-1}(ATPase) = N,

THEN 2. K^{HMM}(ATPase) = (N/(N+1))K^{S-1}(ATPase)

AND 3. V^{HMM}_{MAX} = (N/(N+1))V^{S-1}_{MAX} (PER HEAD)

FIRST NOTE THAT K^{HMM}(DISS)/K^{HMM}(ATPase)=(N+1)/2, AND THEREFORE THIS RATIO IS ALWAYS LESS THAN OR EQUAL TO N (i.e. K(ATPase) APPROACHES K(BINDING) FOR HMM). FOR SKELETAL S-1 WE FIND THAT N=4-5, HENCE IN COMPARISON TO S-1, HMM HAS ABOUT A 20% REDUCED V_{MAX} AND A 20% STRONGER K(ATPase). NOTE THAT THE SLOPE OF THE DOUBLE RECIPROCAL PLOT FOR HMM IS THE SAME AS S-1, ALTHOUGH THE INTERCEPT IS DIFFERENT. PRELIMINARY EXPERIMENTS IN MY LABORATORY ARE CONSISTENT WITH THESE EXPRESSIONS.

(1)GREENE AND EISENBERG(1980),JBC,255,P549
(2)HILL AND EISENBERG(1980),BIOPHYS.CHEM.,11,271

SUPPORTED BY N.Y.STATE AHA AND AMER. CANCER SOC.

W-Pos59

SELECTIVE EFFECTS OF IONIC LIGANDS AT CATALYTIC AND REGULATORY SITES OF ACTO-S1 ATPase.

Jian Feng and Paul Dreizen. (Intr. by Manfred Brust) Graduate Program in Physiology & Biophysics, State University of New York Health Science Center at Brooklyn, New York 11203.

Previous experiments have shown that the interaction between myosin subfragment-1 (S1) and F-actin is highly sensitive to specific ionic ligands. The actin-activated Mg-ATPase of skeletal and cardiac myosin S1 can be analyzed in terms of competitive inhibition of the acto-S1 interaction at a small number (approximately three) of mutually exclusive anionic inhibitory sites and a single Mg^{++} inhibitory site, with different inhibitory constants in the millimolar range for each S1 isoform. The inhibitory sites are presumed to be located away from the catalytic site of acto-S1 ATPase. The original studies are largely based on data in which free Mg^{++} and free nucleotides were varied in the presence of 1 mM MgATP at 25°C. We have extended the earlier studies on rabbit fast-twitch myosin S1 isoforms so as to vary free Mg^{++} and free nucleotide at different MgATP concentrations and at different temperatures in order to distinguish the relative contributions of the selective ionic effects at regulatory sites and catalytic sites on myosin S1. The plots of velocity at constant concentrations of nucleotide or Mg^{++} show characteristic peaks at equimolar Mg^{++} and ATP. The inhibitory effects of free Mg^{++} and free nucleotides above equimolar MgATP are consistent with a kinetic model of 3 anionic sites and 1 Mg^{++} site. The decrease of velocity at free ligand concentrations below equimolar MgATP can also be explained by a model with the same kinetic constants. The overall data are consistent with saturation of the catalytic site, as expected, and a predominant effect of free nucleotide, free Mg^{++}, and MgATP at regulatory sites on myosin S1. Similar phenomena but with different kinetic constants are found for LC1 and LC3 isoforms. These findings confirm that ionic strength effects on acto-S1 ATPase largely involve selective ionic interactions at weak-binding regulatory sites on myosin S1.

W-Pos60

DIFFUSION OF HEAVY MEROMYOSIN IN THE PRESENCE OF ACTIN AND ATP.

Julian Borejdo and Smaranda Burlacu, Baylor Research Foundation, Baylor University Medical Center, 3812 Elm St., Dallas, TX 75226.

We looked for the evidence that diffusion of heavy meromyosin (HMM) is enhanced (facilitated) during its mechanochemical interaction with actin. To be able to observe diffusion in one dimension, we electrophoresed the complex of F-actin and fluorescent HMM in agarose gels in thin capillaries. The intensity profile of the electrophoretic band of the complex showed a sharp peak, which in 1% agarose in the electric field of 17.8 V/cm at room temperature migrated at 3.2 cm/hr. The time evolution of the profile after the electrophoresis was ended was a measure the diffusion of HMM. To enhance fraction of HMM bound to actin in the presence of MgATP, the experiments were done in 20 mM K-Acetate, 5 mM TRIS-Acetate pH 7.5 at room temperature using excess of actin. Fluorescent profiles were measured after 10 min incubation in rigor, relaxing and contracting solutions. In relaxing solution HMM was able to diffuse freely in the gel suggesting that agarose matrix did not impede free diffusion of HMM. In the presence of MgATP, the profile became broader and weaker, and the position of its maximum was unchanged relative to the profile in rigor solution. The diffusion coefficient of HMM diffusing over actin in the presence of ATP, as calculated from the time evolution of the profile, was 3.4×10^{-7} cm^2/sec. This was 5% smaller than the coefficient of freely diffusing HMM. The fact that diffusion coefficient of HMM diffusing in the presence of actin and ATP was by 5% smaller than diffusion coefficient of free HMM is interpreted to indicate that there is 90% probability that during the interaction of F-actin and HMM the facilitated diffusion does not occur.
Supported by NIH RO1 AR40095-01.

W-Pos61

KINETICS OF MYOFIBRILLAR ATPase. A COMPARISON WITH MYOSIN SUBFRAGMENT 1.

M.Houadjeto, F.Travers and T.Barman.INSERM U128, CNRS, BP 5051, 34033 Montpellier Cedex1, France.

A problem in muscle research is to determine the relation between the ATPase activity of the myosin heads and the physiological events involved in contraction. Most kinetic work has been carried out with actin and myosin in solution and under unphysiological conditions. We have studied the ATPase activity of Ca^{2+} activated and relaxed myofibrils in a solvent of pH and ionic strength that are nearly physiological : pH7.4 and 0.1 M K-acetate. Because of the rapidity of ATP hydrolysis at 37°C, the experiments were carried out in a rapid flow quench apparatus at 4°C. Two types of experiment were carried out : cold ATP chase ([γ-^{32}P]ATP + myofibrils reaction mixtures quenched in cold ATP) and Pi burst (reaction mixtures quenched in acid). The first type gives information on the kinetics of the initial binding of ATP and the second on the kinetics of the cleavage and release of Pi steps. Both give information on the steady state rate of ATP hydrolysis.

From the results of chase experiments, it appears that myofibrils (activated or relaxed) bind ATP as tightly as does S1. The second order binding constants were similar for the three materials (1×10^6 M^{-1} s^{-1}). In Pi burst experiments with activated myofibrils there were three phases: a rapid formation of Pi, a short linear ATPase activity (about 2 s^{-1}; this lasted for about 1s) and a progressive loss of activity. From microscopic observations we propose that phases 1 and 2 occur during the shortening of the myofibrils and that phase 3 occurs with overcontracted myofibrils with a progressive loss of structure. With relaxed myofibrils there were only two phases: a rapid formation of Pi (phase 1) followed by a steady state rate similar to that with S1 (0.02s^{-1}). Here the myofibrillar stucture appeared to remain intact. We propose that phase 1 is due to a Pi burst of myosin.ADP.Pi : the amplitude (0.8 mol Pi per mol myosin head) and kinetics (10 s^{-1}) of this are similar for activated and relaxed myofibrils and S1. In conclusion, we find that at 4°C and in a solvent that is nearly physiological, activated myofibrils bind and hydrolyse ATP with transient kinetics very similar to those found with S1. But the kcat of the myofibrils was 100x that with S1. Relaxed myofibrils and S1 could not be distinguished kinetically.

W-Pos62

TIME- AND ANGLE-RESOLVED PHOSPHORESCENCE ANISOTROPY OF EOSIN-LABELED MYOSIN HEADS IN MUSCLE FIBERS

Richard A. Stein and David D. Thomas.
Dept. of Biochem., U. of Minn., Minneapolis, MN 55455

We have measured the phosphorescence emission anisotropy of eosin-maleimide labeled myosin heads in muscle fibers with the fiber oriented at several angles relative to the excitation polarization. Measurements of the initial and final anisotropies (r_o and r_∞) with the fiber at different tilt angles (α) provides information about the orientational distribution (and thus the amplitude of rotational motion) of the probe relative to the fiber axis in different chemical and mechanical states of the muscle fiber. The rate of exponential decay from r_o to r_∞ indicates the rate of rotational motion. When the muscle fiber is oriented parallel to the excitation polarization (α=0°) the anisotropies for rigor, relaxation, and contraction are all positive and contraction is intermediate between rigor and relaxation. Tilting the fiber to α=30° causes changes in r_o and r_∞, but contraction is still intermediate between rigor and relaxation. Further tilting of the fiber to α=60° causes the anisotropy to become negative in rigor and relaxation, whereas the contraction decay is positive and thus not intermediate between the decays for rigor and relaxation. These results clarify the distinct angular and dynamic properties of myosin heads in these chemical and mechanical states.

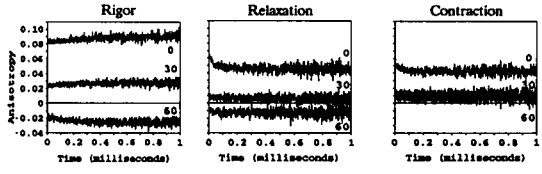

W-Pos63

Microsecond Rotational Motions of Myosin Heads Bound to Actin in the Presence of AMPPNP and ATPγS

Christopher L. Berger and David D. Thomas
University of Minnesota Medical School
Minneapolis, Minnesota 55455

We have previously shown (Berger *et al*, **P.N.A.S.** 1989) that spin-labeled myosin subfragment one (MSL-S1) bound to actin during the steady-state hydrolysis of ATP is mobile on the microsecond time-scale, with an effective rotational correlation time (τ_r) of 1.0 microseconds (μsec). Complementary experiments with the spin-label attached to actin instead of S1 indicate that the S1 is rotating relative to actin under these conditions (Ostap and Thomas, submitted to the **Biophysical Journal**). In the present study we are attempting to determine which actin-attached intermediates of the myosin ATPase cycle correspond to the actin-attached mobile S1 states observed during steady-state ATP hydrolysis. The ATP analogs AMPPNP and ATPγS are being used to trap S1 in states that are assumed to be intermediates in the acto-myosin ATPase cycle. The rotational motion of MSL-S1 bound to actin in the presence of AMPPNP or ATPγS has been measured using saturation-transfer electron paramagnetic resonance (ST-EPR), a technique that is sensitive to microsecond rotational motions. The fraction of actin-attached myosin heads in the presence of either AMPPNP or ATPγS have been determined from sedimentation experiments, and used to analyze the ST-EPR spectra in terms of the actin-attached MSL-S1. MSL-S1 has a high affinity for actin in the presence of AMPPNP, and the actin-attached myosin heads are immobile on the microsecond time-scale, just as in rigor (no nucleotide present). In the presence of ATPγS, MSL-S1 has a weak affinity for actin, and we are attempting to determine an effective rotational correlation time for the actin-attached myosin heads.

W-Pos64

A SPIN LABEL THAT DETECTS DIRECTLY THE AXIAL ROTATION OF MYOSIN HEADS IN MUSCLE FIBERS

Osha Roopnarine and David D. Thomas, Dept. of Biochemistry, University of Minnesota Medical School, Minneapolis, MN 55455

We have attached an indane dione nitroxide spin label (InVSL, kindly provided by Professor Kalman Hideg, Univ. of Hungary, Pecs) to myosin heads in glycerinated rabbit psoas muscle fibers. EPR spectra of fibers parallel to the magnetic field show that this spin label's orientation relative to the head makes it complementary to all spin labels previously studied in this system. In the absence of ATP, the label's principal axis is aligned almost perfectly with the muscle fiber axis. This makes it the first spin label capable of providing unambiguous information about axial rotations of the myosin head, as proposed in most molecular models of muscle contraction. The EPR spectrum of labeled fibers (aligned parallel to the magnetic field) shows an oriented (SH1-bound) and a disordered (non-specifically bound) population of spin labels. For the oriented population, the mean axial orientation of the probe's principal axis, (Θ_o), and the distribution about the mean angle ($\delta\Theta$, full width at half maximum) are 0-5° and 10-20°, respectively (determined from simulated EPR spectra, using the simplex fitting program of Fajer et al, 1990). Relaxation with MgATP broadens (but does not completely randomize) the angular distribution of heads, while MgADP causes a small axial rotation ($\leq$ 8°) of the heads.

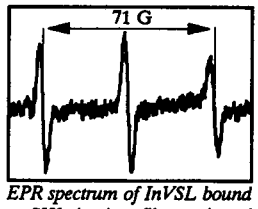

EPR spectrum of InVSL bound to SH1, in rigor fibers oriented parallel to the magnetic field

W-Pos65

STEADY-STATE PHOSPHORESCENCE STUDIES OF THE ROTATIONAL DYNAMICS OF SKELETAL MUSCLE THICK AND THIN FILAMENTS.

Richard D. Ludescher, Nano Mardones, and Zane D. Liu, Department of Food Science, Rutgers University, New Brunswick, NJ 08903-0231.

We have labeled myosin and actin from rabbit skeletal muscle with the triplet probe erythrosin-5-iodoacetamide. Biochemical, enzymatic, and spectroscopic analyses indicate that the probes are attached to the fast reacting sulfhydryl (SH1) in the myosin heavy chain and at cys-374 in actin with labeling stoichiometries of 0.7 to 0.9 probe molecules per polypeptide chain; steady-state fluorescence anisotropy measurements indicate that the probes are rigidly attached to the protein's surface. The probes will thus monitor the rotational motion(s) of myosin and actin filaments on the microsecond time scale.

The steady-state phosphorescence anisotropy (r_p) of erythrosin-labeled proteins has been measured using a pulsed Xe lamp and an average over the time window from 0.07 to 1.0 ms. Under conditions in which the proteins are monomeric (myosin at 500 mM or actin at 5 mM ionic strength) r_p is 0.0 for either protein; isotropic rotational motion of the monomers thus occurs during the dead time of our instrument (0.07 ms). Under conditions that favor filament formation (myosin at 125 mM or actin at 50 mM ionic strength), r_p increases to 0.03 for myosin and 0.05 for F-actin (at 20°C). Titration of the myosin filaments with divalent cation (CA^{++} or Mg^{++}) has little effect on the anisotropy at pH 7.0; at pH 8.2, however, the anisotropy increases. r_p appears to be sensitive to the spread-compact transition that occurs in myosin filaments.

The steady-state phosphorescence emission anisotropy can thus provide a rapid, accurate, and inexpensive measure of slow rotational motions in muscle protein filaments.

(Supported by the American Heart Association--New Jersey Affiliate, the Muscular Dystrophy Association, and the New Jersey Agricultural Experiment Station.)

W-Pos66

ALTERED CARDIAC CONTRACTILE RESPONSE IN THE PRESENCE OF HISTONE PROTEINS. M.V. Westfall*, A.F. Martin*, K.L. Ball*, R.J. Solaro*. *Dept. of Physiol. & Biophys., Univ. of Illinois, College of Medicine, Chicago, IL, and *Dept. of Pharmacol. & Cell Biophys., Univ. of Cincinnati Medical School, Cincinnati, OH.

Histones often co-purify with preparations of cardiac myofibrils. Their effect on myofibrillar function has not been thoroughly investigated. We measured myofibrillar Ca^{2+}-dependent Mg^{2+}-ATPase activity in the presence and absence of exogenous histones (calf thymus; U.S. Biochem. Corp.). Addition of histones (0.05 mg/mg protein) elevated rat heart actomyosin ATPase activity (pH 7.0) at low Ca^{2+} concentrations but significantly reduced maximal ATPase activity. When ATPase values normalized to maximum activity were analyzed with the Hill equation, the pCa_{50} was enhanced and the Hill coefficient was diminished in the presence of histones. A similar trend was observed when myofibrils were incubated at pH 6.50. Addition of histones at higher Ca^{2+} concentrations was also associated with reduced tension in left ventricular cardiac muscle preparations skinned with Triton X-100. The influence of histone proteins on ATPase activity and tension development should be considered when interpreting experiments where variable amounts of histones may co-purify with myofibrils. Supported by NIH Grants HL-22231 and HL-08059.

W-Pos67

OPIOID PEPTIDE INCREASES pH AND CONTRACTILE RESPONSE TO CALCIUM IN CARDIAC MYOCYTES.

Carlo Ventura, Maurizio C. Capogrossi, Harold A. Spurgeon, Edward G. Lakatta (Intro. by Paul S. Blank). Gerontology Research Center, NIA, NIH, Baltimore, MD

The intracellular effects of opioid peptides on cardiac myocytes are incompletely understood (Biophys. J. 57: 294a, 1990). Here we report that a rapid, transient application (via pico spritzes) of a κ receptor agonist, U50,488H (U-50), to individual isolated rat cardiac myocytes causes a transient increase in cytosolic pH (measured via SNARF-1 fluorescence, Fig. A). U-50 spritzed onto the cell also causes a phasic increase in Ca_i (measured via Indo-1 fluorescence) and a contraction (Fig. B); the relation between the Ca_i and contraction amplitude is much steeper than when Ca_i is increased by caffeine (Fig. B and C). Both the pH increase and enhanced contractile response to Ca^{2+} by U-50 are abolished by blockade of the Na/H exchanger by ethyl isopropyl amiloride or by inhibition of protein kinase C (PKC) activity via pretreatment with staurosporine or prolonged incubation with phorbol myristate acetate. Thus, the observed U-50 effects are likely mediated via PKC activation of the Na/H exchanger.

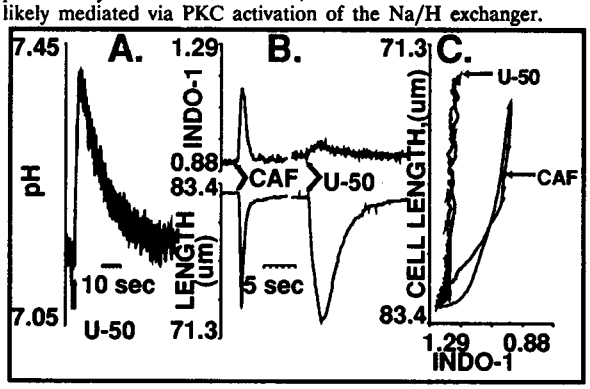

W-VCR1

A VOLTAGE DEPENDENT MOTOR IN THE LATERAL WALL OF COCHLEAR OUTER SENSORY CELLS

F. Kalinec[1], K. Iwasa[2], D. Lim[3] and B. Kachar[1] (Intro. by T.S. Reese). [1]Lab. of Mol. Otol. NIDCD, [2]Biophysics Lab. NINDS, NIH, Bethesda, MD, and [3]Department of Otolaryngology, Ohio State University, Columbus, OH.

We used video enhanced microscopy and freeze-etching electron microscopy to analyze the basis of the electrically evoked rapid contractile activity of auditory outer sensory cells (OSC) isolated from guinea pig cochlea (Kachar et al., Nature, 322: 365, 1986). Cyclic contractile responses in OSC were evoked by sinusoidally modulated electrical potentials applied either by i) electrodes placed across the cell; or ii) by a patch pipette in the whole cell clamp mode; or iii) to small cylindrical membrane blebs obtained from the lateral plasma membrane of mechanically disrupted cells by a suction patch pipette. During elongation and shortening of OSC in response to stimulation with electrodes across the cell body, the lateral wall of the cells shows displacements with amplitudes proportional to the distance to the points where the cell body is fixed to the microscope slide. In whole-cell clamp mode the amplitude of the displacements is proportional to the distance to the pipette attachment site. Application of oscillatory voltage changes to small cylindrical membrane blebs formed by the patch pipette produce elongation and shortening of the bleb. Membrane hyperpolarization always produces elongation and depolarization always produces shortening of the membrane blebs independent on the position along the lateral wall where they were formed, and independent of the remaining cytoplasmic organization of the cell. These results indicate that the voltage sensitive motility is a property ubiquitous to any local microdomain of the lateral wall. The elongation and shortening of the intact cell could result from a cumulative effect of this phenomenon along the entire lateral wall.

When examined by freeze-etching, the lateral plasma membrane of OSC shows a unique distribution of densely packed large intramembrane particles that form a highly ordered orthogonal lattice. We postulate that interacting transmembrane proteins of this lattice respond with conformational changes to changes in the membrane potential. These structurally associated membrane proteins might act in a cooperative manner, and the integrated electroconformational change could power the mechanical response of the cell.

W-Pos68

CHANGES IN INTRACELLULAR SODIUM AND pH DURING RESPIRATORY ACIDOSIS IN RAT VENTRICULAR MYOCYTES.

By Simon M. Harrison, Eileen McCall, Mark R. Boyett & Clive H. Orchard, Department of Physiology, Univeristy of Leeds, LS2 9JT, U.K.

During respiratory acidosis, contractile strength initially falls and then exhibits a slow partial recovery. We have investigated the role of a^i_{Na} and pH_i in this biphasic change of contractility. Rat ventricular myocytes were loaded with the acetoxymethyl ester of either SBFI or BCECF to measure a^i_{Na} or pH_i, respectively. The cells were superfused with bicarbonate buffered salt solutions. To induce acidosis, the superfusate was changed from one equilibrated with 5% CO_2 (pH_o 7.3) to one equilibrated with 15% CO_2 (pH_o 6.8).

The initial acidosis-induced decrease of contractility was associated with a rapid fall of pH_i with little change in a^i_{Na}. The partial recovery of cell shortening during acidosis was associated with an increase of a^i_{Na} from 6 ± 1 mM to 9 ± 1 mM (n=6) with little change in pH_i. During the partial recovery of contractility, twitch shortening was linearly related to a^i_{Na}, the mean slope of the twitch shortening *vs* a^i_{Na} relationship being 2.1 ± 0.4 μm/mM rise of a^i_{Na} (n=5). The slope of this relationship was very similar to that observed in rat ventricular myocytes during inhibition of the Na-pump with strophanthidin (1.8 ± 0.2 μm/mM rise of a^i_{Na}, n=5) suggesting that a^i_{Na} plays a pivotal role in determining contractility during the partial recovery of cell shortening during acidosis.

We conclude that the initial reduction of cell shortening is primarily a result of the decrease in pH_i and may reflect in part a reduction of myofilament Ca^{2+}-sensitivity. The slow recovery of contractility may be a result of Na^+ loading via Na-H exchange leading to an increase of Ca^{2+} via Na-Ca exchange.

W-Pos69

VANADATE PHOTOOXIDATION OF 6S AND 10S GIZZARD MYOSIN: IDENTIFICATION OF AN ACTIVE SITE SERINE

Douglas G. Cole and Ralph G. Yount
Department of Biochemistry/Biophysics
Washington State University, Pullman WA 99164-4660

Vanadate (V_i) forms a stable transition state-like complex with MgADP at the active site of myosin. The half-lives of both 6S and 10S gizzard myosin•MgADP•V_i complexes are >7 days in the dark. Irradiation with UV light for 5 min, however, photomodified the enzyme and destablized the complexes. Reduction of photomodified 6S and 10S myosins by NaB^3H_4 resulted in the incorporation of ^3H into serine (Cole, D. G., and Yount, R. G. (1989) *Biophys. J.* **55**, 77a), suggesting that a serine aldehyde had been generated as previously shown for photomodified skeletal myosin S1 (Cremo *et al.*, (1989) *J. Biol. Chem.* **264**, 6608-6611). The [^{3}H]-serine was localized to the 29-kDa NH_2-terminal tryptic fragment of the heavy chain of both 6S and 10S gizzard myosin. [^{3}H]-Labeled subfragment 1 preparations isolated from both 6S and 10S photomodified and reduced myosins were exhaustively digested by trypsin and a single radioactive peptide was isolated by HPLC. The sequence was E-D-Q-S-I-L-(C)-T-G-E-[^{3}H]S-G-A-G-K, corresponding to residues 169-183 in the gizzard myosin heavy chain (Yanagisawa *et al.*, (1987) *J. Mol. Biol.* **198**, 143-157). These results place Ser-179 at the γ-phosphate-binding site for ATP and provide further evidence that this glycine-rich region provides critical elements to bind the phosphates of ATP. Supported by MDA and NIH (DK 05195).

W-Pos70

PHOTOAFFINITY LABELLING OF SMOOTH MUSCLE MYOSIN WITH 2-N_3-ATP

Shinsaku Maruta and Mitsuo Ikebe
Department of Physiology & Biophysics, School of Medicine, Case Western Reserve University, Cleveland, OH 44106

Photoreactive ADP analogue, 2-N_3-ADP labelled with radioisotope (^{32}P β-phosphate) was synthesized and used as a probe to study the conformational change of adenine binding site of smooth muscle myosin due to phosphorylation of 20kDa light chain and 10S-6S conformational transition. 2-N_3-ADP was trapped in smooth muscle myosin in the presence of AlF_4^-. 0.5-0.6 mol of 2-N_3-ADP/ mol myosin head was trapped. After removing excess amount of 2-N_3-ADP, myosin/2-N_3-ADP/AlF_3 ternary complex was irradiated at 0°C with 450W Hg medium pressure lamp. Short wavelength UV was cut with pyrex petri dish cover. When phosphorylated HMM/2-N_3-ADP/AlF_3 complex was irradiated, about 50% of total incorporated 2-N_3-ADP was observed into 68kDa N-terminus fragment and 25% was incorporated into the 20kDa light chain. On the other hand, when the dephosphorylated HMM was irradiated, only 68kDa fragment was labelled with 2-N_3-ADP. The labelled HMM was digested by trypsin and it was found that tryptic 29kDa N-terminus fragment was labelled specifically. Phosphorylated S-1(SAP) and dephosphorylated S-1 were also labelled with the same method. Only 68kDa N-terminus fragment was labelled specifically for both phosphorylated and dephosphorylated S-1. Since the ATPase activity of HMM is regulated by phosphorylation but that of S-1 is not, these results may suggest that the phosphorylation induces the change in the relative position of the adenine binding site and the regulatory light chain so as to alter the ATPase activity.
(Supported by NIH, AHA & Syntex)

W-Pos71

GIZZARD MYOSIN MODIFICATION WITH THE SULFHYDRYL MODIFYING REAGENT, ACRYLODAN. Susannah J. Rogers and Leslie E. Sommerville, Department of Chemistry, St. Lawrence University, Canton, N.Y. 13617

Attempts at labeling gizzard myosin with sulfhydryl modifying reagents such as N-((2-(iodoacetoxy)ethyl)-N-methyl)amino-7-nitrobenz-2-oxa-1,3-diazole (IANBD), 5-(2-((iodoacetyl)amino)-ethyl)amino)naphthalene-1-sulfonic acid (1,5-IAEDANS), and 2-(4'-maleimidylanilino)naphthalene-6-sulfonic acid (MIANS) have resulted in nonspecific labeling of myosin. Preliminary results with 6-acryloyl-2-dimethylaminonaphthalene (acrylodan) indicate that this modifying reagent could modify gizzard myosin in a more specific way. The ratio of acrylodan to myosin was estimated (determined by UV-VIS absorbance spectroscopy) to be 2 to 1 after modification under conditions where the myosin was in the folded 10S conformation. When the myosin was in the 6S conformation the acrylodan to myosin ratio was found to be consistently higher (3 to 1 or greater.) SDS-PAGE followed by visualization using a UV-light box showed that this modification occurred primarily on the essential light chains (LC17). This modification resulted in a decreased myosin solubility. Due to the change in solubility it was not possible to determine if the modified myosin went through the 6S to 10S transition but a titration of modified myosin from 150 mM KCl to 430 mM KCl resulted in an acrylodan fluorescence intensity decrease of less than 10% and no shift in the emission maximum (λ_{max} = 480 nm). These results suggest that acrylodan is modifying one of four sulfhydryls on each LC17 and that this sulfhydryl residue is in a relatively nonpolar environment. Further studies are being done to characterize this modification to determine if acrylodan can be used as a probe for structural changes in gizzard myosin. (Supported by the PEW undergraduate research program and a St. Lawrence University Faculty Research Grant.)

W-Pos72

DIRECT PHOTOAFFINITY LABELING OF GIZZARD MYOSIN WITH ADP

Todd E. Garabedian and Ralph G. Yount
Department of Biochemistry and Biophysics
Washington State University
Pullman, WA 99164-4660

The active site of smooth muscle myosin has been investigated by direct photoaffinity labeling studies with [^{3}H]ADP. Addition of vanadate (V_i) and Co^{2+} enabled [^{3}H]ADP to be stably trapped at the active site ($t_{1/2}$ > 5 days). The extraordinary stability of the myosin•Co^{2+}•[^{3}H]ADP•V_i complex allowed it to be purified free of excess [^{3}H]ADP before irradiation began, and ensured that only active site residues became labeled. Following UV irradiation, approximately 10% of the trapped [^{3}H]ADP became covalently attached at the active site. Only the 200 kDa heavy chain was labeled; there was no apparent labeling of either LC_{20} or LC_{17}. After extensive trypsin digestion of labeled S1, HPLC separation methods and alkaline phosphatase treatment allowed two labeled peptides to be isolated. Sequence analysis combined with radioactive counting of both peptides identified Glu_{185} as the labeled residue. Since Glu_{185} has been previously identified as a residue at the active site using [^{3}H]UDP as a direct photolabel [Garabedian, T. E. and Yount, R. G. (1990) *J. Biol. Chem.*, in press], this result provides further evidence that Glu_{185}, which follows the phosphate-binding glycine-rich loop, is part of the purine binding pocket of smooth muscle myosin, and represents the first instance of the explicit identification of a purine nucleotide-amino acid adduct from an active site. Supported by grants from NIH (DK 05195) and the MDA.

W-Pos73

SPECIFIC LABELING OF SERINE-19 OF THE REGULATORY LIGHT CHAIN OF CHICKEN GIZZARD MYOSIN

Kevin C. Facemyer and Christine R. Cremo, Dept. of Biochemistry/Biophysics, Washington State University, Pullman, WA 99164-4660.

The phosphorylatable regulatory light chain (LC_{20}) of smooth muscle myosin was labeled with [^{3}H]IAEDANS by a new approach. Reactive accessible thiols of free isolated myosin light chains, native myosin, or V8-Subfragment 1 were treated with the reversible blocking reagent methylmethanethiosulfonate (MMTS) to form the oxidized mixed disulfides. The modified proteins were specifically thiophosphorylated at serine-19 with myosin light chain kinase and ATPγS. The thiophosphate was then reacted with [^{3}H]IAEDANS to form the phosphorothioate ester. The kinetics and optimal conditions for the reaction of the thiophosphate with IAEDANS have been investigated. The oxidized sulfhydryls were then returned to the native reduced form by treatment with reducing agents. The resulting labeling of LC_{20}, as measured by gel electrophoresis and acetone precipitation of the proteins, has been investigated for all three protein preparations. This approach is potentially useful to specifically label thiophosphorylatable serines, threonines and /or tyrosines in other proteins.

W-Pos74

STUDIES OF THE PROTEASE SUSCEPTIBLE SITES AND THE STABILITY OF STRUCTURAL DOMAINS OF AORTA MYOSIN ROD AND LMM.

Lan King and Meei Jyh Jiang. Department of Biochemistry, Chang Gung Medical College and Institute of Biomedical Sciences, Academia Sinica, Taiwan, Republic of China

Our studies have shown that aorta smooth myosin rod, similar to other myosin rod, is composed of LMM and S-2 region. Papain digestion of Aorta myosin produces S-1 and rod, while chymotrypsin digestion yields HMM and LMM from intact myosin or S-2 and LMM from myosin rod. Both chymotrypsin and trypsin digestion of LMM produce a fragment (LMM') which is about 10 kDa smaller than LMM. Chymotrypsin can further digest LMM' into an approximately 10 kDa smaller fragment (LMM"). Aorta myosin rod and LMM show three major thermal helix unfolding transitions in solution containing 0.6 M NaCl at neutral pH, monitored by circular dichroism (CD) at 222 nm. The transition midpoints are 48,52 and 55 °C, respectively. The second transition at 52 °C, which corresponds to more than half of total helix loss, is extremely sharp with a 10%-90% span of about 1 °C. This phenomenon resembles the second thermal unfolding transition of gizzard myosin rod (L. King, S.S. Lehrer & J. Seidel, biophys. J. 55, 77a, 1989). The possible causes of these sharp transitions will be discussed. Supported by the National Science Council of Republic of China, Chang Gung Medical College and Academia Sinica.

W-Pos75

EFFECT OF PAPAIN DIGESTION TIME ON KINETICS OF GIZZARD MYOSIN SUBFRAGMENT-1.

J.S. Drew, L.A. Stein, M.P. White, and C. Moos. Departments of Medicine and Biochemistry, SUNY at Stony Brook, Stony Brook, NY 11794.

We analyzed the kinetic properties of unphosphorylated gizzard myosin digested to S-1 for varying times with papain. We found that the actin-activated Vmax increased gradually from 0.73/s after 30 seconds digestion to 1.6 /s at 20 or more minutes of digestion. However, the ATPase of S-1 alone also increased with digestion time so that the magnitude of activation was unchanged. Activity began to decrease after 60 min. digestion. K ATPase strengthened from 21 μm after 30 seconds digestion to 8 μm actin at 30 minutes, and K binding strengthened from 53 μm at 1 minute to 16 μm at 30 minutes digestion. In the absence of actin, the rate of the initial tryptophan fluorescence enhancement (burst) decreased somewhat from 19/s to 15/s, but the burst magnitude remained the same (~10% over background fluorescence).

These kinetic changes correlated with two changes seen by SDS-PAGE : a decrease in the relative amount of intact LC20 and a cleavage of the 95 KD S-1 peptide to 75KD and 26KD fragments. Gizzard S-1 produced by digestion of unphosphorylated myosin with S. aureus protease, which has intact LC20 but no 95KD peptide, had a K ATPase of 42 μm and a Vmax of 1.4/s. These data suggest that unphosphorylated LC20 inhibits actin binding while cleavage of the 95KD peptide favors increased ATPase activity in gizzard S-1.

Supported by AHA/NY Affiliate 431-3367A to LAS and AHA/NY Affiliate postdoctoral fellowship 431-3337A to JSD.

W-Pos76

FORMATION OF THE STABLE SMOOTH MUSCLE MYOSIN-ADP-AlF_3 COMPLEX AND ITS ANALYSIS USING ^{19}F-NMR

S. Maruta*, G. D. Henry#, B. D. Sykes# and M. Ikebe*
*Department of Physiology & Biophysics, School of Medicine, Case Western Reserve University. Cleveland, OH 44106
#Department of Biochemistry, University of Alberta, Edmonton ALTA. T6G 2H7, Canada

Smooth muscle myosin forms two distinct conformations, a folded (10S) conformation and an extended (6S) conformation and it has been proposed that the some component of the 10S-6S transition is involved in the regulation of actomyosin ATPase by the light chain phosphorylation. In this study, we attempted to use ^{19}F-NMR to investigate the alteration of the active site conformation. AlF_4 and BeF_3 which are known as phosphate analogs were used as probes. Mg^{2+}-ATPase activity of both smooth muscle and skeletal muscle HMMs was inhibited in the presence of either AlF_4 or BeF_3. Further more it was found that ADP was trapped into HMM in the presence of either AlF_4 or BeF_3 but not in their absence. The incorporated ADP is quite stable and more than 70% of ADP was retained with HMM after 4 days of dialysis. These results suggest that HMM forms a stable complex of HMM-ADP-AlF_3 or HMM-ADP-BeF_3. The binding of AlF_4 or BeF_3 was monitored using F-NMR. F^- and AlF_4^- signals were observed at 11 and -24 ppm respectively. In the presencee of S-1, ADP and AlF_4^-, a new line at -11.5 ppm was observed, while in the absence of ADP, this peak was not observed. When S-1 was denatured by addition of solid urea or S-1 was digested by addition of trypsin, the -11.5 ppm peak was disappeared and the free AlF_4^- peak grew large. These results clearly indicate -11.5 ppm peak is due to AlF_4^- bound to S-1. The change in the chemical shift of the peak corresponding to the bound AlF_4^- between phosphorylated HMM and dephosphorylated HMM or 10S myosin and 6S myosin are also studied. (Supported by NIH, AHA & Syntex)

W-Pos77

A QUASI-ELASTIC LIGHT SCATTERING STUDY OF SMOOTH MUSCLE MYOSIN Xufeng Wu, Paul S. Blank, Francis D. Carlson, Department of Biophysics, The Johns Hopkins University, Baltimore, MD 21218.

We have investigated the hydrodynamic properties of turkey gizzard smooth muscle myosin in solution using quasi-elastic light scattering (QELS). Effects of ionic strength (0.05 M KCl--0.5 M KCl) and light chain phosphorylation on the conformational transition of myosin were examined in the presence of ATP at 20°C. In addition to the cumulant analysis, several light scattering models were developed to describe the myosin system in solution. A non-linear least square fitting procedure was used to determine the model that fitted the data best. The conformational transition of the myosin monomer from a folded form to an extended form was clearly demonstrated in a salt concentration range form 0.15 M to 0.30 M KCl. Light chain phosphorylation regulated the transition and favors the extended form in this salt concentration range. These results are in agreement with the observations obtained from sedimentation velocity and electron microscopy studies (Trybus and Lowey, (1984), *J.Biol.Chem.* 259, pp.8564-8571). In addition to the two monomeric forms, myosin polymeric form(s) were found in solution with a weight fraction of ~30%. The size of the polymeric form varied with salt concentration. This observation suggests a dynamic equilibrium between the two configurations of myosin monomer and myosin filaments in solution. (Supported by U.S.P.H.S. NIAMSD Grant AR12803 to F.D.C).

W-Pos78

GEL ELECTROPHORETIC RESOLUTION OF A POSSIBLE FOURTH MYOSIN HEAVY CHAIN IN SMOOTH MUSCLE TISSUES. T. J. Eddinger, Biology Department, Marquette University, Milwaukee, WI 53233.

Two different smooth muscle myosin heavy chains (MHC) have been identified in a variety of smooth muscle tissues. In addition, a non-muscle MHC has been observed. The relative content of these heavy chains is developmentally regulated in a unique fashion in different species and smooth muscle tissues. Further studies of these proteins have resulted in resolution of a fourth band on SDS gels which is believed to be another myosin heavy chain. This fourth band has a MW less than the other three MHC's (approximately 190 kD). It has been most readily resolved in uterine tissue from guinea pig and mouse, but has also been resolved in aortic tissue from these two species. It is unclear if it is also present in any other smooth muscle tissues. It has not been observed in smooth muscle tissues from rat, rabbit or pig. This fourth MHC is present as a relatively small fraction of the total MHC content, similar to the non-muscle MHC content (<10%). It is not recognized by a series of smooth muscle or non-muscle MHC specific antibodies currently available. The observance of this band is consistent, however, with previous reports of two mRNA's for non-muscle MHC in various smooth muscle tissues. Generation of specific antibodies for this fourth band and sequence information will be required to confirm its identity as another MHC. Supported by AHA Grant #90-Ga-30, NIH grant #RR07196, and Marquette University's Biological and Biomedical Research Institute and Committee on Research.

W-Pos79

EXPRESSION OF MYOSIN HEAVY CHAIN (MHC) ISOENZYMES IN THE PREGNANT UTERUS OF RATS AND ITS INFLUENCE ON CA^{2+} SENSITIVITY OF SKINNED UTERUS FIBERS

MORANO I, BOELS, P.. UNIVERSITY OF HEIDELBERG, DEPARTMENT OF PHYSIOLOGY II, INF 326, D-6900 HEIDELBERG

During different stages of pregnancy (6 days, 16 days, and 1 h after partum) uteri were removed from rats of the Sprague Dawley strain and chemically skinned using 1% Triton x-100 and subsequently 50% glycerol under relaxing conditions (pCa >8). The relative concentrations of the MHC isoenzyme expression in myosin crude extracts of skinned fibers were determined by SDS-PAGE according to CARRARO and CATANI, BBRC 116: 793 (1983). MHC and filamin were identified by Western blot analysis using polyclonal antibodies. Isometric tension of skinned fibers was recorded by changing pCa stepwise from 8 to 4.5. Fibers from 6 days and 16 days had a pCa_{50} of 5.75 and 5.88 respectively and a Hill coefficient of 1.8 and 1.34. Uteri obtained 1 h post partum had a pCa_{50} of 5.36 and a Hill coefficient of 1.38 (means of 20 fibers per group; SEM<10%). Maximal force development in fibers from 6 d and from 1 hr post partum was respectively 0.581 and 3.510 mN/mm^2. Two MHC isoenzymes were detected in the extract and designated as Sm1 and Sm2 with increasing mobility in the gel. They showed immunoreactivity with anti-Sm-MHC but not with anti-filamin. The relative amount of Sm2 in skinned fibers increased with increasing duration of pregnancy being 22%, 28%, and 40% after 6 d, 16 d, and 1 hour post partum, respectively. Thus, during pregnancy, Sm2-MHC expression increases. This expression correlates with a decrease of Ca^{2+} sensitivity and cooperativity of the contractile apparatus and an increase of absolute force development.

W-Pos80

FUNCTIONAL RECONSTITUTION OF MIP FROM CHICKEN LENS IN PLANAR LIPID BILAYERS. A. C. Campos de Carvalho, E. Modesto and D. C. Spray. Instituto de Biofisica Carlos Chagas Filho, UFRJ, Rio de Janeiro, Brazil and Dept. Neuroscience, A. Einstein Coll. Med., N.Y. 10461.

We have purified membrane fractions highly enriched in MIP28 from chicken lens and incorporated such fractions into lipid bilayers. In contrast to previously published results we do not need to add the membrane fractions to both chambers to obtain channel activity. Also, the incorporated channels display a higher voltage sensitivity than previously described, with symmetrical voltage dependent closing noticeable at 20-30 mV. Other properties of the incorporated channels (single channel conductance of 200-300 pS in 100 mM salt, and lack of calcium, pH or octanol sensitivity) are identical to those reported by Zampighi et al. (PNAS, 1985) for MIP26. Despite the high enrichment of the membrane fractions used in these studies, the possibility of the observed channel activity being contributed by a minor contaminant in the samples can not be discounted. To overcome this problem we reconstituted electro-eluted MIP into liposomes that were then incorporated into planar bilayers. We have been able to functionally reconstitute electro-eluted MIP28 following the procedure described by Hanke et al. (Europ. Biophys. J., 1990). The channel properties of the reconstituted protein are very similar to those obtained from incorporation of membrane fractions highly enriched in MIP28, indicating that the channel activity observed in these fractions is indeed due to MIP channels.

Supported by NIH grant EY 08969-01 and FAPERJ.

W-Pos81

DIFFUSION OF A FLUORESCENT PROBE IN A MONOLAYER OF CULTURED, HEPATOCYTE-DERIVED EPITHELIAL CELLS

Bonnie L. Bunch, M.D.

Intro. By Peter R. Brink, Department of Anatomical Sciences, SUNY-Stony Brook, Stony Brook, NY

The diffusion of fluorescent probes in the median giant axon of earthworm was well-characterized by Brink and Ramanan (Biophys. J., 48:299-309, 1985). The diffusion model assumed a simple cylindrical cellular geometry and allowed computation of an apparent cytoplasmic diffusion coefficient, a junctional membrane permeability, and a plasma membrane permeability for each probe. The current work tests the analytical power of a similar model written for the more complex geometry of a monolayer of identical polygonal cells coupled at a constant number of interfaces per cell (Ramanan and Brink, Biophys. J., 58:631-639). Clone 9 normal rat liver cells (ATCC CRL 1439) were grown in culture and studied using the fluorescent probe 5-(and 6-) fluorescein sulfonic acid. Fluorescent intensity was measured using a video image analysis system. The model separates junctional permeability and cytoplasmic diffusion in spite of deviations from the ideal geometry. In theory, this should allow separation of effects due to direct actions on the gap junction channel (gating) from effects due to alterations of cytosolic characteristics such as viscosity. The use of monolayers of cells in secondary culture allows easy application of hormones and other mediators of cell function while minimizing the transient effects on junctional coupling seen in preparations of freshly dissociated cell pairs in primary culture.

This work was supported by NIH grant LH-31299.

W-Pos82

FUNCTIONAL RECONSTITUTION OF HPLC-PURIFIED LENS CHANNEL PROTEIN MIP26 IN LIPOSOMES AND PLANAR BILAYERS. L. Shen, P. Shrager, S. Girsch, P. Donaldson and C. Peracchia (Intro. by B. C. Spalding). Department of Physiology, University of Rochester, Rochester, NY 14642.

The putative lens gap junction protein (MIP26), purified by HPLC from bovine lens fibers, was incorporated into liposomes. Permeability of reconstituted channels was studied by a spectrophotometric-osmotic assay (Girsch and Peracchia, J. Membr. Biol., 83, 217, 1985) and channel electrical properties were monitored in planar bilayers following liposome fusion. Intramembrane particle formation in proteoliposomes was determined by freeze-fracture EM. Consistent with previous data, channels made of HPLC-purified MIP26 were permeable to molecules larger than small ions (sucrose). In planar bilayers, channel activity was observed after addition of liposomes to both chambers and with holding potentials greater than 20 mV. Channel open time decreased progressively as the holding potential increased, such that at 60-80 mV the open probability was approximately 50%. This indicates that the channels are voltage-dependent and are permanently open at voltages lower than 20 mV. Histograms of single channel current-amplitudes at 80 mV holding potential showed Gaussian distributions that peaked at 9.5 pA (~120 pS). The curves describing frequency distribution of open and closed times at 80 mV followed single exponential functions with time constants of 0.16 and 1.3 sec respectively. Open time-constants ranged from 0.1 to 0.3 sec and closed time-constants from 1 to 7 sec. Cs^+ did not alter channel conductance, but reduced mean open time from 0.22 to 0.05 sec and mean closed time from 1.5 to 0.43 sec. Most often this increase in channel flickering with Cs^+ occurred in bursts. In contrast, TEA affected neither channel conductance nor channel open and closed times. Channel events were also observed in Na^+-solutions (zero-K^+), indicating that the MIP26 channels are not cation selective. Various characteristics of these channels, including: permeability to molecules larger than small ions, conductance greater than 100 pS, absence of selectivity, long open and closed times, etc., are consistent with those of gap junction channels.

Supported by NIH GM20113.

W-Pos83

GAP JUNCTION UNCOUPLING BY HEPTANOL, HALOTHANE AND ISOFLURANE. A Ca^{++}- AND H^+-INDEPENDENT PHENOMENON ENHANCED BY CAFFEINE AND THEOPHYLLINE. Camillo Peracchia, Department of Physiology, University of Rochester, Rochester, NY 14642.

This study has monitored junctional (R_j) and non-junctional (R_n) resistances, and either $[Ca^{++}]_i$ or $[H^+]_i$ (with ion-selective microelectrodes; Peracchia, C., J. Membr. Biol. 113,75,1990), in crayfish septate axons exposed to anesthetics. Heptanol (0.04-0.08%, v/v) and halothane (0.1-0.3%, v/v) caused a 1.5-2 fold increase in R_j, while isoflurene (0.3%, v/v) increased R_j to a lesser extent. The effects of anesthetics on R_j were significantly potentiated by 10-20 mM caffeine or theophylline. R_j maxima with either heptanol-caffeine or halothane-caffeine were 3 times greater than those with heptanol or halothane alone, and R_j maxima with isoflurane-caffeine were 1.5-2 times greater. However, unlike the effect of caffeine on low pH_i-induced uncoupling (Peracchia, C., J. Membr. Biol. 117,79,1990), the xanthine effect on anesthetic-induced uncoupling did not involve an increase in $[Ca^{++}]_i$. In fact, heptanol caused a decrease in $[Ca^{++}]_i$ and $[H^+]_i$ both in the presence and absence of either caffeine or theophylline, and a similar but transient effect on $[Ca^{++}]_i$ was observed with halothane. Negative results obtained with different $[Ca^{++}]_o$ (7-27 mM), Ca^{++}-channel blockers such as nisoldipine (1-10 μM) and Cd^{++} (500 μM), and ryanodine (10 μM), also speak against a Ca^{++} participation in uncoupling by anesthetics. Similarly, negative results obtained with IBMX (1mM), forskolin (5 μM), CPT-cAMP (0.5 mM), 8Br-cGMP (200 μM), adenosine (5mM), phorbol ester (TPA, 162 nM) and H7 (100 μM), tested in the presence and absence of caffeine and/or heptanol, exclude the participation of cyclic nucleotides, adenosine receptors and kinase C. Curiously, 4-aminopyridine (5 mM) was found to strongly inhibit heptanol-induced uncoupling. The data suggest a direct effect of anesthetics on gap junction channels, possibly involving both polar and hydrophobic interactions with channel proteins. Xanthines and 4-aminopyridine may influence polar interactions. The potentiating effect of xanthines on anesthetics-induced cell-uncoupling may explain the nature of cardiac arrhythmias in patients treated with theophylline during halothane anesthesia.

Supported by NIH GM20113.

W-Pos84

PROPERTIES OF SINGLE GAP JUNCTION CHANNELS BETWEEN NEONATAL HAMSTER CARDIAC MYOCYTES. By H-Z. Wang, †I. Li, †L.F. Lemanski, and R.D. Veenstra, Depts. of Pharmacology and †Anatomy & Cell Biology, SUNY Health Sci Ctr, Syracuse, NY 13210.

The immunohistochemical and electrophysiological properties of gap junction channels were examined in paired myocytes isolated from 3-day neonatal hamster ventricles and cultured for 1 day in vitro. Immunolocalization with a site-specific antiserum directed against amino acids 252-272 of rat connexin43 (courtesy of Dr. E.C. Beyer, Washington Univ., St. Louis, MO) specifically stained zones of contact between cultured myocytes. The dependence of macroscopic gap junctional conductance (g_j) on transjunctional voltage ($V_j = V_2 - V_1$) was examined using the double whole cell patch clamp technique. Instantaneous and steady-state junctional current (I_j) measurements were taken from the beginning and end of a two sec step in V_j ranging from 0 to ±100 mV. The instantaneous I_j-V_j relationships of neonatal hamster myocyte pairs were linear over the entire voltage range examined, as observed for all gap junctions examined to date. However, the steady-state I_j-V_j relationship was nonlinear for $V_j > \pm 50$ mV. V_j-dependence was observed in all pairs where $g_j < 12$ nS and was not observed in three pairs where $g_j > 30$ nS. These g_j values are at least six times higher than those required for loss of V_j-dependence in neonatal rat heart. Once normalized to the instantaneous g_j recorded at each V_j, a plot of the steady state g_j produces a bell shaped curve which can be adequately described by a two-state Boltzmann equation previously described for other voltage-dependent gap junctions. From the theoretical fit of the steady-state g_j-V_j relationship for neonatal hamster heart, the minimum g_j was 0.39; the half-inactivation voltage was 73.6 mV; and the valence of the voltage sensor was 2.22 electrons. Gap junction channel current (i_j) records yield a linear i_j-V_j relationship with a slope conductance of 50 pS, although a lower single channel conductance of 32 pS was also observed in another cell pair. These channel conductances are consistent with that observed in neonatal rat heart. Real time amplitude histograms of the channel recordings indicate that the channel open time probability was decreased at larger V_j values, supporting the view that regulation of g_j occurs by the open-closed gating of individual gap junction channels. Polarity reversal experiments exhibited a transient recovery in I_j, which indicates that the channels reopen prior to closing in response to the reversal in V_j. This work was supported by NIH HL-42220 and HL-37702.

W-Pos85

RECONSTITUTED COMMUNICATING JUNCTIONS: VOLTAGE DEPENDENCE AND STRUCTURE

E.J.A. Lea, G.F. Clunn, A. Tickner and R.W. Horne. Introduced by University of East Anglia, School of Biological Sciences, Norwich, NR4 7TJ, UK.

In vivo, communicating junctions are composed of regular arrays of conducting units, each unit consisting of two connexons, one in each of the adjacent communicating cell membranes. Some junctions are sensitive to cell membrane PD[1] such that junctional conductivity decreases if either cell membrane is depolarized. Other junctions are sensitive to transjunctional PD, such that junctional conductivity decreases with increasing polarization[2]. Both types of behaviour have been described in terms of Boltzmann functions. A fundamental question in reconstitution studies concerns the nature of the reconstituted channel in the single membrane of the liposome or planar bilayer. Does it consist of two connexons as appears to be the case in reconstituted liver junctions[3] or one connexon, and if so how is it arranged in the bilayer, and what is its functional relationship to a communicating channel in vivo? In the lens reconstitution studies, the situation is complicated by the presence of more than one type of channel but electron microscope evidence revealing 4-subunit structures seems to support the proposition that in the reconstituted system only hemichannels are present[4]. A voltage dependence model is presented, based on the voltage dependence of populations of hemichannels, which may be helpful in the interpretation of the different types of voltage dependent conductivity seen in different tissues and in planar bilayers.

1 Obaid, A.L., Socolar, S.J. & Rose, B. J. Membrane Biol. 73, 69-89 (1983). 2 Spray, D.C., Harris, A.L. & Bennett, M.V.L. J. gen. Physiol. 77, 75-94 (1981). 3 Spray, D.C., Saez, J.C., Brosius, D., Bennett, M.V.L. and Herzberg, E.L. Proc. Natl. Acad. Sci. (USA) 83, 5494-5497 (1986). 4 Tickner, A.L., Lea, E.J.A. and Horne, R.W. Micron 21, 91-99.

W-Pos86

LARGE CHANNELS FORMED BY IMMUNOPURIFIED CONNEXIN32 IN SINGLE PHOSPHOLIPID MEMBRANES. S.K. Rhee[1] and A.L. Harris[2]. [1]Dept. of Biology and [2]Dept. of Biophysics, Johns Hopkins Univ., Baltimore, MD 21218.

Gap junction channels are formed by connexin protein. We have affinity-purified connexin32 from rat liver with a monoclonal antibody attached to a bead matrix. The connexin32 is highly pure, soluble in octylglucoside, and is not exposed to the denaturing conditions involved in isolation of gap junction membranes. When the immunopurified connexin32 was incorporated into the membranes of unilamellar phospholipid vesicles, the vesicles became highly permeable to sucrose, and to Lucifer Yellow (diam. ~12Å), which is near the upper size limit for permeation through junctional channels *in vivo*. Exposure to pH below 7.5 reversibly decreased the sucrose permeability. For a given amount of connexin, the number of vesicles that became sucrose-permeable can be accounted for if the connexin distributes randomly among the vesicles as hexamers, and if a single hexamer can form a sucrose-permeable pore. Distribution as dodecamers (two connexons) cannot account for the data. We conclude that connexin32 purified under these conditions can form large, gated channels through single phospholipid membranes, and that the channels may be single functioning connexons. These single-membrane connexin channels may therefore represent a form of the junctional channel accessible for detailed studies of permeation, gating and modulation that are not possible *in situ*. Supported by ONR grant N00014-89-J-1570 to ALH, NIH BRSG S07RR07041 to Johns Hopkins University, and an America Liver Foundation Award to SKR.

W-Pos87

GAP JUNCTIONS EXPRESSED IN XENOPUS OOCYTES: pH DEPENDENCE. Lisa Ebihara. Columbia University, New York, New York, 10032.

The dependence of gap junctional conductance on intracellular pH(pH_i) was measured in pairs of Xenopus oocytes expressing either Xenopus connexin38 or rat connexin43. G_j was monitored using a double voltage-clamp technique. A pH-sensitive microelectrode located close to the junction was used to measure pH_i. The general conclusions of this study are: 1) In pairs of oocytes expressing connexin38, the junctional conductance could be nearly abolished by perfusing with 10% CO_2 equilibriated MB corresponding to a reduction in pH_i from 7.2 to 6.8. The changes in junctional conductance closely paralleled changes in pH_i. 2) In contrast, in oocyte pairs expressing connexin43, reduction of pH_i from 7.2 to 6.8 was associated with either no change or a small increase in G_j. When pH_i was lowered to 6.1-6.0 by perfusion with 100% CO_2 equilibriated MB G_j was reduced. In some cell pairs G_j could be totally abolished while in others G_j was reduced by only 10-20% even when the pH_i was held at 6.0 for 5-10 minutes. The G_j-pH_i relationship on recovery resembled that reported in adult rat heart cell pairs(1). Since both connexin38 and connexin43 are being expressed in the same cell type, these differences in pH sensitivity most likely reflect differences in structure of the junctional proteins.

(1) R.L. White et al.(1990) J Gen Physiol. 95:1061-1075.

Supported by grants from NIH(HL 45377-01, HL 28958), AHA and a Hirschl Career Scientist Award.

W-Pos88

MEMBRANE CHOLESTEROL AND GAP JUNCTION FORMATION. Barbara Malewicz[a], Susan B. Johnson[a], Ross G. Johnson[b], and Wolfgang J. Baumann[a], The Hormel Institute[a], University of Minnesota, Austin, MN 55912 and Department of Genetics and Cell Biology[b], University of Minnesota, St. Paul, MN 55108.

Gap junctions (GJ) are important regulators of cellular function. They provide channels for the movement of small molecules between cells and control cell-to-cell communication. Although the cluster of GJ proteins that are assembled in the junction do function in a lipid environment, there is a paucity of information on the role of lipids in gap junction assembly and function (Malewicz et al., *Lipids 25*, 419-427, 1990). We have evidence that cholesterol affects the gap junction assembly process. We found that in Novikoff hepatoma cells (NHC) grown in cholesterol-supplemented medium containing 10% serum, GJ assembly and permeability can be stimulated, or inhibited, depending on the level of cholesterol supplementation. Maximum stimulation was observed when cells were grown for 24 hr in 20 μM cholesterol-supplemented medium which resulted in up to a seven-fold increase in the number of aggregated GJ particles and in up to a three-fold increase in GJ plaque areas (Meyer et al., *J. Cell Sci. 96*, 231-238, 1990). Maximum stimulation occurred when cell cholesterol levels reached about 64 nmol/mg cell protein and cell membrane cholesterol levels reached 250-280 nmol/mg protein. At that point, the membrane cholesterol-to-phospholipid ratio reached 0.34 to 0.45 as compared to 0.22 to 0.25 for control cells. When NHC were grown in >40 μM cholesterol-supplemented medium, and cell cholesterol levels doubled, GJ formation became inhibited. Stimulation as well as inhibition of GJ formation by cholesterol supplementation can be counteracted by lysophosphatidylcholine. We suggest that cholesterol may be involved in the assembly and function of gap junctions by facilitating the ordering and anchoring of the clusters of GJ proteins in the microdomain of the gap junction plaque. (Supported by NSF Grant DCB-8517726, NIH Grant HL08214, and by The Hormel Foundation)

W-Pos89

PERMEABILITY PROPERTIES OF DISSOCIATED LENS CELLS AND OF A CELL LINE TRANSFECTED WITH THE cDNA FOR MIP26.
A.G. Miller, N.M. Kumar, N.B. Gilula, and J.E. Hall, Dept of Physiology and Biophysics, University of California at Irvine, Irvine Ca 92717, Dept of Molecular Biology, Research Institute of Scripps Clinic, La Jolla, California 92037.

Single membrane conductances and cell-to-cell membrane coupling of freshly dissociated embryonic chicken lens cells and three baby hamster kidney (BHK) cell lines (a parental cell line, a cell line transfected with the cDNA for the major intrinsic protein of eye lens membranes (MIP26), and a cell line transfected with the β_1 cDNA for a liver gap junction protein) were investigated using the patchclamp technique. We previously reported a survey of the permeability properties of the dissociated lens cells (Biophys. J. 57:245a 1990) and of two of the cell lines (ASCB abstract). This abstract reports the analysis of these permeability properties, and some new observations.

Lowering pH reduces coupling between dissociated lens cells. In mammalian ringer (pH 7.4), passage from cell to cell of Lucifer Yellow injected via a patch pipette was seen in 90% of the dissociated lens cell pairs or clusters. Internal pH was lowered by perfusing the cells with solutions containing NaAcetate. 100% of the cell pairs or clusters showed coupling at pH 6.8, 30% showed coupling at pH 6.4 and none showed coupling at 6.0. It was not possible to reverse the block of coupling, however a stable seal was formed at each pH.

Preliminary nuclear staining experiments with a DNA binding dye indicate that two types of nuclei are present in the dissociated preparation. A large percentage of the cells contain rounded nuclei and a small percentage contain elongated nuclei. Also three types of currents were found in whole cell clamp: 48% of the cells tested contain only a linear, voltage-independent current, 14% contain an inward rectifier which turns off at about -40 mv and 38% contain a current which turns off at positive voltages (10-40 mv) over a period of seconds. Thus the dissociated cells comprise a heterogeneous population.

A current similar to the positive voltage-dependent current was found in 30% (8 out of 27) of the BHK cells transfected with the cDNA for MIP26, but was absent in both the parental cells (0 out of 12) and the cells transfected with the β_1 cDNA for the liver gap junction protein (0 out of 4). The current versus voltage relationship is similar to that found in the dissociated lens cell preparation, but the current turns off over hundreds of milliseconds, rather than over seconds as the current in the dissociated cells does. Supported by NIH grants EY05661 (to JEH), EY06884 (to NMK) and GM37907 (to NBG and NMK).

W-Pos90

HUMAN CONNEXIN43: CHANGES IN GAP JUNCTION PROPERTIES AFTER SITE-SPECIFIC MUTAGENESIS. A.P. Moreno, G.I.Fishman, L.A. Leinwand, and D.C. Spray. Depts. Neuroscience, Medicine and Microbiology/Immunology, A. Einstein College of Medicine, Bronx, N.Y.

Features that distinguish the gap junctions expressed in different tissues are gating properties (e.g., sensitivity to voltage, pH and second messengers) and channel size (i.e., unitary conductance and permeability). To begin to identify domains of the connexin molecules conferring functional attributes, we have compared properties of human connexin43 (Cx43) gap junction channels in stably transfected SKHep1 cells with those of mutant Cx43 channels. Two classes of mutants have been characterized: a) Truncation mutants, with premature stop codons resulting in cytoplasmic tails that are similar in length to connexin26 or connexin32; and b) Single amino acid substitutions in the predicted third membrane spanning domain of the molecule (M3). The major effect of the truncation mutations was to alter unitary conductance (γ_j). Wild type human Cx43 channels exhibit γ_j values of about 60 and 90 pS (using CsCl pipette solutions); γ_j of the Cx26 analogue was about 50 pS and of the Cx32 analogue about 150 pS (the latter consistent with γ_j's in the same parental cell line stably transfected with rat Cx32). Sensitivity of junctional conductance (g_j) to transjunctional voltage (V_0 about 60 mV, g_{min} about 50% g_{max}) was unaffected by these mutations. For the second type of mutation, SER158 (presumed to lie within the M3 domain) was replaced with LYS, PHE or ASP; in separate constructs, PHE161 was replaced with GLY. For all of these constructs, mutant connexin expression was similar to wild type Cx43 levels. Lucifer Yellow failed to pass between any of these mutants involving the M3 domain, whereas g_j attributable to the transfected channel proteins was still observable for the SER158 mutants. We conclude that the carboxyl terminal tail is an important determinant of γ_j, that consensus carboxyl-terminal phosphorylation sites are not necessary for correct membrane insertion, assembly or function, and that SER158 may play a role in the characteristic permeability of gap junction channels to moderately large molecules.

W-Pos91

KINETIC PROPERTIES OF VOLTAGE DEPENDENCE OF RAT CONNEXIN 26 AND 32 JUNCTIONS EXPRESSED IN XENOPUS OOCYTES. L.C. Barrio, T. Suchyna*, T. Bargiello, R. Roginsky, R.S. Zukin, B. Nicholson* and M.V.L. Bennett. Albert Einstein College of Medicine, Bronx, NY 10461 and *SUNY Buffalo, Buffalo, NY 14260.

Xenopus oocytes were injected with cRNAs encoding either rat Cx26 or Cx32 and paired to form Cx32-32, Cx26-26 or Cx32-26 junctions. Antisense cDNA oligonucleotides to Xenopus Cx38 were coinjected to block endogenous coupling selectively. Junctional conductance, g_j, was measured using the dual voltage clamp technique. "Instantaneous" g_j (time resolution c.10ms) was roughly constant for Cx32-32 junctions at large transjunctional voltages, V_j, of either sign, but for Cx26-32 junctions it increased with V_j positive on the Cx26 side and decreased with opposite V_j with a slope of 5.5/V. For Cx26-26 junctions "instantaneous" g_j increased with depolarization and decreased with hyperpolarization of either cell with a slope of 1.3/V, indicating a dependence on the potential between inside and outside of the cells, V_{i-o}. During large V_j steps of either polarity, g_j at Cx26-26 and Cx32-32 junctions decreased slowly to a new steady state value. The time course of these decays was well fit by a single exponential; the time constants were several seconds and decreased for larger V_j. The changes were slightly asymmetric for Cx26-26 junctions reflecting the V_{i-o} sensitivity. For Cx26-32 junctions, this slow g_j decrease was only present for relative positivity the Cx26 side. If V_j closes the hemichannels on the positive side (as amphibian blastomeres), the Cx32 hemichannels lose their V_j sensitivity in Cx26-32 junctions. Also in these heteromeric junctions, Cx26 hemichannels may convert their fast V_{i-o} sensitivity to fast V_j sensitivity opposite in sign to the slow changes. Boltzmann parameters of steady state g_j/V_j relations were for Cx32 A=0.09 and V_o=±55; for Cx26 A=0.15 and V_o=±85mV and Cx26-32 A=0.19 V_o=+75mV. During a small V_j step following a large V_j that decreased g_j, g_j increased again, but the time course was not a single exponential. Also, steady state g_j could be smaller than during a single V_j step to the same level. In summary: a) g_j at Cx32-32 and Cx32-26 junctions is dependent exclusively on V_j while Cx26-26 junctions also exhibit some V_{i-o} dependence; b) Cx26-26 and Cx32-26 junctions show both fast and slow changes in g_j suggesting the coexistence of two different types of gating; c) the properties of the heteromeric Cx26-32 junctions would not be predicted from those of the homomeric junctions and d) although slow decays in g_j during single V_j steps were exponential, recovery was more complex and steady state g_j could show hysteresis; thus, their gating is not a simple first order process.

W-Pos92

MODULATION OF INTERCELLULAR COMMUNICATION AFFECTS DEVELOPMENT OF EARLY MOUSE EMBRYOS.

M. L. Pressler, K. Elias*, J. English*, J. A. Lash & E. S. Critser*. Krannert Institute of Cardiology & Roudebush VAMC, Indiana University Sch. of Medicine, and *Methodist Hospital, Indpls, IN

Intercellular communication seems to be needed for compaction and determination of cell fate of early embryos but a complete understanding of the role of cell-cell coupling in embryogenesis has not been attained. We used a B6D2F$_1$ mouse expression model to study changes in development after premature induction of coupling (normally occurs at 4- to 8-cell stage). *In vitro* transcribed connexin43 (CXN43) mRNA (0.5-1 pg of wild type or deletion mutants) was microinjected into fertilized B6D2F$_1$ eggs to induce coupling at the 2-cell stage (60-80% of injected eggs). *In vitro* development was followed for 96 hr and cell coupling assessed by Lucifer Yellow dye transfer. Developmental arrest occurred with induction of CXN43 channels missing 98 aa at the C-terminus (31% morula/blastocysts (M/B) at 96 hr) but not after induction of wild type CXN43 (62% M/B) or in uninjected controls (75% M/B). To further explore the relation between junctional communication and growth, we studied a strain (ICR) of embryos which is known to arrest in culture at the 2- to 4-cell stage. Two-cell ICR embryos were usually coupled (17 of 33) in contrast to the B6D2F$_1$ 2-cells (0 of 24). ICR development to the blastocyst stage could be fostered by culture in medium containing glutamine but no glucose (CZB medium): 48 ± 6% (CZB medium) vs 21 ± 5% (controls in mod. Whitten's; n=80; P<0.05). Together with the enhanced development, the rate of 2-cell coupling of ICR embryos markedly decreased: 1/18 (CZB medium) *vs* 12/18 controls (mod. W). Expression of junctional channels at very early embryonic stages may be a harbinger of subsequent problems in mouse development.

W-Pos93

Arachidonic Acid and Lipoxygenase Metabolites Uncouple Neonatal Rat Cardiac Myocyte Pairs.

Kenneth D. Massey and Janis M. Burt University of Arizona, Physiology Department, Tucson, AZ 85724.

Cardiac myocytes are coupled via gap junctions which provide a low resistance pathway between cells and allow for rapid propagation of the action potential through the heart. Cardiac gap junctions are regulated by pH, pCa, second messengers and certain lipophilic compounds. Tissue ischemia causes decreased pH and increases in both $[Ca^{2+}]_i$ and tissue content of non-esterified fatty acids. Additionally, ischemia is often accompanied by electrical conduction abberancies. In previous investigations exposure of cardiac myocytes to perfusates containing oleic, decanoic and doxyl stearic acids have been demonstrated to reversibly uncouple gap junctions while leaving the cells in an electrically excitable state. In the myocardium an area of partially uncoupled cells which retain the ability to conduct action potentials is a prime focus for re-entrant type arrhythmias. Work from this laboratory previously reported reversible uncoupling for 1 and 5 μM AA which was delayed by pretreating the cells with phenidone, a non-specific AA cascade blocker but not by blockers of the cyclooxygenase pathway, indomethacin or ibuprofen. In this investigation we have extended these observations to include specific inhibitors of the lipoxygenase cascade, autooxidized products of arachidonic acid (AA) and protective effects of α-tocopherol, if any. Junctional conductance (g_j) between cells of neonatal rat cardiac myocyte pairs was measured using dual, whole-cell voltage clamp techniques. Cell pairs were superfused with physiological buffer or buffer supplemented with AA or the AA-containing superfusate was bubbled with 100% O_2. In several experiments cells were pretreated with an inhibitor of the 5-lipoxygenase (LPI) enzyme, U-70344A (Upjohn), 1μM for 60 min or α-tocopherol 100 μM for 18 hr. The data in this study demonstrate reductions of g_j in a dose and time-dependent fashion with exposure to 10, 25 and 100 μM AA. Time from intervention to complete uncoupling for various treatments are shown in the following table:

Intervention	n	Time to uncoupling Mean ± SE
10 μM AA	3	6.97±0.64 min
25 μM AA	10	4.43±0.60 min
100 μM AA	6	2.48±0.47 min*
25 μM AA+LPI (1μM)	5	3.12±0.29 min
25 μM AA+LPI (2μM)	3	5.40±1.36 min

(*p<0.05) Further, pretreatment of the cell cultures with α-tocopherol had no discernible effect. Oxidation of AA solutions prior to superfusion tended to increase the time required for uncoupling. Thus, arachidonic acid and oxidative products thereof uncouple cardiac cells in a dose and time-dependent fashion. The uncoupling effect of AA is attenuated by blockade of the 5-lipoxygenase metabolic pathway. Suggesting that end products of the 5-lipoxygenase cascade are involved in the uncoupling process. These studies were supported by PHS: HL31008 and AHA-Az Affiliate G-2-28-90.

W-Pos94

JUNCTIONAL CURRENTS IN ADULT MAMMALIAN SINUS NODAL CELL PAIRS.

By J.M.B. Anumonwo, H-Z. Wang, R.D. Veenstra, M. Delmar and J. Jalife, Dept. of Pharmacology, SUNY/HSC, Syracuse, NY 13210.

Electrophysiological studies have suggested that pacemaker cells in the sinus node (SN) synchronize their activity by electrotonic interactions mediated by gap junctions. Some ultrastructural studies, however, have reported that gap junctions are rare or totally absent in the SN. In this study, the double whole cell patch clamp technique was applied to isolated rabbit SN cell pairs to determine whether indeed SN cell pairs are coupled electrically through gap junctions. In all pairs examined (n = 7), we could record junctional currents (I_j) which ranged from 250 to 1655 pA at a transjunctional voltage (V_j) of 100 mV. Instantaneous and steady-state I_j measurements, taken from the beginning and the end of two sec steps in transjunctional voltage (from 0 to ± 100 mV, 10 mV increments), were linear over the entire range examined. The slope conductance (g_j) taken from the I_j-V_j relationship of each cell pair ranged from 2.5 to 16.5 nS with an average of 7.46 ± 6.01 nS (mean, ±sd). Previous experimental and theoretical studies have shown that action potential transfer between adjacent cells occurs when the ratio of junctional resistance to input resistance (r_j/r_{in}; transfer index) is less than 12. Input resistance in the isolated SN cells was 0.90 ± 0.18 GΩ (n = 5). Given that $r_j = 1/g_j$, the transfer index in the SN cell pairs equals 0.15. Electrical coupling in the cell pairs was sensitive to n-alkanols, which previously have been shown to reversibly block gap junction channels. For example, I_j was completely abolished by 1-10 mM octanol in a reversible manner. In two experiments, following the reduction of g_j with octanol, individual gap junction channel currents could be resolved. In one of these experiments, single channel currents ranged from 2.39 to 3.79 pA (V_j = 40 mV), corresponding to a mean single channel conductance (γ_j) of 65 pS (43 openings). In the second experiment, single channel currents ranged from 3.34 to 4.90 pA (V_j = 100 mV), giving a mean γ_j of 42 pS (95 openings). These data provide, for the first time, direct evidence for electrical coupling between pacemaker cells in the mammalian SN. They also strongly support the hypothesis that SN pacemaker cells synchronize their activity by electrotonic interactions mediated through gap junctions. Supported by grants HL-39707, HL-42220, HL-29439 and a fellowship from AHA (New York State Affiliate).

W-Pos95

COMPARTMENTAL ANALYSIS OF DYE SPREAD IN MONOLAYERS.

Peter Gates, Mitchell A. Watsky, Kim Cooper and James L. Rae. Dept. of Physiology and Biophysics, Mayo Foundation, Rochester, MN.

We present a new method of obtaining quantitative estimates of junctional permeabilities in a monolayer of cells. This method yields estimates of the individual junctional permeabilities along with an estimate of the error associated with each permeability determination. The procedure used is an N dimensional analog of linear regression which makes use of the singular value decomposition algorithm.

The experimental preperation is the corneal endothelium of the rabbit. Data is taken by patch clamping a cell of the monolayer in the whole cell configuration and allowing dye to diffuse from the electrode into the source cell and its neighbors. The fluorescent intensity in each cell is then measured at several points in time. This data can then be used to generate an overdetermined system of equations.

We assess the performance of the algorithm by randomly assigning junctional permeabilities to each of the junctions in an ideal monolayer of hexagonal cells. The pattern of dye spread is computed by integrating the associated system of differential equations. This computed data can then be altered in a variety of ways to simulate experimental data and used as input to the fitting algorithm. This procedure is repeated with different sets of permeabilities each randomly generated from the same distribution. The resulting statistics can be used to determine the ability of the algorithm to fit permeabilities depending on the precision of the data, the distance of a junction from the source cell, and the orientation of the junction relative to the direction of the dye spread.

Supported by NIH grants EY06206, EY03282, and EY06005

W-Pos96

INTRACELLULAR TRAFFICKING PATHWAYS IN MALARIA INFECTED ERYTHROCYTES VIEWED BY CONFOCAL FLUORESCENCE IMAGING MICROSCOPY. **Jill A. Hunter, Stella M. Hurtley, Marianne Murray and Theodore F. Taraschi, Dept. of Pathology & Cell Biology, Jefferson Medical College, Philadelphia PA 19107.** Erythrocytes infected with the malaria parasite, *Plasmodium falciparum*, exhibit stage-specific changes in morphology, structure, composition and antigenicity during the parasites 48 hour intraerythrocytic life cycle. We have found alterations in the host cell phospholipid and fatty acid composition that suggest bi-directional exchange of phospholipids between the erythrocyte and parasite membranes. To investigate lipid trafficking pathways, *P. falciparum* infected erythrocytes were incubated in vitro with NBD-labeled phospholipids and the timecourse of lipid uptake by the parasite membranes and distribution of labeling was assessed by laser-scanning confocal fluorescence imaging microscopy (CFIM). Unlike in uninfected erythrocytes, the fluorescent lipids rapidly crossed the erythrocyte membrane and heavily labeled the internal parasite membranes. Numerous, highly mobile membranous structures (0.1 - 1.0 μm diameter) were observed in the erythrocyte cytoplasm. In addition, structures suggestive of membrane continuity between the parasite and erythrocyte membranes were observed. NBD-ceramide, a lipid precursor that is not metabolized by uninfected erythrocytes, was synthesized into NBD-sphingomyelin by the parasite and actively trafficked to the host cell membrane. A number of parasite proteins are synthesized and exported to or secreted from the erythrocyte membrane during intraerythrocytic maturation. In order to investigate protein trafficking pathways, synchronous cultures of infected erythrocytes were temporally analysed for the production of parasite proteins. These proteins were visualized by conventional immunofluorescence microscopy and CFIM using monoclonal antibodies. Malarial proteins were often localized in structures in the erythrocyte cytoplasm at the same developmental stage and in strutures that were similar in size to the mobile vesicles labeled with the NBD-phospholipids. These vesicles may be part of a parasite directed lipid/protein trafficking pathway. **Supported by PHS grant AI 27247 and the UNDP/World Bank/WHO Special Program for Research and Training in Tropical Diseases.**

W-Pos97

ASYNCHRONOUS RELEASE AND TRANSMITTER-RECEPTOR INTERACTION ON THE NEUROMUSCULAR JUNCTION OF *Bufo marinus* TADPOLE'S TAIL: CADMIUM EFFECT. **Legier Rojas, Carmen L. Loureiro, and Marino DiFranco.** (Intr. by Ernesto Gonzalez). Centro de Biología Celular, Facultad de Ciencias. U.C.V. Apartado 47144, Caracas 1041-A, Venezuela.

Scanning electron microscopy of tadpole's tail (2-4 weeks old) from the tropical toad *Bufo marinus* revealed an elevated nerve fibers ramification on the muscle fibers. We took advantage of this structural feature to study releasing and transmitter-receptor complex properties of the asynchronous spontaneous neuro-muscular synaptic transmission and its dependence on extracellular Ca^{2+} and Cd^{2+} (a calcium conductance blocker).

Macropatch technique (Parnas et al., 1989) was used to record the miniature end-plate currents (mepc's). The solutions in both pipette and bath contained (in mM): 125 KCl, 10 mM HEPES, pH 7.2; $CaCl_2$ was changed in the range 0.1-10 mM in pipette and bath. The probability to record mepc using pipettes of about 10 μm of diameter was high (about 0.6). Synaptic transmission was blocked by d-tubocurare, decamethonium and α-Bungarotoxin when applied to the bath, indicating a cholinergic transmission. At room temperature (22-24 °C), amplitude distribution of asynchrounus spontaneous mepc's was multimodal and at -100 mV holding potential the mepc's amplitude ranged between 0.1 and 2 nA. The peak of the mepc was reached between 100-900 μs and time to peak increased linearly on the mepc amplitude. The stationary mepc's frequency calculated over 120 s, increased sigmoidally when the external calcium concentration was increased (0.1-10 mM), with a $K_{Ca} = 0.9 mM^{-1}$. A dual effect on mepc's frequency was observed when Cd^{2+} was used in solutions containing 8 mM of Ca^{2+}. The stationary frequency decreased at low concentrations 100-600 μM, whereas it increased between 0.6-4 mM of Cd^{2+}. The decay time of the mepc's (τ_{mepc}) was fitted with one exponential and the values obtained were between 2-8 ms depending of the tadpole age. τ_{mepc} was smaller for old tadpoles.

Kinetics characteristics of the transmitter release and the transmitter-receptor interaction will be discussed based on Rahamimoff and sequential models respectively. (Grants CDCH-03.10.2065.89 and C-054.89)

Parnas, H.; Hovav, G. and Parnas, I. Biophys. J. 55: 859-874, 1989.

W-Pos98

EXTRACELLULAR SPACE IN ISOLATED BARNACLE MUSCLE CELLS UNDER ISOTONIC AND HYPOTONIC CONDITIONS. M. Holmgren., D. Berman. and H. Rasgado-Flores. Dept. Physiol. & Biophys., UHS/Chicago Med. Sch., North Chicago, IL 60064.

Barnacle muscle cells are able to regulate their volume in response to hypotonic solutions. The regulatory volume decrease (RVD) depends on the presence of extracellular Ca^{2+} (Ca_o). To determine whether a net lost of intracellular ions is responsible for the RVD, it is necessary to accurately know the values of the extracellular space (ECS). We measured the ECS in isolated barnacle muscle cells exposed to isotonic and hypotonic conditions in the presence and absence of Ca_o. Hypotonic solutions were obtained by varying the sucrose concentration while maintaining constant the ionic concentrations. Ca_o was replaced mole-for-mole by Mg^{2+}. ^{14}C-polyethylene glycol 4000 was used as the ECS marker. Since barnacle muscle cells possess deep invaginations, equilibration of ^{14}C-polyethylene glycol took an average of 3 hours. In the presence or absence of Ca_o, the ECS measured under isotonic conditions (-Ca = 12.4 ± 0.56, n = 26; +Ca = 8.16 ± 0.38, n = 41) were significantly higher than under hypotonic conditions (-Ca = 7.11 ± 0.33, n = 30; +Ca = 4.02 ± 0.12, n = 39). This may be due to obliteration of the invaginations upon hypoosmotic stress. Interestingly, the ECS values measured in the absence of Ca_o were significantly higher than the ones obtained in the presence of this cation. This may result from expulsion of water from the invaginations as a consequence of the contraction that the cells undergo when they are cut (to be analyzed) in the presence of Ca_o. Supported by NIH R29-AR39522 (H.R-F).

W-Pos99

ASPECTS OF THE INTERACTIONS OF RETINOL WITH RAT SERUM RETINOL-BINDING-PROTEIN (RBP) AND WITH RAT CYTOSOLIC RETINOL-BINDING-PROTEIN (CRBP I). Noa Noy, Dept. of Medicine, Cornell University Medical College, New York, NY.

The rates of transfer of retinol initially bound to rat RBP or to rat liver CRBP I to vesicles of egg phosphatidylcholine were measured by monitoring the decrease in retinol fluorescence that occured upon transfer from the proteins. Transfer occured via the aqueous phase and the rates of transfer represented the rates of solvation of the ligand from the two proteins. This was evidenced by the independence of the rate constants for transfer on the concentrations of protein or vesicles. The rate constants for dissociation of ligand from the proteins could thus be directly obtained from rates of transfer.

The equilibrium binding constants of retinol with the two proteins were measured by studying the partitioning of radioactively labelled retinol between proteins, plasma membranes of rat liver cells, and an aqueous phase.

The implications of the data for the mechanism by which retinol moves from its binding site on RBP in blood onto its binding site on CRBP in the cytosol of cells will be discussed.

W-Pos100

REGULATION OF BACTERIAL PORIN STRUCTURE AND FUNCTION. J.C. Todt, W.J. Rocque, and E.J. McGroarty. Porin is a trimeric channel forming protein in the outer membrane of gram negative bacteria. The importance of bacterial porin lies in its control of the flux across this membrane and its similarity to other channel-forming proteins. The primary and secondary structure of many porins has been well characterized, and its function has been analyzed both in vivo and in reconstituted membrane systems. Despite such studies, discrepancies concerning porin channel size and voltage gating are not yet resolved. We have initiated functional studies on OmpF, OmpC and PhoE porins from Escheriohia ooli K12 and have found that the size and voltage regulation of the channels are altered by such variables as pH and the amount of bound LPS present. Initial studies indicate that porin channels are smaller and induced to close by lower transmembrane potentials at acidic pHs. We propose that porin can adopt two or more conformations having different channel sizes and gating voltages. We have preliminary evidence of a pH-induced conformational change using DSC and intrinsic tryptophan fluorescence. These results could explain some of the discrepancies in porin (functional) studies.

W-Pos101

INTRACELLULAR pH REGULATION IN PREIMPLANTATION MOUSE EMBRYOS

Jay M. Baltz[1], John D. Biggers[1] and Claude Lechene[1,2]
[1]Harvard Medical School and [2]Brigham and Women's Hospital Boston, MA 02115.

We have investigated the regulation of intracellular pH (pH_i) in 2-cell stage mouse embryos using the pH-sensitive dye, BCECF. After the cells are acid-loaded, pH_i recovers back to approximately the baseline level. However, we have found that, unlike in differentiated cells, this recovery is not mediated by any specific plasma membrane mechanism. Na^+/H^+ exchange, found in almost every other vertebrate cell type, is not present, as evidenced by the insensitivity of the recovery to absence of external Na^+ or the presence of amiloride (JM Baltz, JD Biggers and C Lechene, Dev. Biol. 138:421, 1990). We have now also found that Na^+ dependent HCO_3^-/Cl^- exchange, found in many cells, is also inactive, since the recovery is insensitive to lack of Na^+, lack of HCO_3^-, or the presence of DIDS. These conditions also rule out a Na^+,HCO_3^- cotransport mechanism. In addition, neither CN^- nor NEM slowed the recovery rate, indicating that no H^+ ATPase was involved. Apparently, protons are in equilibrium across the plasma membrane of two-cell mouse embryos and the recovery is a passive process of re-establishing this equilibrium: pH_i is extremely sensitive to the external concentration of K^+, and resting pH_i has the value predicted by the Nernst relation. In contrast, however, we have found that these cells do possess a mechanism for alleviating alkaline loads--a Na^+-independent HCO_3^-/Cl^- exchanger. Recovery from alkaline loads is inhibited by DIDS, Cl^- starvation, or the absence of HCO_3^-. This system is active in the two-cell stage mouse embryo above pH_i 7.15-7.20, with the rate of alkali extrusion mediated by this system increasing monotonically with increasing pH. It may be important for the development of the early embryo for it to possess an alkaline-load alleviating system but not any for relieving acid-loads. Perhaps this reflects the embryos' *in vivo* environment.

W-Pos102

Identification of a new class of growth factors: tumor-derived lymphocyte mitogens. Beverly S. Packard. Division of Cytokine Biology, CBER, FDA, Bethesda, MD. 20892

One of the functions thought to be required for the antitumor activity of lymphocytes is their proliferation at tumor sites. Two classes of stimuli -- one derived from cell-cell contact between tumor cells and immunocytes and the other from soluble factors -- represent the extremes in the spectrum of physical states describing the initiation of tumor-induced lymphocyte proliferation. Currently, immunologically competent cells such as monocytes and lymphocytes are believed to represent the major source of soluble lymphocyte mitogens. This study was aimed at exploring the possible presence of T-lymphocyte mitogens of tumor origin. It was found that the presence of at least four irradiated human tumor cell lines could stimulate the proliferation of human T-lymphocytes; the observed proliferative stimulation was due to secreted factors as activity was present in the serum-free tumor cell supernatant (**PNAS 87**:4058-62 (1990)). Immunologic and proliferative assays using ELISAs, neutralizing antibodies, and recombinant lymphokine standards indicated nonidentity of at least one secreted factor with any previously characterized lymphokine. Furthermore, tumor cell-derived mitogenic stimulation of growth-arrested lymphocytes reached a maximum by 24 hours compared with 48 hours, the time necessary to approach maximal stimulation by interleukin-2, a well-known pan-T-lymphocyte mitogen. This new factor(s) is being purified by a combination of ion exchange and gel filtration chromatography in addition to reverse phase HPLC. Identification of a secreted factor(s) from tumor cells as a source of mitogenic activity for lymphocytes supports the idea that the tumor immunoenvironment as recognized by lymphocytes is defined by soluble mediators in addition to the well-studied cell-cell contact interactions.

W-Pos103

CROSS-TALK BETWEEN SECRETING BOVINE CHROMAFFIN CELLS AND OTHER MEDULLARY CELLS: A FURA-2 IMAGING STUDY. M. Diverse-Pierluissi, E.W. Westhead and D.J. Gross. Program in Molecular and Cellular Biology, University of Massachusetts, Amherst, MA, 01003.

Upon stimulation chromaffin cells release the contents of their secretory granules. These granules contain adenine nucleotides, catecholamines and neuropeptides. The purpose of this study was to determine the effects of the released granule contents on the cells that normally surround the adrenal chromaffin cells. Fura-2 imaging of primary cultures of chromaffin cells and other contaminating cells allowed us to simultaneously measure the response of several cell types to stimulation. When cells were stimulated with 50 μM ATP a fast elevation in the levels of cytosolic calcium was observed. As soon as the agonist was removed the calcium levels of bovine chromaffin cells went back to basal. In the other cell types present, a second calcium response was observed after removal of the agonist. The lag period for the development of this second response was proportional to the distance between chromaffin cells and the other cell. This suggests that the other adrenal cells were responding to an agent secreted by chromaffin cells. When cells were stimulated with a nicotinic agonist the chromaffin cells and cells that morphologically resemble smooth muscle cells responded with an elevation in the calcium levels. A third cell type did not respond to the nicotinic agonist but it had a strong response to ATP. We believe these cells are endothelial cells. Chromaffin cells that were close to endothelial cells showed an inhibition of the cytosolic calcium response to a subsequent stimulus after removal of the initial stimulant. Endothelial cells are known to produce nitric oxide which elevates the levels of cGMP by activating guanylate cyclase. Preincubation with 50 μM cGMP decreased the ATP-evoked calcium response.
Support: NSF DMB-8803826, NIH NS26606, BRSG RR 07048.